This electronic thesis or dissertation has been downloaded from the King's Research Portal at https://kclpure.kcl.ac.uk/portal/

Neural Repair and Robotics
The In-cage automation of a test for dexterity after stroke.

Gadiagellan, Dhireshan

Awarding institution:
King's College London

The copyright of this thesis rests with the author and no quotation from it or information derived from it may be published without proper acknowledgement.

END USER LICENCE AGREEMENT

Unless another licence is stated on the immediately following page this work is licensed

under a Creative Commons Attribution-NonCommercial-NoDerivatives 4.0 International

licence. https://creativecommons.org/licenses/by-nc-nd/4.0/

You are free to copy, distribute and transmit the work

Under the following conditions:

- Attribution: You must attribute the work in the manner specified by the author (but not in any way that suggests that they endorse you or your use of the work).
- Non Commercial: You may not use this work for commercial purposes.
- No Derivative Works - You may not alter, transform, or build upon this work.

Any of these conditions can be waived if you receive permission from the author. Your fair dealings and other rights are in no way affected by the above.

Take down policy

If you believe that this document breaches copyright please contact librarypure@kcl.ac.uk providing details, and we will remove access to the work immediately and investigate your claim.

Download date: 08. Oct. 2023

NEURAL REPAIR AND ROBOTICS:

The in-cage automation of a test for dexterity after stroke.

Dhireshan Gadiagellan

Thesis submitted to King's College London for the degree of
Doctor of Philosophy in Neuroscience
October 2017

Department of Neurorestoration
Wolfson Centre for Age-Related Diseases
The Institute of Psychiatry, Psychology and Neuroscience
King's College London

Abstract

Stroke is a chronic and debilitating disease that affects millions of individuals worldwide. The collective medical and socioeconomic costs reach into billions of pounds annually. Pre-clinical research into neurorestorative treatments for this disease often involves the behavioural assessment of rats using the Single Pellet Reaching Task (SPRT). This task is executed by placing a pellet in front of a rat beyond a slit, offsetting the pellet to the left or right so that it can only be reached with the right or left paw respectively. This allows for independent evaluation of the more or less-affected forelimb after unilateral stroke. The animal is scored on the number of pellets it consumes by reaching through the slit. After a cortical stroke, rats will drop more pellets than naïve rats, and despite some spontaneous recovery, without treatment, recovery is incomplete. It is an effective assessment method which yields information about motor skills, coordination, dexterity, reach, and grasping ability. However, it is labour intensive and time-consuming, resulting in lower powered experiments than that desired by researchers.

This thesis describes the development of robotic equipment to provide the in-cage automated training, rehabilitation and assessment of the grasping of sucrose pellets by large cohorts of rats. The goal of this new assessment paradigm is to help accelerate the identification of therapies for patients with central nervous system (CNS) injuries that impact dexterity.

With the use of rapid prototyping methods and technologies, an in-cage robotic apparatus (RatBot™) has been developed and validated to automatically train rats in the SPRT and assess their grasping ability before and after a CNS injury. The apparatus comprises of a programmable 45mg sucrose pellet dispenser with features to prevent pellet jamming and reduce grinding, and a programmable pellet positioning system which can present the pellet to a variety of locations within the reach space of a rat. Pellet consumption statistics, rat identification and trial participation information are automatically gathered and persisted to a database for remote access and offline analysis.

With minimal infrastructure and maintenance requirements, an array of RatBots has been shown to be sensitive to the individual reaching capabilities of the rats tested, successfully identifying grasping deficits in two independent cohorts of rats with unilateral cortical stroke. The device can operate in parallel in both bench top as well as overnight unattended in-cage operation.

Declaration of authenticity and copyright

I declare that all the work presented in this thesis is a result of my research and has not been accepted for any other degrees. Contributions, references and outsourced work have clearly been stated as appropriate in this text.

The copyright and intellectual property associated with this thesis rests with the author and no quotation from it or information derived from it may be published without proper acknowledgement or commercialised without prior written agreement.

Dhireshan Gadiagellan

October 2017

Acknowledgements

To my supervisor, Dr Lawrence Moon who is a remarkable individual and a great mentor with a generous and positive outlook on life. Thanks for all the support, advice, motivation and direction throughout this PhD, and to Dr Thrishantha Nanayakkara who shares a passion for making quality of life contributions to science and robotics.

To my family for supporting me selflessly over the duration of this PhD. To my daughters Kayla and Talia for being understanding about the lack of dad time. To my wife and life partner Vishnee for ensuring that I had the best possible chance at success!

To my friend and business partner Mike Counsell, thanks for carrying the key business workload over these last few years. Your support was key to ensuring the success of our venture, and I could not have done it without your support.

Thank you to Sotiris Kakanos, Claudia Kathe, Natalie Duggett and Aline Spejo for the advice and support and assistance throughout my stay at the college.

A big thank you to Claire Pearce, Gary Fulcher and the rest of the Hodgkin Building Biological Services Unit team for the advice and unending support in animal care and for catering to my bespoke requests during my experiments.

To Andy Grant for working with me to ensure I had a smooth PhD track.

To everyone at the Wolfson Centre for Age-Related Diseases for allowing me the opportunity to take over part of the behaviour and animal holding rooms.

A large appreciation goes out to the European Research Council for funding this work and the subsequent route to the commercialisation of the developed device.

And a special thanks to King's College London for giving me the opportunity to expand my knowledge and contribute to science through this PhD.

Contents

Figures

Appendix Figures

Tables

Abbreviations

Abbreviation	Meaning
CNS	Central nervous system
MRI	Magnetic Resonance Imaging
CT	Computerised Tomography
ACE	Anglotensin Converting Enzyme
NT3	Neurotrophin-3. A nerve growth factor
ID	Inner diameter
OD	Outer diameter
PLA	Polylactic acid
SPRT	Single pellet reaching task
SMD	Surface mount device
BSU	Biological Services Unit
VAT	Value added tax
RFID	Radio frequency identification
DC	Direct current
FDD	Floppy disk drive
CDD	Compact disk drive
Gb	Gigabit 1000000000 bits per second
LED	Light emitting diode
GUI	Graphical user interface
PIC	Programmable integrated circuit - Microchip
LAN	Local Area Network
NTP	Network Time Protocol
AIC	Akaike’s Information Criterion
SPSS	Statistical Package for the Social Sciences
PoC	Proof of Concept
ERC	European Research Council
ABS	Acrylonitrile butadiene styrene
PFA	Paraformaldehyde
PBS	Phosphate buffered solution
OS	Operating System
Ra	Average Roughness
PCT	Patent Cooperation Treaty
HD	High Definition

Chapter 1

Introduction

Neuroscience is an interdisciplinary field (Holley, 2008) that fuses a broad spectrum of subjects and techniques and encourages a creative ingenuity that allows scientists to push the boundaries of experimental research (FINK et al., 2007). Quantification of the results of a study or an experiment is crucial to its success and scientists are constantly innovating by developing and improving experimental methods and analytical techniques. Part of this analysis relies on strategically designed behavioural assessments that enable researchers to highlight and assess various physiological characteristics of an animal (Cenci et al., 2002; Kleim et al., 2007; Schlinger, 2015).

With the high pace of technological advancement, electronic miniaturisation becomes more evident (Schaller, 1997) and we notice an increase in the use of novel robotic assistive technologies in both animal and human studies (Fasoli et al., 2003; Chang et al., 2007; Cheng, 2012; Dominici et al., 2012; Kleinholdermann et al., 2013; Vigaru, 2013). This trend encourages research groups to embrace cross-discipline teams and research environments, and more closely integrate biological sciences with engineering. The output from these multi-discipline teams has been more evident in recent years with high-tech innovations in neuroprosthetics (Borton et al., 2011; Pappas and DeVoll, 2012; Courtine and Bloch, 2015; Eapen et al., 2017), brain-machine interfaces (Rowe, 2014; Moxon and Foffani, 2015) and biologically inspired and assistive robotics (Hakim et al., 2016; Dukelow, 2017; Pourghodrat and Nelson, 2017).

In the UK, less than $1/10^{th}$ of research funding is available per stroke patient compared to cancer (Luengo-Fernandez et al., 2012). With the increase in labour costs, limited research time, and the need to make efficient use of limited funding by generous grant bodies, automation becomes an attractive method of optimising long-term spending and research goals.

This project aims to assist with the streamlining and optimisation of the Single Pellet Reaching Task (SPRT) (Whishaw and Pellis, 1990b) through robotic automation. This thesis presents the development, refinement, validation and testing of an in-cage automated solution capable of training and assessing a cohort of rats with the SPRT.

1.1 What is a stroke?

The Stroke Association defines a stroke as a '*brain attack'* that '*happens when the blood supply to part of the brain is cut off and brain cells are damaged or die*'.

Stroke is a neurological disability affecting approximately 100 000 people in the UK every year (Stroke Association, 2017). It is one of the leading causes of adult disability (Stroke Association, 2017) and results in about 1.9 million deaths in Europe each year (European heart network, 2017). In England alone, £2.8 billion is spent each year on stroke treatment and places a tremendous burden on medical services (Stroke Association, 2017).

1.1.1 Types of Stroke:

The two main types of stroke are:

1. **Haemorrhagic** (Figure 1.1a) - The wall of a blood vessel in the brain is compromised and ruptures causing blood leakage into the brain, preventing the delivery of oxygen and nutrients to brain cells resulting in cellular damage or death.
2. **Ischemic** (Figure 1.1b) - A vessel blockage due to blood clotting or vessel constriction that prevents the supply of oxygenated, nutrient rich blood to a specific part of the brain which also results in damage or death of brain cells. Ischemic stroke accounts for approximately 85% of strokes (Stroke Association, 2017).

a.	b.
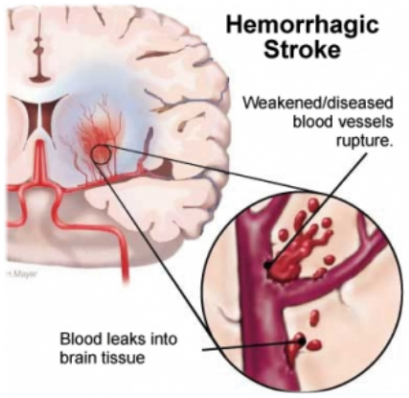	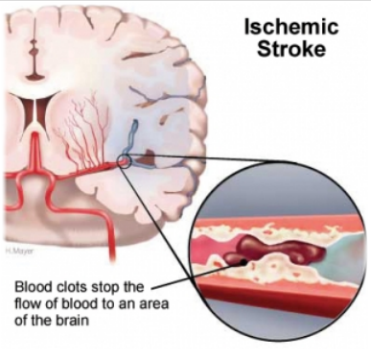

Figure 1.1 - A graphical representation of the two main types of stroke.

a. Haemorrhagic stroke due to a breakage in the vessel wall causing blood to flow into the surrounding tissue.
b. Ischemic stroke caused by an obstruction or constriction of a supply vessel limiting or eliminating the flow of blood to the brain.

(Image: topmedicaljournal.com)

1.1.2 Stroke Deficits

a.	b.
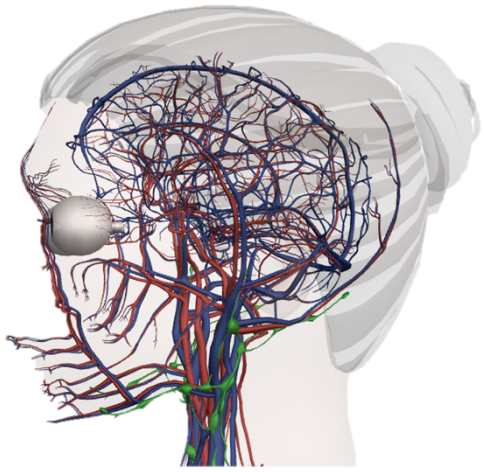	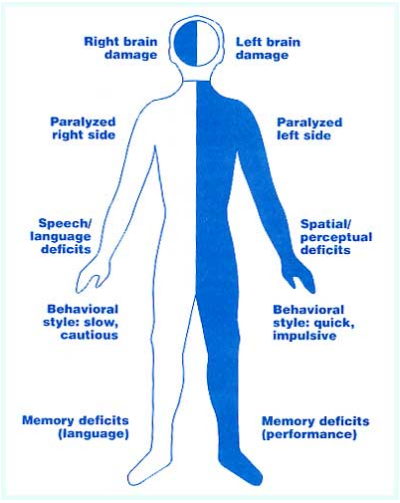

Figure 1.2 - Brain circulatory system and human deficit map.

a. A representation of the larger veins and arteries within the human brain. (zygotebody.com)
b. A chart indicating the contralateral relationship with brain damage and the affected side of the body. Major deficits are also highlighted. (nasam.org)

Disruption to the blood supply can occur in various parts of the vessel-rich brain (Figure 1.2a), which means that cellular death can occur in a variety of areas resulting in different kinds of deficits including but not limited to: speech and language, memory and motor skills. These deficits along with the contralateral relationship between the affected brain hemisphere and affected side of the body are depicted in Figure 1.2b.

1.2 Stroke treatment

In order to determine the most appropriate treatment for a stroke victim, first, the type of stroke needs to be determined i.e. ischaemic or haemorrhagic. This diagnosis is usually achieved via a computerised tomography (CT) or magnetic resonance imaging (MRI) brain scan.

For ischaemic stroke, ‘clot-busting’ alteplase may be administered to dissolve the blood clots but is only effective within 4.5 hours after the onset of stroke (del Zoppo et al., 2009; Otwell et al., 2010; NICE, 2017). This treatment is usually followed up with the use of

anticoagulants such as heparin and warfarin to prevent further clots from forming (Donnan et al., 2008)

In the case of haemorrhagic stroke, surgery is required to repair the damaged vessel. The patient is given angiotensin converting enzyme (ACE) inhibitors post-surgery to lower blood pressure and prevent further strokes from occurring (Hankey, 2003).

Outside of the 4.5-hour critical window for ischemic strokes, the only treatment available is rehabilitation (del Zoppo et al., 2009; Lees et al., 2010). The lack of available treatments indicates a need for more treatment options that can be administered outside of this critical period.

A variety of neurorestorative stroke treatments have been developed and studied, but very few have been translated into clinical applications. These treatments range from neurorestorative therapies such as Chondroitinase to promote plasticity (Soleman et al., 2012), the suppression of the myelin-derived inhibitor Nogo-A (Tsai et al., 2010) to exercise (Nielsen et al., 2013; Tian et al., 2013) and robotic rehabilitation (Fasoli et al., 2003; Chang et al., 2007; PhD et al., 2014; Schwartz and Meiner, 2015) therapies incorporating mechanical and brain-machine interfaces. A vast number of neuroprotection studies have taken place over the past few decades, but the success rate of translation into the clinical environment has been low (O'Collins et al., 2006). This, coupled with high mortality rates and the short effective treatment window, results in an urgent need for more treatment options and further studies that are more relevant to the clinic.

1.3 Behavioural analysis in stroke research

Like in-vitro analysis, in-vivo behaviour analysis plays an important role in assessing the outcomes of central nervous system (CNS) injury related studies such as stroke (Schaar et al., 2010). Various tests have been developed to assess and quantify physiological recovery or deficits in studied animals. Table 1.1 shows a subset of behaviour assessment tasks that attempt to test motor skills and coordination.

Test	Description
Montoya Staircase	Forelimb reaching ability (Montoya et al., 1991)
Cylinder	Paw preference (Montoya et al., 1991)
Pasta	Grip strength (Schallert et al., 2000)
Pasta Matrix	Reach (Ballermann et al., 1999)
Sunflower seed	Dexterity and motor coordination (Ballermann et al., 2001)
Horizontal Ladder	Coordination and motor skills (Soblosky et al., 1997; Gonzalez et al., 2004)
Whishaw Single pellet reaching	Reach, dexterity, grasping, coordination of motor skills, olfactory-based pellet location. (Whishaw and Tomie, 1988; Whishaw and Pellis, 1990a; 1990b; Metz and Whishaw, 2013)
Isometric pull task	Quantification of forelimb force generation. (Hays et al., 2013)

Table 1.1 - Commonly used behavioural tests for the assessment of motor skills in rats.

1.4 The single pellet reaching task

Rodent reaching has been shown to be similar to non-human primate (Alaverdashvili and Whishaw, 2008) and human (Whishaw et al., 1992) reaching models, hence may be more relevant in research. The modern day single pellet reaching task (Smith and Metz, 2005) described in Figure 1.3, evolved from handedness experiments (Alaverdashvili and Whishaw, 2013) and cage-bar based pellet retrieval studies (Wentworth, 1933). This task was designed to minimise the effects of posture abnormalities that other skilled reaching exercises such as the conveyor belt task (Whishaw et al., 1986a) and test tube task (Evenden and Robbins, 1984) suffered from (Schneider and Olazabal, 1984).

Briefly, a rat is placed in a custom-designed acrylic pellet reaching apparatus (Figure 1.3a) (Girgis et al., 2007) and is allowed to reach through a 1cm wide opening to grasp a sucrose pellet placed at specific locations on a shelf. The shelf is located approximately 3cm above the base of the apparatus (Figure 1.3b). Two pellet positions are generally used; one to the left of the slit and one to the right of the slit. If a sugar pellet is placed to the left of the slit, then the rat can only retrieve it with its right paw; it is unable to reach the pellet with its left paw. This allows the researcher to evaluate the use of a specific forelimb; for example, after unilateral stroke the researcher can quantify dexterity of the affected paw and the less affected paw separately. Slow-motion videography reveals that a successful grasp involves the rat advancing, grasping, withdrawing and releasing the pellet (Figure 1.3c). The rat is trained to move away from the slit before it is presented with another sucrose pellet (Whishaw and Pellis, 1990b; Whishaw and Coles, 1996). This requires the rat to present and reposition itself to the slit again thereby removing any advantage that it may have gained from the previously adopted posture (Miklyaeva et al., 1994; Field and Whishaw, 2005).

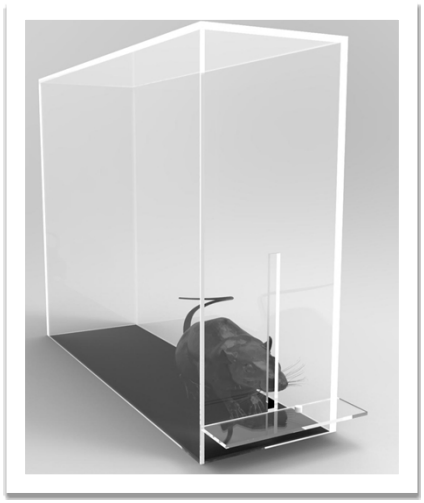

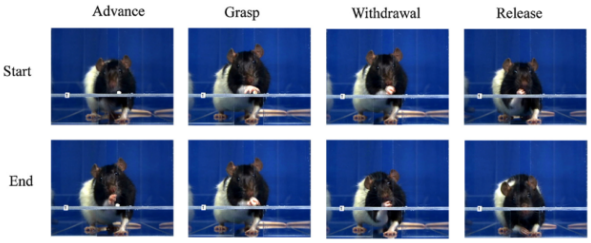

Figure 1.3 - Single pellet reaching task setup and motion breakdown.

a. The single pellet reaching apparatus constructed out of clear acrylic.
b. Side view of a rat reaching through the 1cm opening for a sucrose pellet.
c. Front view breakdown of the reaching task into Advance, Grasp, Withdrawal and Release components.

Images b & c: (Karl and Whishaw, 2011)

The reaching and consumption success rates as well as the quantized reaching movements (Alaverdashvili and Whishaw, 2013) may be assessed to provide information about the motor skills of a naïve or post CNS injury animal.

Preparation, execution and analysis of the SPRT can be broken down into various phases as follows (Alaverdashvili and Whishaw, 2013):

1. ***Device Acclimation*** - The process of familiarising animals with the test environment.
2. ***Pellet Habituation*** - The process of familiarising animals with the reward (sucrose pellet) by introducing the pellets into their cage for up to a week before the initial training commences.
3. ***Reach Training*** - The process of teaching the animal to grasp and consume the pellet by varying the complexity of the task; initially making the task easy, allowing

pellet access directly with the tongue (Figure 1.4a). The pellet is moved further away coercing the animal to use its forepaw to obtain the pellet (Figure 1.4b-c).

4. ***Distraction Training*** - To ensure that the animal does not benefit from maintaining the same posture and orientation, it is taught to move to the rear of the apparatus between reach attempts. The animal would then approach the shelf to execute the next reaching trial.
5. ***Task Execution*** - Once trained, the task is executed on a regular schedule defined by the researcher. Due to the manual nature of the task, a researcher may test only one animal at a time.
6. ***Offline Assessment & Analysis*** - Execution of the task may be video recorded for offline analysis. Often this analysis is done on a frame-by-frame basis to assess the individual facets of the reach i.e grasp, retraction and consumption movements.

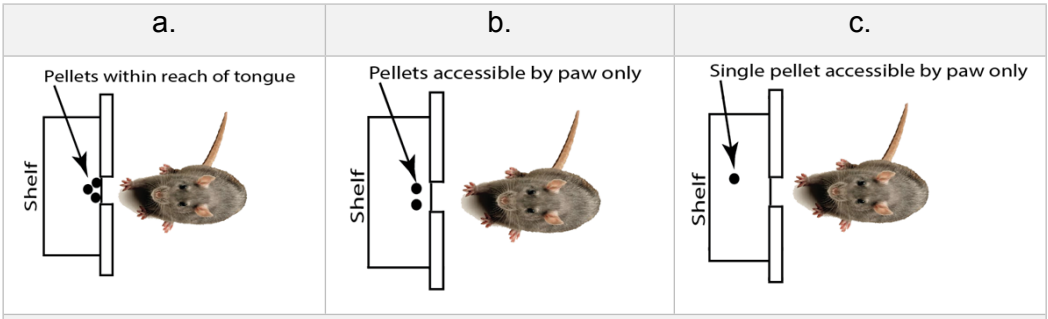

Figure 1.4 - Training by varying the distance of the sucrose pellets.

a. Multiple pellets are placed near the animal so that it may obtain one or more using its tongue.

b. Pellets are moved away so that they are no longer accessible with the tongue. This encourages use of the forepaw.

c. A single pellet is presented further away requiring an extended reach and a targeted reach trajectory for the single pellet compared to possible random reaches where many pellets are present.

1.5 Why Automate

Automation is a natural path forward when dealing with repeatable monotonous tasks that may benefit from higher throughput. In a general sense, automation provides the opportunity and ability to increase the repeatability of a task and increase throughput while reducing operator or researcher subjectivity. Robotic appliances developed to carry out rehabilitation and other neurotherapies (Hesse et al., 2003a; Schmidt et al., 2004; Hesse et al., 2006) are progressing, but the field is still in its early stages (Loureiro et al., 2014) and may benefit from more research and investment (Loureiro et al., 2011). The single pellet reaching task is one such task that research will benefit from being automated.

The SPRT is a rich behavioural test but unlike behavioural tasks such as the Montoya staircase test (Whishaw et al., 1986b; 2008a; Alaverdashvili and Whishaw, 2013) which may be executed in parallel, the SPRT is a labour intensive assessment (Montoya et al., 1991; Hurd et al., 2013; Fenrich et al., 2016) requiring a researcher to test or train only a single animal at a time due to the manual pellet loading and pellet retrieval observations necessary. This one-to-one labour-intensive nature of the task results in lower experimental numbers and sparse testing schedules. Although it is a labour-intensive task, it is still important in stroke models of research (Farr and Whishaw, 2002; MacLellan et al., 2006; Silasi et al., 2008)

With the automation of the SPRT, we may assess larger cohorts of rats in parallel and achieve a larger number of trials per subject. Researchers and technicians are free to carry out more research rather than spending time assessing these behavioural tasks. Automating this task may also reduce researcher influence on experiments allowing for a greater level of objectivity. In doing so, more consistent and objective incomes will be achieved by mitigating the low repeatability of positive results (Fouad, 2013). Consistency of execution and data integrity may further facilitate collaboration between research groups leading to larger powered studies. Collaborations may also have a positive impact in reducing the number of repeat studies that take place as data may be reused, hence reducing the overall number of animals used.

It has been shown that early rehabilitation through repetitive skilled movement improves motor performance after stroke in rats (Whishaw et al., 1986a). This has also been seen in healthy humans (Tian et al., 2013) as well as in humans suffering from a CNS injury (Hesse et al., 2003b; Livingston-Thomas and Tasker, 2013). Research also shows that early rehabilitation (Lum et al., 2002) promotes plasticity (Stinear et al., 2013) and motor

recovery is related to the repetitive action patterns that form part of these rehabilitation exercises. In addition to plasticity, rehabilitation also promotes the development of compensatory motor function and strategies (Whishaw et al., 1991; Metz et al., 2005; Gharbawie and Whishaw, 2006; Girgis et al., 2007; Alaverdashvili and Whishaw, 2010), which is a form of recovery i.e. regaining lost ability. It should be noted that forced rehabilitation may have an adverse impact on functional recovery if it took place soon after the brain damage occurred (Humm et al., 1998). There is also evidence of more effective and positive outcomes when therapies are complimented by rehabilitation (García-Alías et al., 2009; Weishaupt et al., 2013; Ishikawa et al., 2015).

The manual variant of the task may be considered an anxiogenic practice (Hurst and West, 2010) as it is assessed in a well-lit environment outside of the animals' home cage, requiring handling and transportation, which may lead to increased stress levels within the animal and thus may provide inaccurate data. Although not disclosed in many studies, it is assumed that the task is executed during the light cycle outside of the animal holding room, when the animal is least active. It has been shown that animals participate more accurately in reaching tasks during the dark cycle (Whishaw et al., 2008a; Hurd et al., 2013) so an in-cage device capable of operating 24 hours a day would be advantageous. It has also been shown that sleep disturbance may have a negative impact on stroke recovery in rats (Zunzunegui et al., 2011). Having a device that can run overnight also prevents the need for reversing the day/night cycle in animal houses which may affect other ongoing studies.

With automation, we aim to:

1. Maximise animal comfort and reduce the possibility of increased stress and anxiety levels by executing the task within the confines of the animal's home cage. In-cage operaton will be achieved by creating a miniature device to fit inside the cage without encroaching on the 'free-roam' space available.
2. Increase experimental numbers achievable with minimal overhead by automating as many of the phases as possible.
3. Make the task more objective and repeatable by reducing the human interaction and assessment subjectivity.
4. Minimise or eliminate manual data capture and data recording errors.

1.5.1 Design tracks considered

Two design models were initially considered for the automation of the SPRT. A stand-alone assessment station (Figure 1.5a) which would allow a greater variety of

assessments as robotic equipment may be chosen without space and size limitations. This approach, however, may not solve the problem of throughput and animal anxiety. It also introduces additional complexity for unattended operation, which would require automated animal transport facilities via a network of transport tubes to and from the testing station. This may increase the workload on both the animal and the researcher as the animals will require training simply to use the transport facility. This setup may not be feasible as a long-term installation in typical biological services units because it takes up space that otherwise could be occupied by housing.

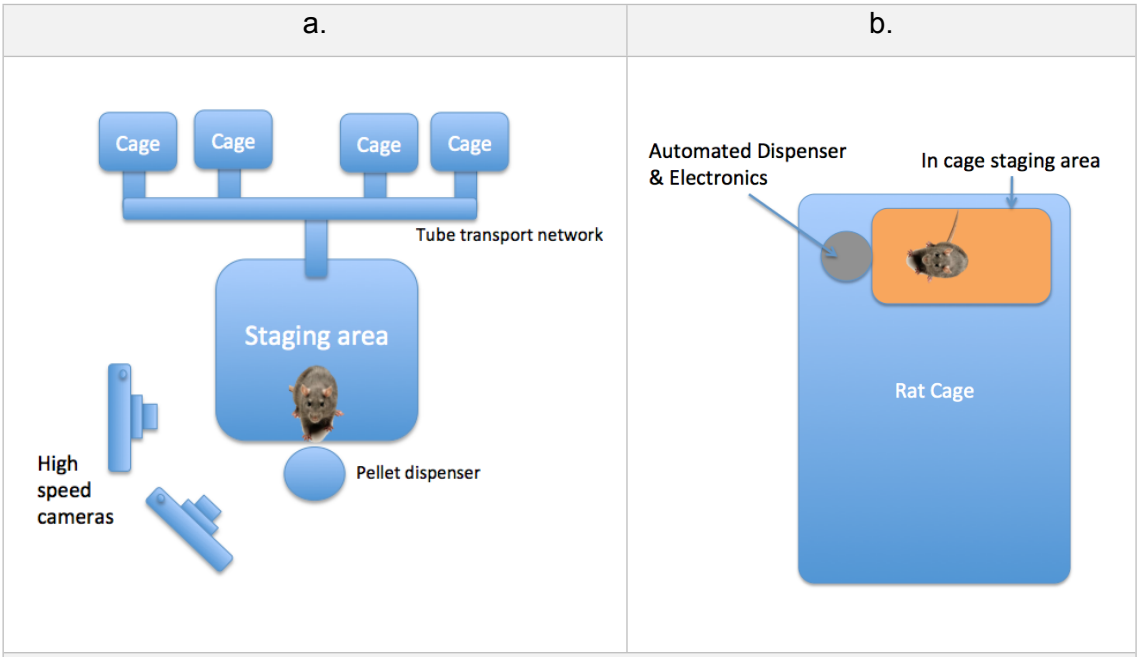

Figure 1.5 - Two design variations considered in the initial phases of the project.

a. An apparatus-rich stand-alone assessment station that allows the animals to commute via a series of tube networks to a staging area for assessments to be carried out. An automated dispenser and an array of feedback equipment may be used to acquire information on the various aspects of the reaching task. Space considerations are relaxed in this design scenario.
b. An apparatus with self-contained dispensing and assessment facilities is designed to fit inside a rat's cage. Miniaturisation design considerations are imperative to the success of this design track.

(Images: bugaboopest.com)

An in-cage approach shown in Figure 1.5b solves the problem of throughput, transport, training and animal anxiety, but limits our ability to extend the feature set to include larger off the shelf data capture and analysis equipment. This design track is less invasive to the typical Biological Services Unit (BSU) environment and is likely to be well supported due to lower maintenance and infrastructure requirements.

Typical BSU operations adopt group housing strategies where multiple rats are housed per cage, with multiple cages in a rack, and multiple racks in a typical holding room. These facilities are routinely cleaned weekly or fortnightly. Both racks and animal cages are washed in automated washing facilities such as the Techniplast ARES and Pegasus systems. These cleaning regimes would suggest that any additional infrastructure must be separate to, or easily detachable from the existing racks and cages in the room so that maintenance routines are unhindered. Typically, these holding rooms are shared by multiple departments running multiple studies and their access to animals is to remain unhindered. Taking these operational and collaborative requirements into account, it was decided that the most feasible approach would be the development of a small in-cage robotic device to execute and assess the task. The device would require minimal supporting infrastructure and can be easily removed and replaced per the BSU cleaning schedule.

1.6 Currently available pellet dispensers

Four vendors supply stand-alone pellet dispensers (Table 1.2) that are capable of dispensing either 20mg or 45mg sucrose pellets.

Vendor	Product Image	Price	Dimension
Med Associates		£324	235(H)x112(W)x127mm(D)
Coulbourn		£425 ex VAT	Not available
Lafayette	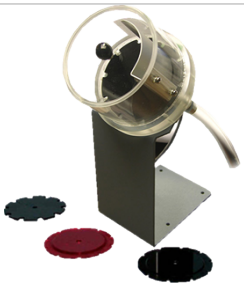	£409 ex VAT[1]	250(H)x95(W)x117mm (D)
Noldus[2]		Not available. *(No response from supplier)*	200(H) x100mm (Diameter)

Table 1.2 - Commercially available pellet dispensers.

Pellet dispensers designed for laboratory behavioural studies that are capable of dispensing either 20mg or 45mg sucrose pellets. This table outlines the vendor, product images, pricing and dimensional information where available.

[1] $660. Exchange rate 1.61 ($/£) - 17 Nov 2013

[2] 20mg pellets only

Except for the Noldus dispenser, these devices (Table 1.2) are too tall to fit into a standard rat cage such as the Techniplast™ 1354G. None of the devices can dispense a single pellet to a variable location and are more suited to static dispensing experiments. Instruments such as the Lafayette dispenser are noisy and display signs of excessive pellet grinding, which causes excessive dust and results in broken pellets, which may jam the device.

The decision was made to design and fabricate a new automated pellet dispensing system to address the lack of facilities and size restrictions that come with off the shelf dispensing equipment. This approach provides the flexibility to tailor a dispenser to meet the dynamic needs of this project and allow us to incorporate appropriate sensors and electro-mechanical mechanisms as required.

1.7 Automation in behaviour

Automation is used extensively in in-vitro research in areas such as high-throughput screening (Kodandaramaiah et al., 2013) in the drug discovery sector where a variety of robotic technology is employed. Prohibitive costs may have limited the uptake of expensive automation within research organisations with limited budgets. With the reduction in rapid prototyping and device development costs, automation and robotics are beginning to play a bigger role in in-vitro research. To facilitate this, cross-discipline research teams are becoming more apparent and necessary.

Attempts have been made to automate various animal behavioural assessments (Peikon et al., 2009; Palmér et al., 2012; Poddar et al., 2013; Vigaru, 2013; Fenrich et al., 2015b; Meyers et al., 2016) with robotic solutions, and various commercial devices such as the Digigait (Mouse Specifics Inc.), Rat Touch Screen Systems (Lafayette Neuroscience), modular chambers (Lafayette Neuroscience), Rota-Rods (Panlab), Grip strength systems, activity monitoring and tredmill systems (Panlab) have been developed to automate motor and activity assessments but due to the size of these devices and systems, they are more suitable as station based systems rather than in-cage solutions.

Attempts have also been made to automate the assessment of forelimb function and even the single pellet reaching task in rats using image processing techniques and electro-mechanical devices (Palmér et al., 2012; Fenrich et al., 2015a; Wong et al., 2015; Ellens et al., 2016). Like the aforementioned commercial devices, the design and size of these solutions precludes each from being an in-cage apparatus. These attempts at automating the task are creative solutions encompassing a variety of technologies and can execute the basic SPRT. However, these devices do not currently offer the following set of desirable features:

- Automatic identification of the rat executing the task.
- Automatic assessment of whether the pellet has been retrieved.
- A programmatic pellet positioning facility to vary the task complexity by presenting the pellet either closer to or further away from the rat.

1.8 Aim

The work presented in this thesis describes the iterative development of an automated in-cage solution to the single pellet reaching task which achieves all the desirable features described previously with the added objectives of reducing animal stress, reducing researcher time commitments, streamlining the experimental workflow and producing larger data sets for more powerful and repeatable studies.

The key aims of this PhD are as follows:

1.8.1 Key Aim 1

Develop a device that can fit in a cage of group housed rats and automatically train and asses them using the SPRT. The device must be capable of uniquely identifying each rat. It should operate day and night on a programmable schedule. Using sensor feedback, the device must detect if a pellet has been retrieved or dropped.

1.8.2 Key Aim 2

Assess the ability of the device to train cohorts of group housed rats with the SPRT.
Assess the ability of the device to detect a deficit and any recovery after unilateral cortical stroke in adult rats.

Chapter 2

Pellet characteristics and Reach Assessment

2.1 Introduction

In this investigation, we will examine the height, diameter and integrity of the 45mg sucrose pellets so that we may understand the pellet characteristics when designing the dispensing component of the automated in-cage solution. We will also examine the reaching capabilities of adult rats to determine the appropriate pellet placement capabilities of the automated device.

2.2 Pellet Characteristics

A previous study by (Metz and Whishaw, 2000) has shown that rats displayed optimal reaching success rates with pellet sizes of 20mg, 45mg, 75mg, 94mg, 190mg and 300mg. Based on olfactory pellet location studies (Metz et al., 2000; Metz and Whishaw, 2013) and common pellet usage across a variety of other studies (Whishaw, 1989) as well as current availability and usage within the Wolfson Centre for Age-Related Diseases (CARD), the 45mg TestDiet™ sucrose pellet (supplied by Sandown Scientific) depicted in Figure 2.1 was chosen as the reward to be dispensed. An alternative 45mg pellet product, which is commonly used in studies, is the Bio-Serv Dustless Precision Pellet. These pellets are not spherical but instead have a cylindrical height and diameter, with rounded ends (Figure 2.1). Pellets break during manufacturing, storage, transport or dispensing (Figure 2.2) and therefore, to facilitate the efficient design of the dispensing mechanism we first needed to quantify the pellet dimensions and the variations therein. This information will allow us to develop the following:

1. A pellet reservoir with sufficient capacity for two days of operation. (at least 200 pellets: 50 trials per day per rat and 2 rats per cage)
2. Pellet separation and de-stacking mechanisms to allow the isolation of a single (ideally unbroken) pellet.
3. Facilities to resolve jamming due to damaged or irregularly shaped pellets.

2.3 Reach and acclimation assessment

Animal-device and animal-pellet acclimation is an important variable that needs to be considered to design the training and acclimation algorithms for the device more efficiently. The standard operating procedure (Whishaw et al., 2008c), involves placing pellets into the rat's home cage so that they become familiar with the pellets (Bar-Yona et al., 1994). The second step involves the rats being placed into the experimental

apparatus, so they familiarise themselves with the environment. We will refer to these processes as ‘Acclimation’. We need to determine if the pellet dispenser needs to follow the same protocol of dispensing pellets into the cage, or may we adjust the protocol to present pellets at the slit and provide sufficient time for rats to find the presented pellets. Understanding how far the rat can reach beyond the slit will give us an indication of where the pellets need to be positioned during the task.

With this study, we aim to obtain acclimation and reach information for adult male and female Lister hooded rats.

In this study, we aim to answer the following questions:

a. How long does it take for the animals to acclimate to and start consuming the sucrose pellets?
b. Is food restriction sufficient motivation to ensure rapid acclimation?
c. How far can the rats reach through the slit to obtain sucrose pellets?

The results of this investigation will assist in the design and implementation of the appropriate acclimation protocols and pellet positioning facilities within the automated in-cage dispenser.

Before the design of the acclimation study a short investigation was run to determine how best to approach a longer-term investigation. Two naïve adult male Lister Hooded rats were placed in a standard pellet reaching apparatus (Figure 1.3a) and introduced to 45mg sucrose pellets both inside the apparatus on the floor and on the shelf. Each rat had access to water and food ad-libitum prior to being placed in the testing apparatus. Consumption of the first pellet was observed almost immediately inside the apparatus and within 8 minutes from the shelf for both rats. This rapid consumption was a sufficient basis for design of an experiment to test the unattended in-cage acclimation requirements of the animals.

2.4 Methods and materials

2.4.1 Pellet characteristics

A random sample of one hundred 45mg sucrose pellets was obtained from within a new 1.8kg container of TestDiet™ pellets purchased from Sandown Scientific. Pellet diameter and height measurements has been achieved with a digital calliper (DURATOOL; Resolution 0.1mm, Accuracy 0.2mm). Pellets were assessed for damage by approximating the percentage of the pellet that was missing as depicted in Figure 2.2.

a.	b.
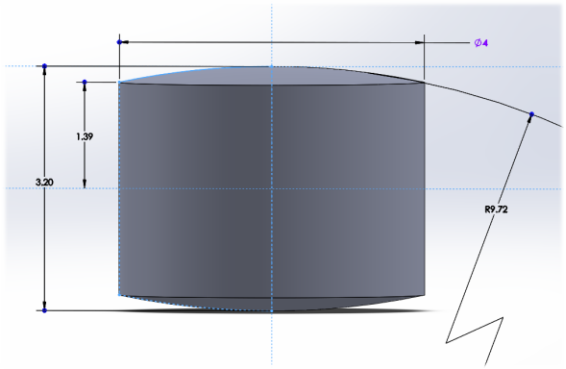	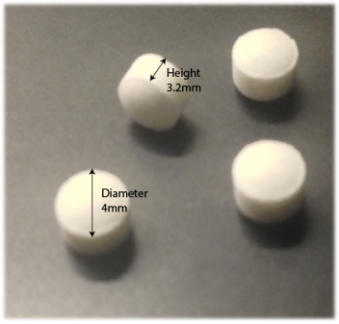

Figure 2.1 - Dimensions of the 45mg TestDiet sucrose pellet.

1. Dimensioned 3D model of a TestDiet™ 45mg sucrose pellet.
2. 45mg sucrose pellet, 4mm in diameter and 3.2mm height.

a.	b.	c.	d.
	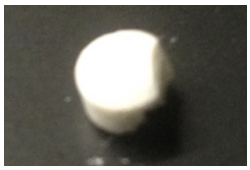		
0%	20%	40%	50%

Figure 2.2 - Pellet damage assessed as a percentage of the amount of pellet that is missing.

(a-d) Estimated damage as a percentage of the amount of the pellet that is missing.

2.4.2 Reach and Acclimation

Three adult male (420-460g) and three adult female (220-240g) Lister Hooded rats (sourced from Charles River UK) were injected with Radio Frequency Identification (RFID) tags (*Figure 2.3*a) in the scruff behind the neck (*Figure 2.3*b) while under anaesthesia (Induced with O_2 at 1L/min containing 5% Isoflurane and maintained at 2% Isoflurane for the duration of the procedure) a week prior to the study under sterile conditions. Analgesia (Carprieve 20:1 2.5ml/kg) was given post-surgery to prevent any postoperative discomfort. Animals were placed in an incubator at 34 °C until conscious and then returned to their cage.

A box shown in *Figure 2.4* was designed and fabricated out of 5mm-thick clear acrylic to be placed inside the rat's cage. An enclosed shelf with a magnetically attached, removable cover was designed so that pellets may be loaded, photographed or removed as required during the study. In an attempt to prevent dragging of the pellet through the opening as seen in post-stroke animals (Whishaw et al., 2008b) a 3mm diameter plastic bar was glued in place (*Figure 2.4*b) with the expectation that a grasp is required to lift the pellet over the obstacle. This however may not completely prevent dragging to the bar and retrieving the pellets using the tongue.

a.	b.
	

Figure 2.3 - RFID tag size comparison and implant location overview

a. Comparative scale reference of an RFID tag with a US Quarter.
b. Dorsal and side view of the RFID tag Implant location
(image: popsci.com)

Animals were assigned to two groups as shown in Table 2.1, housed singly and the amount of food was restricted overnight to 13g standard chow per animal. Water was provided ad libitum for the duration of the study and food was provided ad libitum during the day cycle. The boxes remained in the same cage for the length of the study.

Box	Group	RFID tag number	Gender	Pellets on shelf (g)	Pellets scattered (g)
1	1	050 563 560	F	7	0
2	1	050 576 626	F	7	0
3	2	050 598 320	F	6.1	0.9
4	1	050 619 333	M	7	0
5	2	050 574 315	M	6.1	0.9
6	2	050 678 291	M	6.1	0.9

Table 2.1 - Acclimation study animal grouping, gender and pellet distribution.

Group 1 - 7g of pellets arranged on the pellet shelf only. Two females and one male Lister hooded rats.
Group 2 - 0.9g of pellets scattered randomly inside the acclimation box in addition to 6.1g being arranged on the pellet shelf. This was done to provide extra motivation to consume the pellets. There were two males and one female Lister hooded rats in each group.

The boxes were prepared with a total of 7g of 45mg sucrose pellets between 15:30 and 16:30 daily using the pellet distribution specified in Table 2.1,. Pellets were arranged on the shelf and scattered inside as depicted in *Figure 2.5*. Group 1 had access to pellets placed on the shelf only. Group 2 had access to pellets present on the shelf as well as scattered inside the acclimation box. Pellets were scattered inside the acclimation box to determine if this added encouragement facilitated faster acclimation. Once the boxes were placed inside the rat cage, the food restriction of 13g per animal was put in place.

a.	b.
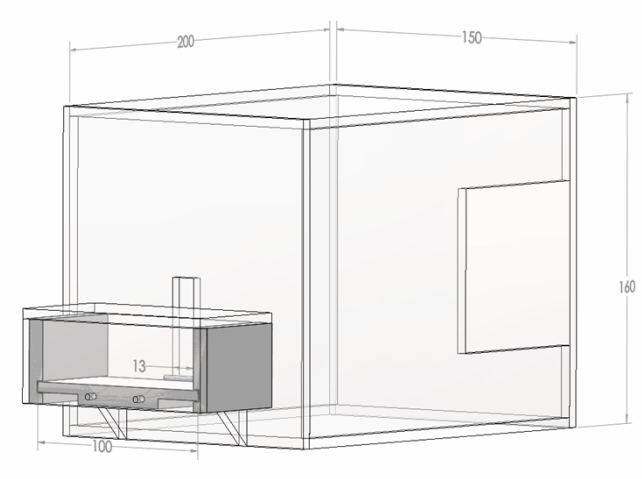	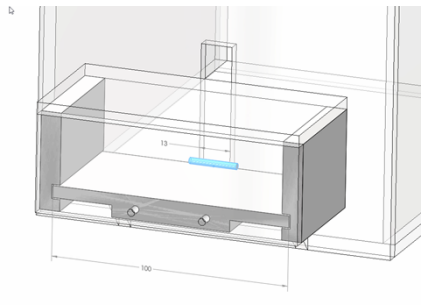
	c.
	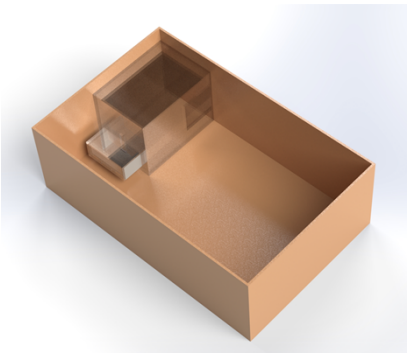

Figure 2.4 - Dimensional overview of the acclimation box and in-cage location.

a. Isometric dimensioned view of an acrylic box (150x200x160mm) used to test pellet acclimation and consumption.
b. Pellet shelf (100mm wide) with a mechanism to prevent the rat from sliding the pellet through the opening.
c. A model of the acclimation box placed inside of a rat cage to indicate a small footprint.

The animals could consume the sucrose pellets at their own free will and the boxes were left in-cage overnight. The food restriction was lifted two weeks into the experiment to investigate its effects on pellet consumption.

a.	b.
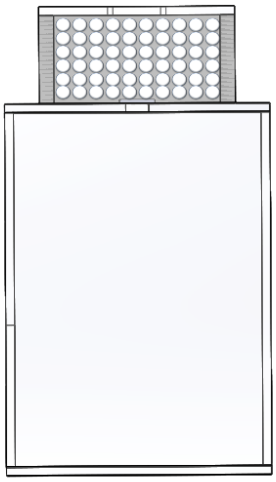	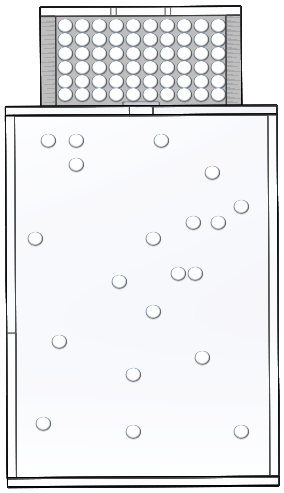

Figure 2.5 - Pellet distribution within the acclimation box.

a. Arrangement of 7g of 45mg sucrose pellets on the shelf of the box only.
b. In box distribution of 0.9g of sucrose pellets in addition to 6.1g of pellets on the shelf.

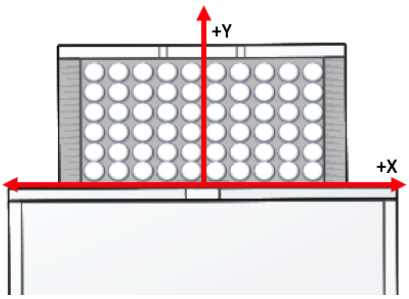

Figure 2.6 - The coordinate system used during maximum reach measurement.

The Cartesian coordinate system used to record pellet locations on the shelf. The (0,0) position at the outside centre of the 11mm wide slit is located at Cartesian origin depicted above.

Mondays were setup days and marked the start of the experiment for that week. Pellet consumption data was acquired between Tuesday and Friday. Rats were weighed from Monday to Friday. The study was not run over Saturday and Sunday, but the acclimation boxes remained in cage during that period.

Photographs of the shelves were taken (iPhone 5 at 5-megapixel resolution) the following morning between 9:30am and 10:30am such that the region of interest was the full height and width of the shelf. All remaining pellets were collected and weighed. Shelf photographs were cropped and straightened (using the edge of the shelf cover as a reference) using Adobe Photoshop CS5. Throughout the study, all pellets scattered inside relevant acclimation boxes were consumed so no pictures were obtained for the insides of the boxes. Results were analysed using Prism 7 (Graphpad) to perform a two way repeated measures ANOVA.

With the aid of a bespoke image analysis application (*Figure 2.7*a) that was developed using VS2012 C# .Net 4.5, the reach of the individual animals was calculated. The application allows the user to specify the slit point (origin) on the image as well as the locations of pellets closest to the slit. It is then assumed that the animals did not consume the remainder of the pellets because these were out of reach. For instances where all pellets were consumed along the lateral edge of the shelf, an assumption was made about the location of the furthest consumed pellet (phantom pellet). Locations were marked approximately one pellet diameter (4mm) apart as depicted in *Figure 2.7*b. The application normalized the images based on the known slit width and calculated the XY coordinates of each marked point. The data was then exported as a Comma Separated

Variable (CSV) file for analysis. Pellet locations were recorded based on the Cartesian coordinate system (*Figure 2.6*).

a.	b.
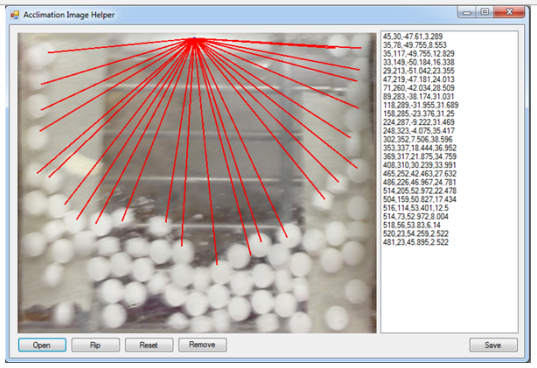	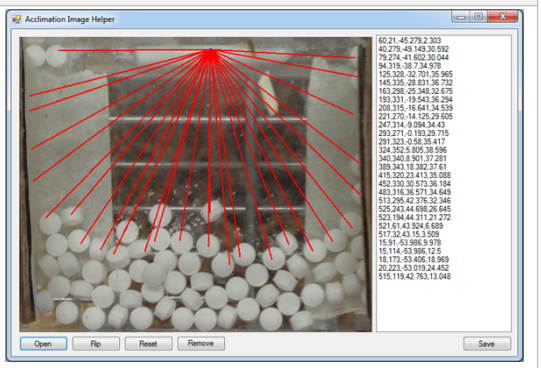

Figure 2.7 - Reach analysis using a bespoke image processing application.

A bespoke analysis assistant application was developed in VS2012, C# and allows the user to interactively map the location of the pellets with respect to the slit.

a. Partial pellet consumption mapped via the application.
b. Maximum shelf consumption pattern with phantom pellet locations. Phantom pellet locations are locations in which pellets no longer exist due to the device boundaries being within the maximum reach of the animal. These phantom positions were marked as an indicator of the animal's maximum reach.

2.5 Results and discussion

2.5.1 Pellet Characteristics

In our test sample, we found an average height of 3.14mm with a minimum of 2.4mm and a maximum of 3.3mm with a standard deviation of 0.16mm (Figure 2.8a). Diameters averaged 3.91mm with a minimum of 3.9mm and a maximum of 4mm with a standard deviation of 0.03mm (Figure 2.8b). These size characteristics will assist us in later design studies relating to the design of the reservoir, dispensing and pellet delivery mechanisms.

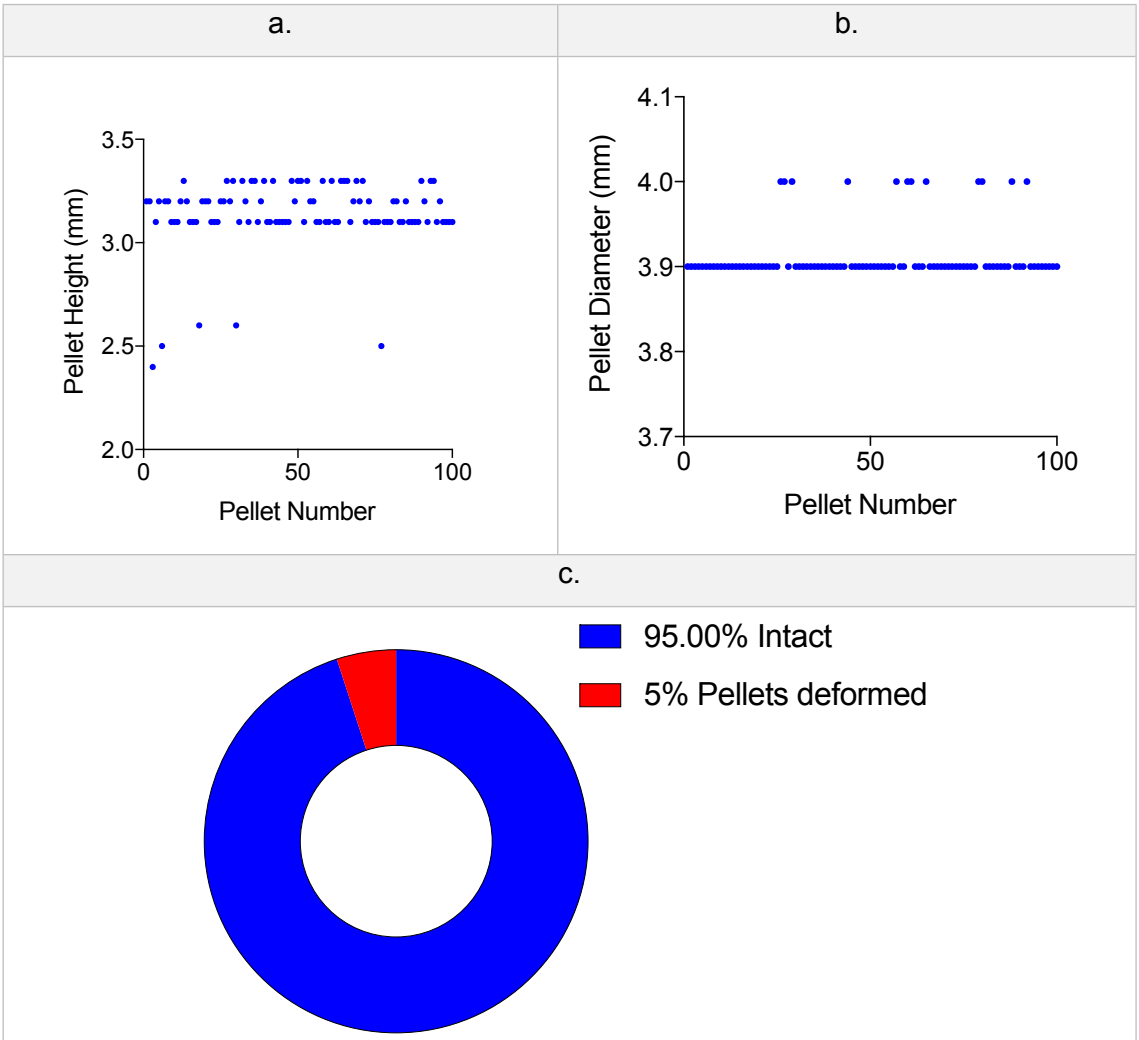

Figure 2.8 - Pellet height, diameter and deformation characteristics.

a. Analysis indicates a height range of 2.5→3.2mm for the current sample. Standard Deviation: 0.16mm.
b. Pellet diameter analysis indicates a diameter range of 3.9→4.0mm. Standard Deviation: 0.03mm.
c. Pellet deformation. 95% of the pellets tested were intact.

A 5% (Figure 2.8c) deformation rate was observed which indicates that jamming may be a potential obstacle to overcome when designing the reservoir and dispenser. From these results, we can conclude that the device must be able to resolve or detect jamming and allow the user to unjam the device quickly and easily, preferably without the use of tools.

2.5.2 Reach and Acclimation

Animals showed interest in the pellets from day one (day zero being setup day) with all pellets scattered inside the boxes being consumed. Pellets were consumed from shelves from day one in boxes 2, 3 and 6 as shown in *Figure 2.9*. From day 4 onwards the reach patterns remained similar as shown in the consumption data in *Figure 2.10*. The rats began consuming pellets from day 1 indicating a short acclimation phase is possible. Pellet consumption plateaued from day 4 at 51% (*Figure 2.11*). There was no observable variation between groups (*Figure 2.11*a; two way repeated measures ANOVA; n=6, $F_{1,4}$=0.2227, p=0.662) or between genders (*Figure 2.11*b; two way repeated measures ANOVA; n=6, $F_{1,4}$=1.712, p=0.261). This allows for the design of training and execution schedules without extended acclimation and to adopt a 'shelf-only' approach whereby pellets are introduced only via the automated dispenser. Based on this evidence, there is no need to sprinkle pellets into the cages.

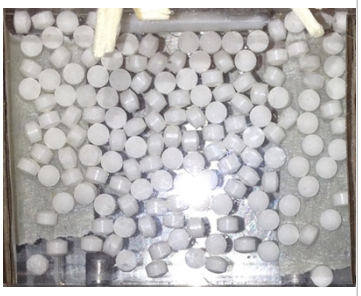

Box 1

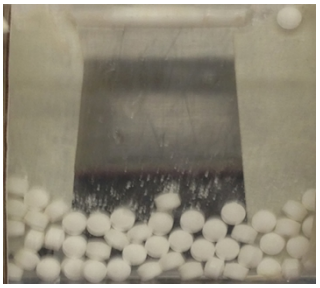

Box 2

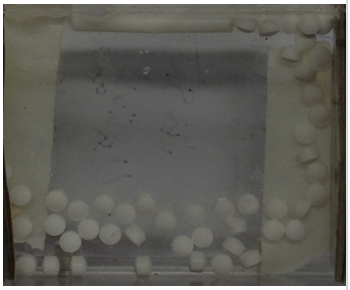

Box 3

Box 4

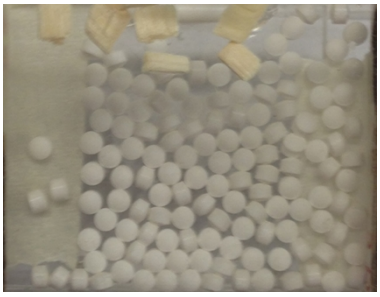

Box 5

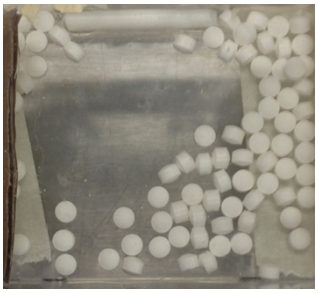

Box 6

Figure 2.9 - Day 1 images of shelves before pellet clean up.

Rats could grasp pellets from the slit (shown on the top side of the image)
Images from Boxes 1, 4, 5 show that the respective rats did not retrieve any pellets from shelves. Boxes 2,3,6 show that many pellets were retrieved from the shelves. The absence of pellets inside the acclimation box or the cage indicates that the rats consumed the pellets.

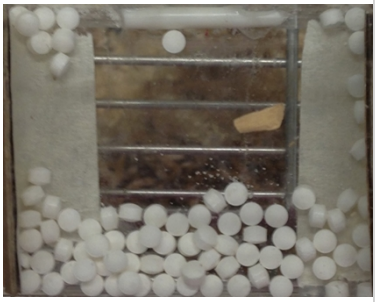

Box 1

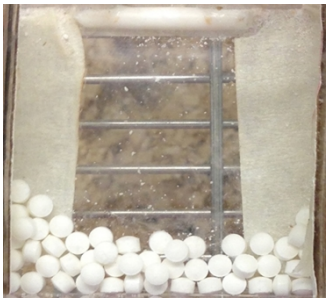

Box 2

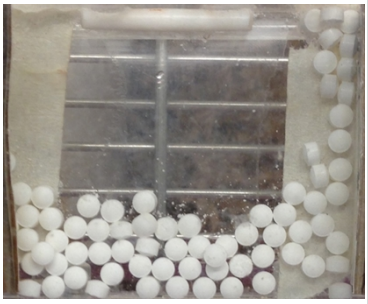

Box 3

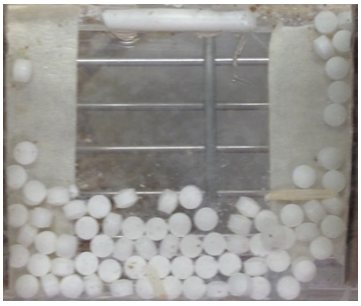

Box 4

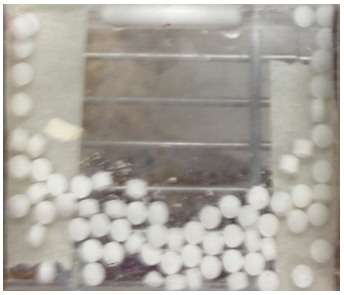

Box 5

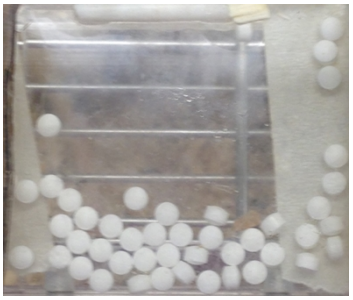

Box 6

Figure 2.10 - Day 4: images of shelves.

Rats could grasp pellets through the slit (shown on the top side of the image).
Rats in all six cages were consuming pellets from the shelf by day 4.

a.

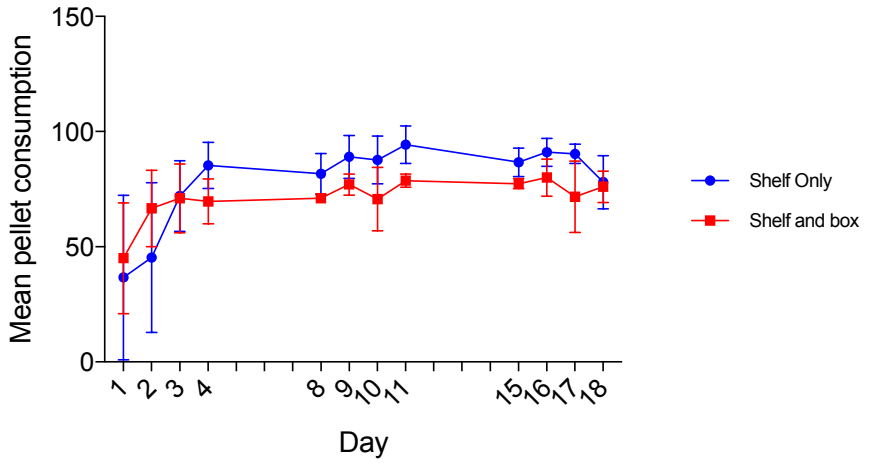

b.

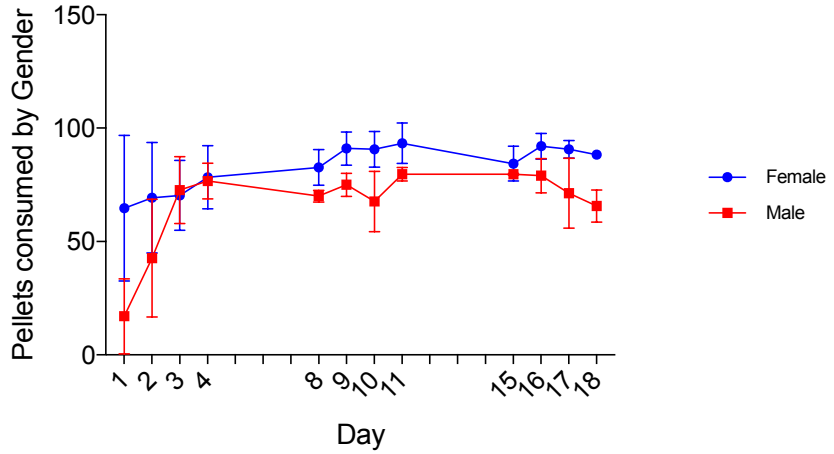

Figure 2.11 - Pellet consumption of rats grouped by pellet dispersion and gender.

a. There was no interaction between group and time ($F_{11,44}$=0.6487, p=0.777). There was no overall difference between the groups ($F_{1,4}$=0.2227, p=0.662). There was an overall effect of time ($F_{11,44}$=3.292, p=0.0023).
b. There was no interaction between group and time ($F_{11,44}$=0.835, p=0.607). There was no overall difference between the groups ($F_{1,4}$=1.712, p=0.261). There was an overall effect of time ($F_{11,44}$=3.42, p=0.0017)

n=6

Error bars indicate ±SEM.

F, p-values calculated using two way repeated-measures ANOVA

The result of the reach analysis (*Figure 2.7*,*Figure 2.12*) indicates that the rats are capable of reaching approximately 40mm in the Y direction and approximately 30mm in the ±X direction through an 11mm slit. As reported with the consumption data, no observable difference in X reach was observed between gender groups (*Figure 2.12*a; repeated-measures ANOVA; n=6, $F_{1,4}$=0.247, p=0.645), similarly, there was no observable difference between gender groups (*Figure 2.12*b; repeated-measures ANOVA; n=6, $F_{1,4}$=0.935, p=0.388) for reach in the Y direction.

a.

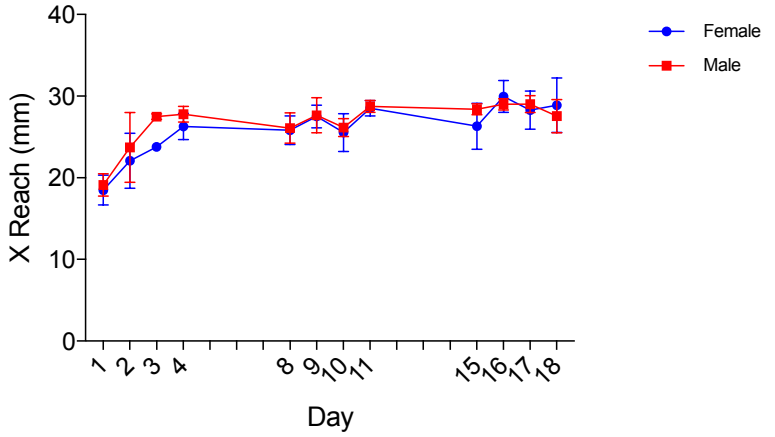

b.

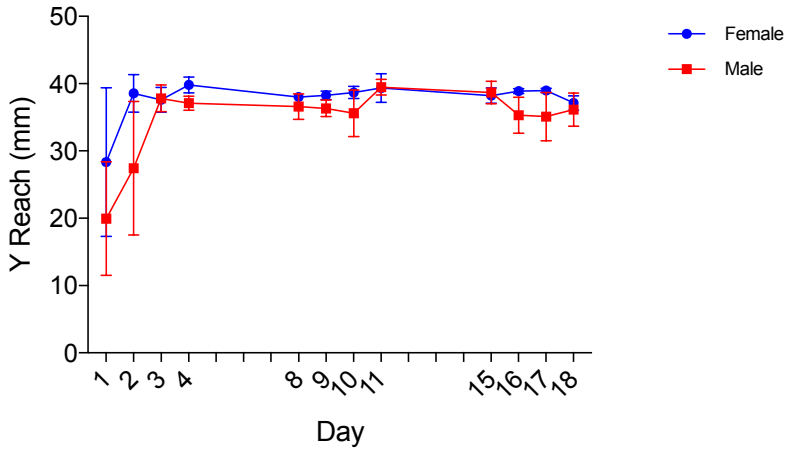

Figure 2.12 - Overall maximum reach results in the X and Y directions past the slit.

The X (Lateral) & Y (Longitudinal) reach of the rats were measured based on furthest reached pellet on the shelf.

a. A maximum average reach of approximately 30mm was recorded in the positive and negative X axis, with no observable difference between gender (repeated-measures ANOVA; n=6, $F_{1,4}$=0.247, p=0.645).
b. A maximum average Y reach of approximately 40mm was recorded with no difference between gender (repeated-measures ANOVA; n=6, $F_{1,4}$=0.935, p=0.388).

Error bars indicate ±SEM.

Weight information shown in *Figure 2.13* revealed no noticeable weight loss over the two weeks (day 0-11) during which nightly food restrictions were in place. This will lead the path for longer experimental studies (with nightly food restrictions if required) later in the project. It was also evident that when the food restriction was lifted, there was no change in the average pellet consumption by the animals. This leads us to believe that the food restriction may not be a necessary form of motivation, at least in the later phases of the experiment. In future, we may determine whether food restriction can be omitted altogether.

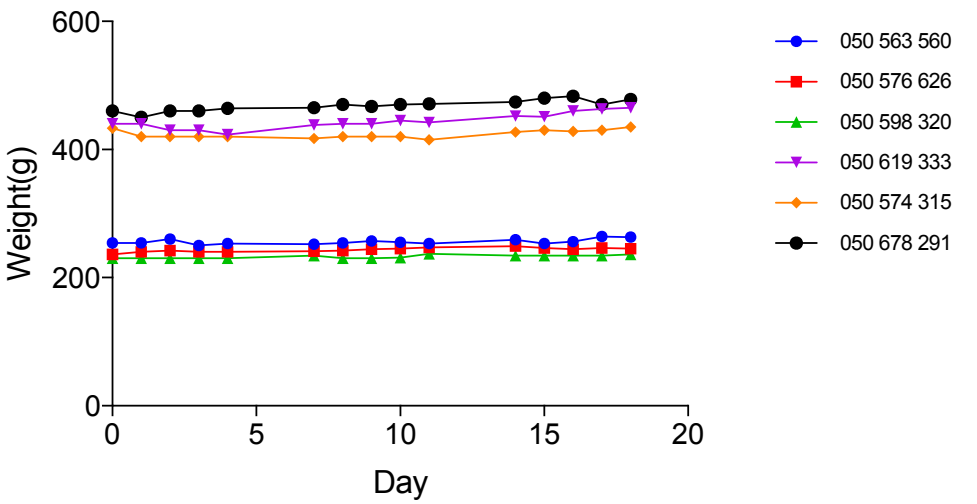

Figure 2.13 - Animal weight captured over the duration of the study.

No weight loss observed during the course of the study. Animals were food restricted overnight during week 1 and 2 (Day 0-11). Food restrictions were lifted for the 3rd week (Day 12-18) of the study. Series show RFID tag number for each rat.

There was no observable difference between male and female Lister Hooded rats in both reach capability and pellet consumption. This allows for the use of either gender in future studies as it may less likely affect the outcome. However, we have decided that for the sake of consistency and size characteristics (females being smaller), that all future studies will include the use of female Lister Hooded rats only. Further, group housing will be maintained moving forward to ensure that isolation does not affect performance (Einon, 2007). It was also observed that the extra sprinkling of the pellets into the cage did not affect the consumption or reach data. This would imply that this pellet-sprinkling

acclimation step may not be required during the acclimation phase and that we may fully automate the acclimation using an automated device.

Chapter 3

RatBot™ mechanical design and fabrication

3.1 Introduction

The primary objective of this PhD is to develop a device capable of automating the single pellet reaching task (SPRT). The first phase of this development process involves the mechanical design of the dispenser and pellet positioning mechanisms. To accomplish this, functional objectives and targets were first defined. This was followed by an iterative development cycle of design → test → iterate. As part of this process, multiple device variants (Appendix A, Appendix B) were developed using various pellet dispensing and delivery mechanisms. In this section the final version (v99) of the device will be described and discussed.

3.1.1 High level device objectives

1. Dispense a 45mg sucrose pellet to a programmable location.
2. Determine if a rat has successfully consumed or dropped the pellet.
3. The overall footprint of the device should be sufficiently small such that it fits inside a large rat cage (Techniplast 1354G) and allows for a total floor area of 250cm^2 per rat (250-350g) as per the minimum space requirements as defined in the 2010 European Union Directive 2010/63/EU and Section 21(5) of the Animals (Scientific Procedures) Act 1986 (Table 3.1). Note that from 2017, this requirement increases to 250cm^2 per rat up to 300g (Table 3.2)
4. The rat executing the task must be uniquely identifiable allowing multiple rats to be housed in the same cage.
5. The daily maintenance required should be minimal and kept under 10 minutes per cage.
6. The device must be capable of unattended overnight operation, 7 days a week.
7. The dispenser should be designed to reduce pellet grinding and jamming.
8. Safety is paramount to in cage operation of the device so this must be a key design requirement for both the operator and the animals involved.

Weight of Animal (g)	Minimum floor area for one or more rats (cm^2)	Minimum floor area per group house animal (cm^2)	Minimum Cage Height (cm)
<50	500	100	18
50-150	500	150	18
150-250	500	200	18
250-350	700	250	20
350-450	700	300	20
450-550	700	350	20
>500	800	400	20

Table 3.1 - Code of Practice for the Housing and Care of Animals Bred, Supplied or Used for Scientific Purposes - (Table 1-2-6) valid up to 2016.

Rows highlighted in green indicate the weight range of animals used in studies described herein.

Weight of Animal (g)	Minimum floor area for one or more rats (cm^2)	Minimum floor area per group house animal (cm^2)	Minimum Cage Height (cm)
<200	800	200	18
200-250	800	250	18
250-300	800	250	20
300-400	800	350	20
400-600	800	450	20
>600	1500	600	20

Table 3.2 - Code of Practice for the Housing and Care of Animals Bred, Supplied or Used for Scientific Purposes - (Table 2-2-8) valid from 2017.

Rows highlighted in green indicate the weight range of animals used in studies described herein.

3.2 Methods

The device development was an iterative process, which resulted in multiple variants (Appendix A - CAD, Appendix B) totalling 99 iterations. Each iteration comprised of a set of mechanical design changes to the device based on issues discovered during each study and other offline testing. Similar design and fabrication methods were used across versions and iterations. To protect intellectual property and patentability of the device, where possible, the fabrication was done in-house or in an ambiguous fashion with a variety of suppliers i.e. component suppliers and custom fabricators were not privy to the intended use or greater function of the supplied goods.

Designs were created using Computer Aided Design (CAD) software Solidworks™ (2013-2017) by Dassault Systems. Plastic components were fabricated out of Polylacticacid (PLA) using a MakerBot 2 Replicator 3D Printer. Metal components were machined on a Clarke CL300 Metal Lathe and a Computer Numeric Controlled (CNC) Router. Final designs were 3D Printed by Shapeways.com, a 3D printing service. Device enclosures were fabricated using acrylic bonding techniques. A bill of materials and list of suppliers are contained in BOM.xls, in the attached DVD (Appendix A - CAD)

3.3 Results and Discussion

In this section, the latest version of the RatBot™, its various components and operation will be discussed. A history of all device versions and iterations have been included in the attached DVD (Appendix A - CAD). Key versions of the device are presented in Appendix B to demonstrate the design progression.

3.3.1 High-level operational overview

The RatBot (Figure 3.1, Figure 3.2, Figure 3.3), which fits inside a large rodent cage (Figure 3.5) dispenses a 45mg sucrose pellet from a pellet reservoir onto a spoon (Figure 3.8). The spoon then moves the pellet to a programmable location in the XY reach space of the rat (Figure 3.13). The rat may attempt to retrieve the pellet from this position by reaching through an 11mm wide slit (Figure 3.2-2, Figure 3.3-4). The pellet is programmatically positioned either to the left or the right of the slit such that the rat is required to use the contralateral forepaw to reach for the pellet.

The chute sensor (Figure 3.6) provides the ability to detect a successful pellet dispense from the pellet reservoir. Reach, drop and proximity sensors (Figure 3.3) provide pellet consumption feedback indicating whether the rat has removed the pellet from the spoon or if the pellet has fallen into the drop box (Figure 3.26). The Radio Frequency Identification (RFID) tag of the rat (Figure 3.1) is read by an RFID reader (located in the archway above the slit) and stored in a database with the result of the trial.

The RatBot is designed to be sufficiently small enough to be placed inside a large cage (Figure 3.5) and is connected to a private network (Figure 3.7). Power and data communications is achieved using Power over Ethernet (PoE) transmission technology reducing the overall infrastructure and cabling requirements of the system to just one Ethernet cable per device. The RatBot is controlled by custom designed electronics and a Raspberry PI 2.

3.3.2 The RatBot enclosure

The core electromechanical components of the RatBot is housed within a 200mm(d) x 175mm (h) x 180mm(w) box (Figure 3.1) fabricated using 5mm clear acrylic. The enclosure is elevated 20mm on 4 feet to allow for a bottom mounted pellet drop box to capture and store dropped pellets. When placed inside a large Techniplast 1354g cage (Figure 3.5) the top of the enclosure is accessible to the rat allowing the area of the device to contribute an overall available ‘floor space’ of 2020cm^2 (Figure 3.5). This allows

for up to 8 rats to be housed in the same cage (Home Office, 2014). The enclosure is connected to the control electronics that resides outside of the cage with a concealed 30-way ribbon cable that is outside of the reach of the rat.

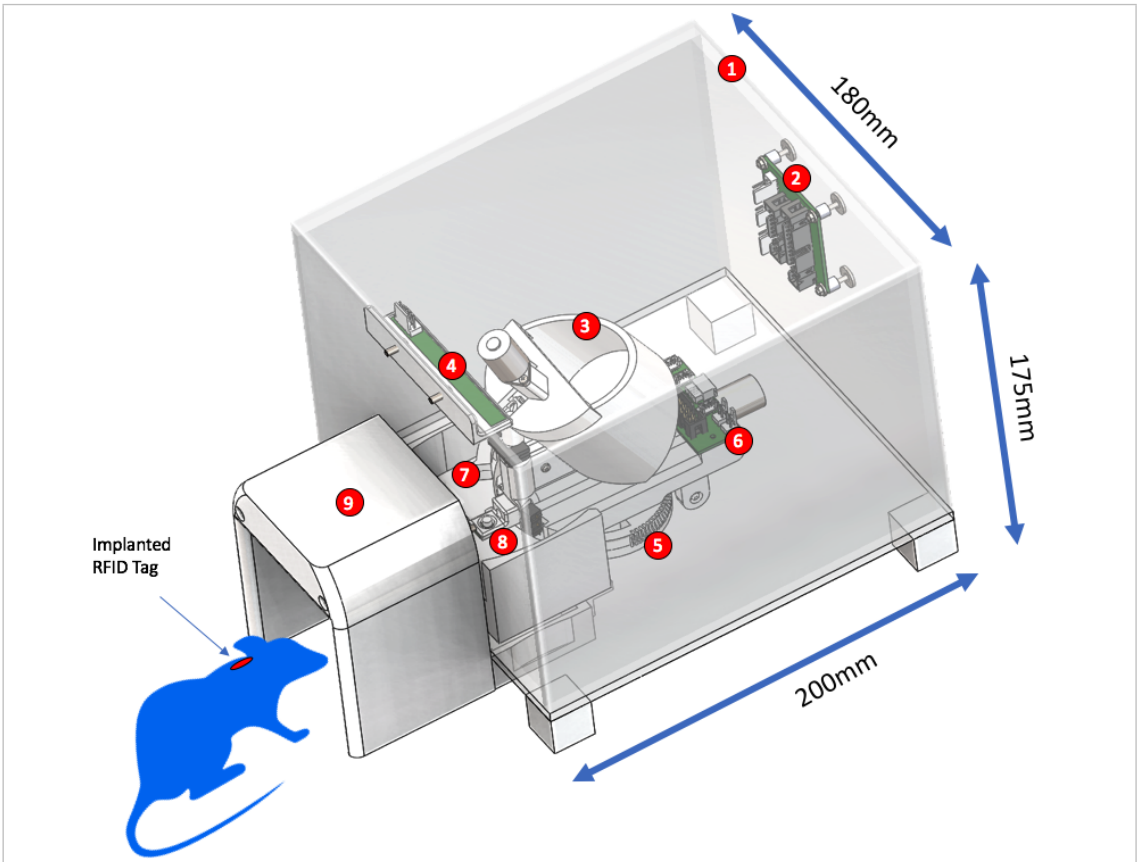

Figure 3.1 - Left orthogonal overview of a RatBot 3D CAD rendering. (Iteration 99)

1. Acrylic enclosure to allow for maximum visibility during testing.
2. Inside distribution board facilitates easily replacing internal and or external hardware without replacing all wire looms.
3. A pellet reservoir with a capacity for 1000 45mg sucrose pellets.
4. LED warm light array to provide an artificial light source during trial execution to reduce the effect of the lack of pellet visibility.
5. Rotational base to allow for worm gear driven positioning of the spoon.
6. Local adapter board allowing easy replacing of motors and removal of the device without the need to remove all wire looms.
7. Cleaning station containing a brush used to automatically clean the spoon between trials.
8. The Spoon which presents a 45mg sucrose pellet in front of the rat at a programmable location. The spoon is embedded with a proximity sensor to detect the presence or removal of a pellet.
9. RFID tunnel in which an RFID sensor reads the implanted identification tag of the rat that is executing the task. This information is associated with the trial result.

The rat may approach the 11mm wide slit from the front of the device through a tunnel (Figure 3.2) 70mm(w) x 80mm(h). The tunnel contains an embedded 134.2khz RFID reader (Priority1Designs Model: RFIDREAD-mRW-134) capable of reading the 134.2khz FDX-B RFID tag that was implanted subcutaneously into the rat (*Figure 2.3*). The slit contains an Omron through beam sensor that allows the embedded firmware to determine when the animal has begun interaction with the device. Rat interaction is defined as the movement of a limb, snout or tongue through the slit. This is not necessarily an indication of forelimb reaching. The slit sensor may also be used to identify when the slit is obstructed with bedding or other debris.

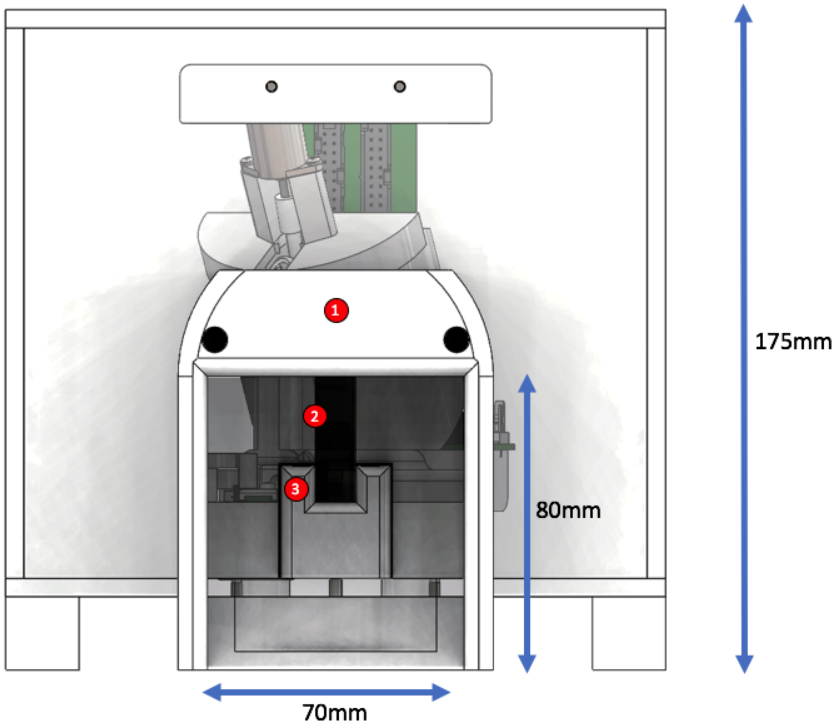

Figure 3.2 - Front view of a RatBot 3D CAD rendering.

1. An RFID (Priority1Designs 134.2khz FDX-B) reader is embedded within a tunnel which reads the implanted identification tag of the rat executing the task.
2. An 11mm wide slit through which the rat reaches for a 45mg sucrose pellet.
3. An Omron through beam sensor is embedded into the slit to record engagement of the rat. This may be in the form of a snout penetrating the slit during sniffing or licking of the pellet or the forelimb of the rat passing through the slit while reaching for a pellet.

A cleaning station (Figure 3.3-2), which contains a custom designed and manufactured brush (Figure 3.4), provides the device with the ability to clean the proximity sensor embedded into the spoon. The cleaning position serves two functions:

1. It prevents the accumulation of dust and dirt, which may obstruct the sensor and provide false positive results when detecting the presence of a pellet on the spoon, and
2. It is used to remove any pellets that are present on the spoon before or after a trial. This may be because of abrupt termination of a trial after the pellet was dispensed onto the spoon. Other scenarios where a pellet will be left on the spoon include trial timeouts where there is no interaction with the device over a pre-defined period, or when the maximum number of reach attempts allowed has been reached without either a successful grasp or drop.

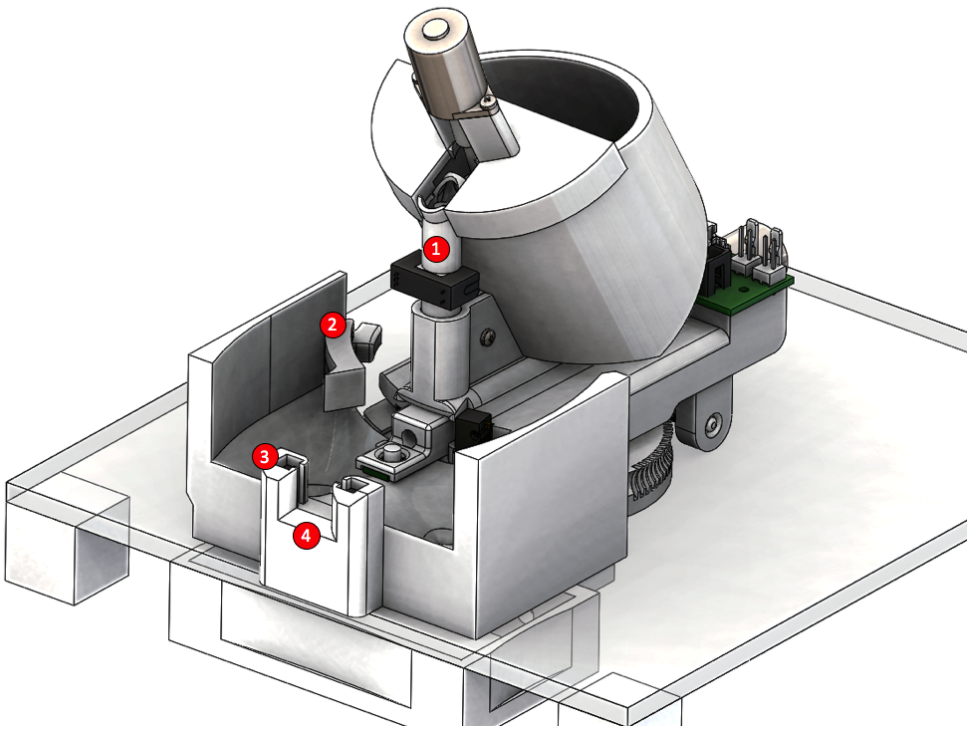

Figure 3.3 - Assembled device (omitting RFID tunnel and acrylic enclosure for clarity).

1. The pellet chute sensor used to detect the dispense of a pellet from the reservoir.
2. A cleaning station containing a brush used to clean the spoon from dust and debris as well as any pellets remaining on the spoon after the end of a reaching trial or abrupt termination of a trial operation.
3. A through beam slit sensor used to determine when the rat is interacting with the device.
4. An 11mm wide slit through which the rat reaches for the pellet.

a.	b.
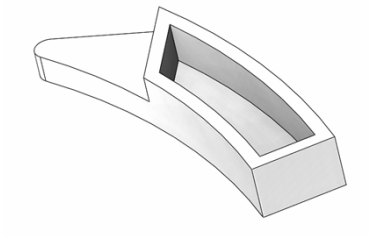	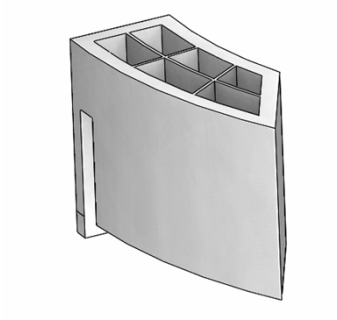
c.	d.
	

Figure 3.4 - The cleaning station brush assembly process.

a. A blank 3D printed brush without the bristles.
b. Bristle placement tool that allows for securing of the bristles during the assembly process.
c. Bristles assembly using the bristle placement tool. Bristles are glued to the holder.
d. The assembled, trimmed brush that will be installed into the cleaning station of the device.

a.

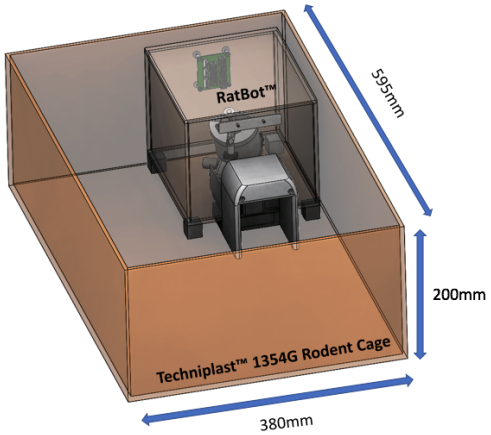

b.

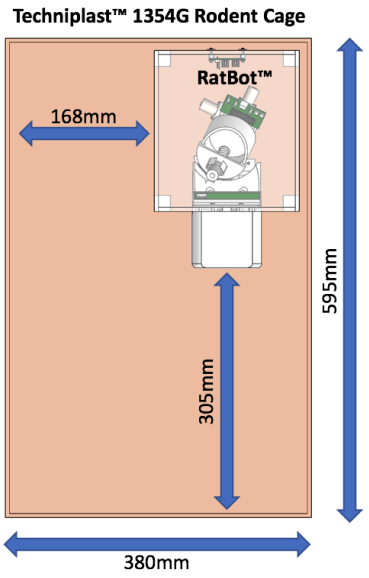

c.

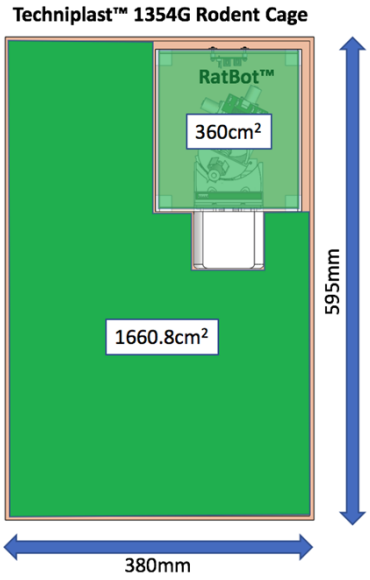

Figure 3.5 - Top view of the assembled device inside a large rodent cage highlighting the available floor space.

a. A representative rendering of the RatBot placed inside a Techniplast 1354G large rodent cage 380mm(w) x 200mm(h) x 595mm(d). The top of the RatBot is accessible to the rat as 'available floor space' and as a result, the Home office recommended area per animal is maintained (Home Office, 2014) Table 3.1,Table 3.2.

b. The RatBot is placed in the rear right corner of the cage.

c. The total remaining floor area is approximately 1660cm^2. The Top of the RatBot is accessible to the rats and may be included in the total area available bringing the total area available to 2020cm^2. This allows for a maximum of 8 rats up to 300g to be housed in this device configuration (Home Office, 2014).

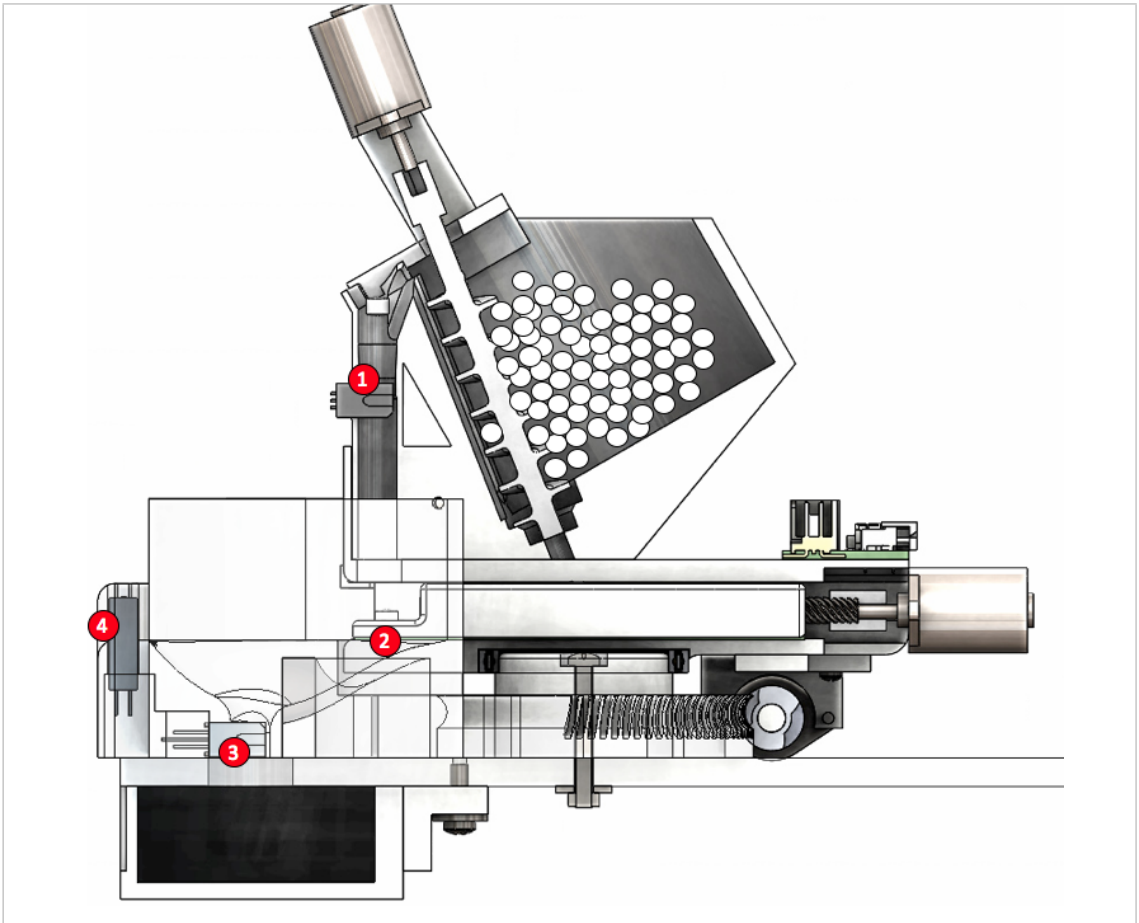

Figure 3.6 - RatBot sensor locations.

1. Chute sensor. A through beam sensor detects the passing of a pellet through the drop chute.
2. A proximity sensor (VCNL4000) embedded into the spoon detects the presence of a pellet on the spoon.
3. A pair of drop sensors detect pellets falling from the spoon and into the drop box.
4. Slit sensor. A through beam sensor detects if there is snout, tongue or reaching activity at the 11mm slit.

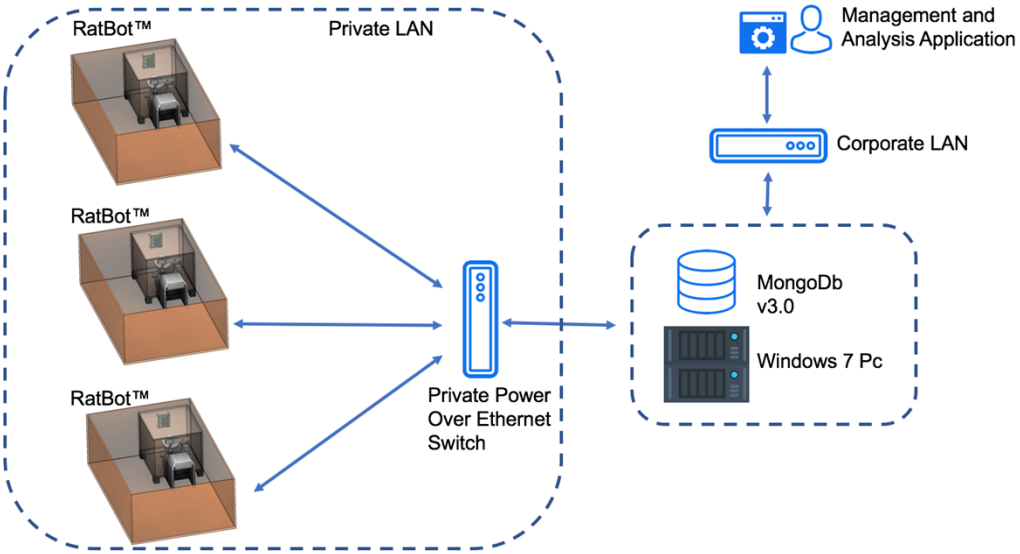

Figure 3.7 - RatBot high-level connectivity schematic.

An array of RatBots and a local PC connect are connected via a POE switch creating a private LAN. The PC serves as a DHCP server and database host (Mongo Db v3.0). The PC connects to the corporate LAN via a second Ethernet adapter, which allows the RatBot Management application to access device generated data, and to provide instructions to the device via the database. This configuration isolates the RatBot network from the main corporate network so that any interruption in the corporate network will not affect the operation of the RatBots.

3.3.3 The pellet dispenser

A pellet dispenser consisting of a pellet reservoir and a pellet feeding system has been designed (Figure 3.8) to store up to 1000 45 mg sucrose pellets. A bespoke auger (Figure 3.9) with 12mm diameter and 4mm pitch, was designed and fabricated to facilitate the movement of pellets up a pellet guide (Figure 3.11) as it is rotated counter clockwise (Figure 3.8 - 1). The auger is rotated using a 50:1 geared 18º/step bipolar stepper motor (Goot Motor - PG15S-020-01/50) which is attached via a keyed coupling (Figure 3.12). The motor is controlled by a low voltage stepper motor controller (Pololu DRV8344) attached to a Raspberry Pi 2 along with custom designed firmware described in section Chapter 4 and Chapter 5.

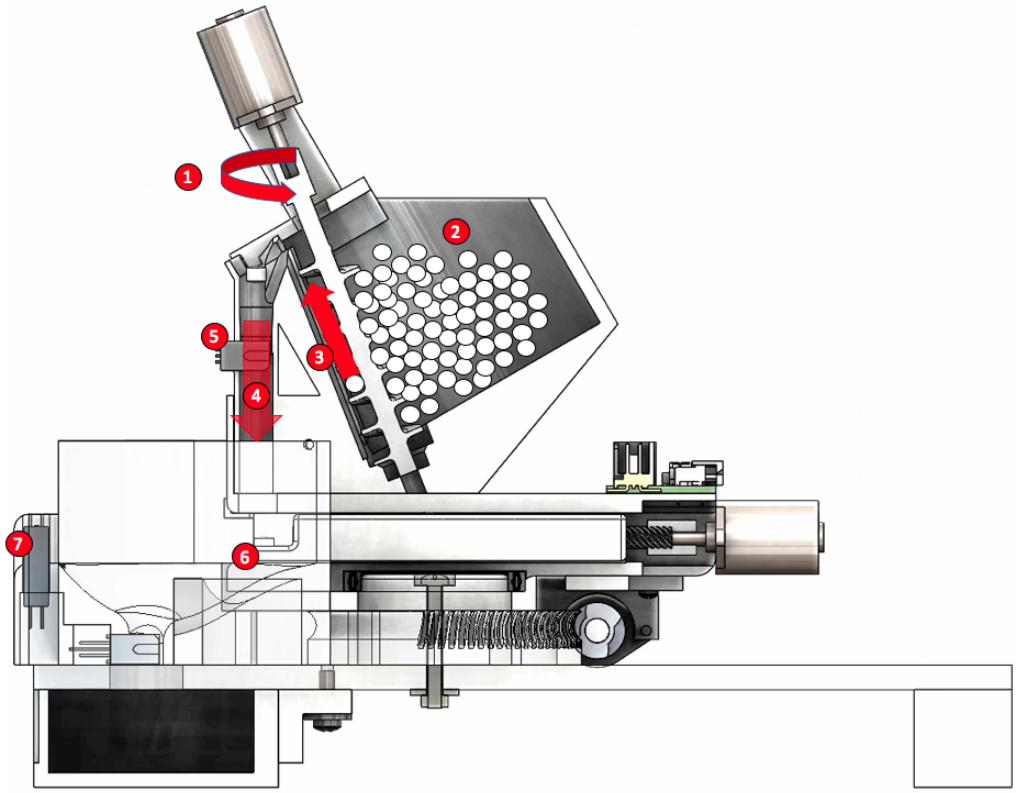

Figure 3.8 - Cross section of the RatBot showing the dispense route of the sucrose pellet.

1. The auger is rotated counter clockwise to facilitate the flow of pellets along a pellet guide as indicated in 3.
2. Pellet reservoir with a capacity to hold 1000 45mg sucrose pellets.
3. The direction in which the pellet moves when the auger is rotated counter clockwise.
4. The pellet drops down a drop chute and onto the spoon.
5. A through beam sensor to identify when a pellet falls through the chute, indicating a dispense has taken place.
6. The spoon with a pellet placed on top of the proximity sensor (VCNL4000).
7. The through beam sensor used to detect a reach, snout or tongue engagement by the rat.

An auger (Figure 3.9), in combination with pellet guidance features (Figure 3.11) designed into the reservoir, facilitates the upward flow of a single file of pellets from the reservoir and into the pellet chute, until one finally lands on the spoon (Figure 3.18) at which point the auger stops rotating.

Various auger designs with varying pitch and flight dimensions, as well as various materials were designed, fabricated and tested (Figure 3.10). The latest version of the

auger with a pitch of 4mm (Figure 3.9-a) and a flight of 1mm (Figure 3.9-b) was incorporated into the latest version of the device to facilitate the dispensing of 45mg sucrose pellets. Nylon was the material of choice as it was the smoothest of the 3D printed variants from the 3D printing service provider Shapeways.

a.	b.
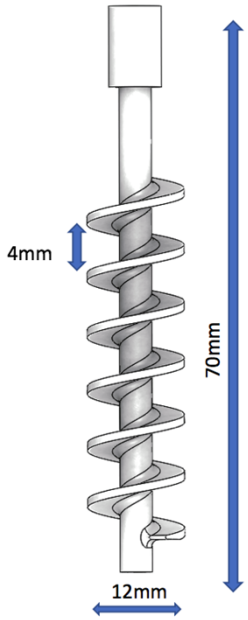	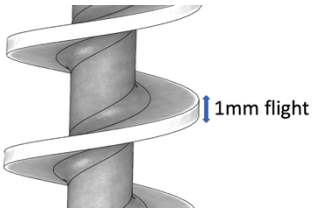

Figure 3.9 - The bespoke designed auger dimensions.

An auger (a) 70mm tall, 12mm diameter, 4mm pitch and 1mm flight (b) was designed to facilitate the flow of pellets from the reservoir to the spoon.

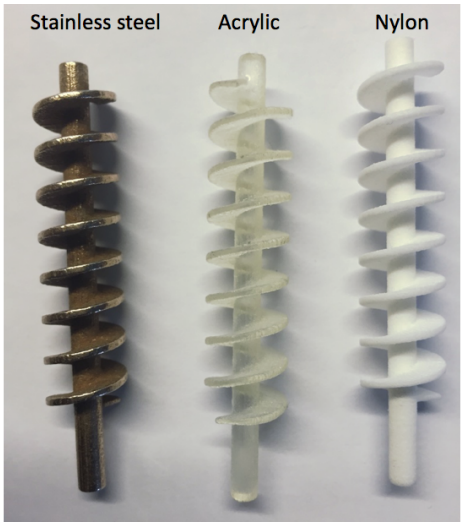

Figure 3.10 - Material variants of the auger printed by Shapeways.

Augers were fabricated out of stainless steel, acrylic and nylon by the 3D printing service, Shapeways. The Nylon variant provided the smoothest surface of the 3 materials and chosen to facilitate a smoother flow of pellets up the pellet guide. The choice was made to reduce the grinding of pellets and increase its efficiency of dispensing.

A pellet chute (Figure 3.11-3) guides pellets upwards and out of the reservoir. Since it may be possible for more than one pellet to move upwards in unison, a pellet redirection feature (Figure 3.11-2) was introduced to counteract this dual pellet flow occurrence and reduce the frequency of multiple pellets being dispensed onto the spoon at the same time.

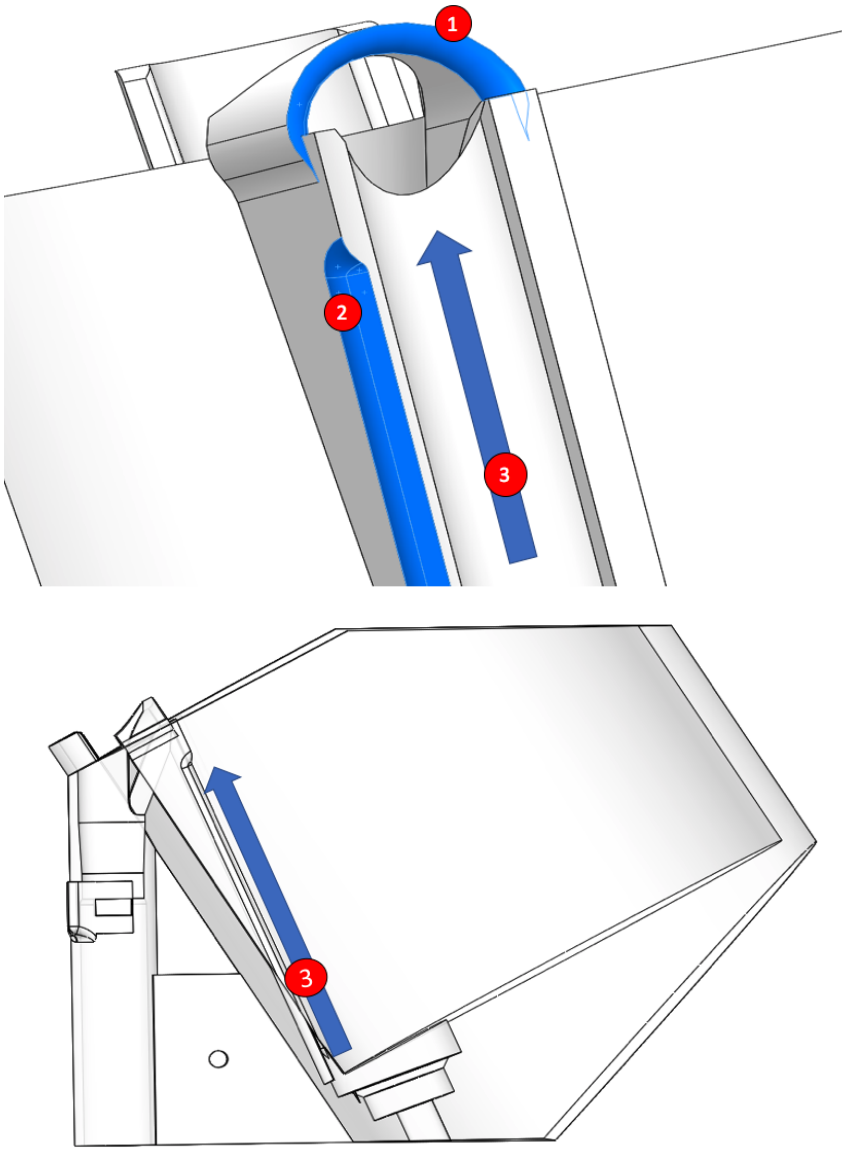

Figure 3.11 - A side view of the pellet reservoir indicating pellet guide features.

1. Pellet overflow protection. An arch ensures that pellets flow out of the reservoir in single file preventing the potential jamming of the pellet chute.
2. A pellet redirection feature directs pellets that are not in the pellet guide (3), to the side and back into the main reservoir
3. A pellet guide directs pellets upwards in combination with the rotational movement facilitated by the rotating auger.

a.	b.
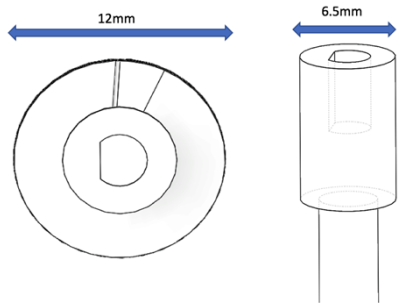	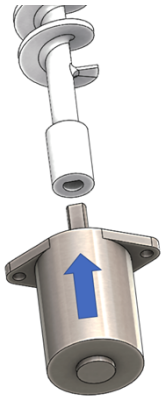

Figure 3.12 - The auger to motor coupling arrangement.

A keyed coupling (a) was designed into the shaft of the auger, which allows for easy connection between the stepper motor and the auger as shown in b.

3.3.4 Anti-jam dispensing action

To reduce pellet jamming due to the granular jamming phenomenon (To et al., 2001), an anti-jam movement inspired by vibrational un-jamming (Janda et al., 2009) has been implemented. This is accomplished by rotating the auger anticlockwise (1°) momentarily during the dispensing operation, which is normally a clockwise operation. This oscillatory motion introduces a vibration element to the dispensing and assists with releasing pellets that may have been jammed due to friction between the auger and the internal surface of the reservoir.

3.3.5 Pellet positioning

The RatBot can position a 45mg sucrose pellet within the Cartesian (X, Y) (Figure 3.13) reach space (25 x 60mm) of the Rat as determined in Chapter 2. Position (0,0) is the position of the pellet when closest to the slit. This position 15mm away from the rat approach hence providing an overall positioning capability of Y = 40mm (25+15mm) and X = +- 30mm. Future references in this text differentiates between positions relative to the device and rat by using the subscript ‘device’ and ‘rat’ respectively i.e. XY_{device} and XY_{rat} where $XY_{rat} = X_{device}, Y_{device}$+ 15mm. The rat may only access the pellet via the slit and depending on the position of the pellet presentation, the Rat is required to use a

specific forepaw to grasp the pellet. If the pellet is offset to the left of the slit, then the rat is required to use its right forepaw to grasp the pellet and vice versa.

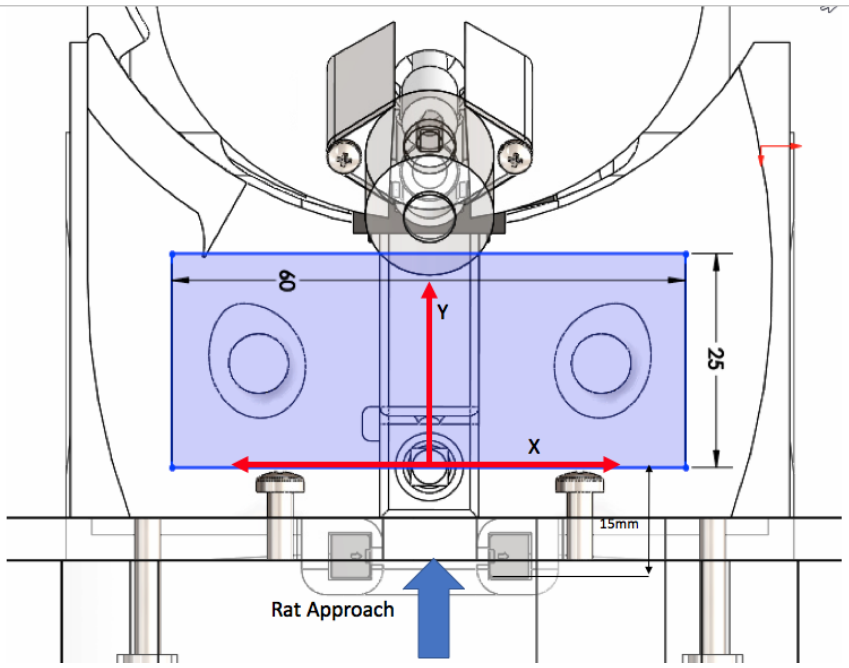

Figure 3.13 - Cartesian frame of reference for pellet positioning.

Position (0,0) is the furthest position that the spoon can reach central to the slit. This position is set back 15mm from the closest rat approach position. The overall reach Y_{rat} required is therefore up to 40mm in the Y direction, and ± 30mm in the X direction.

3.3.6 Rotational motion of the RatBot spoon base

A worm gear configuration (Figure 3.14-2, Figure 3.16) is used to provide rotational movement (Figure 3.21) of the spoon base. A worm screw with a lead of 4mm (Figure 3.15) provides 4mm of linear translated movement for each full rotation of the worm screw. The worm screw is driven by a 20:1 18º/step stepper motor (Goot Motor - PG15S-020-01/20) and is attached by a keyed coupling (Figure 3.16) to prevent slip within the coupling. The worm screw mates to a matching gear (Figure 3.14-3) that has been designed into the fixed base. The fixed base is static (being bolted to the floor of the RatBot) and hence any rotational force caused by the worm screw rotating will rotate the Spoon Base.

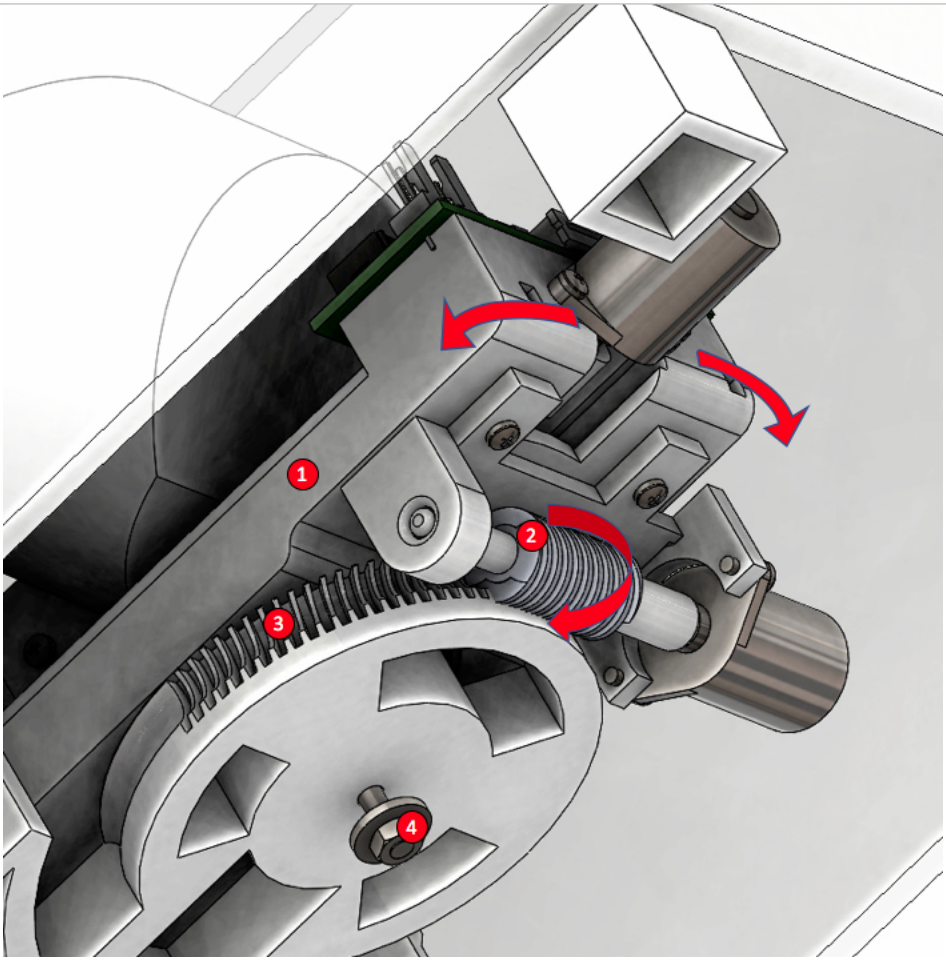

Figure 3.14 - Worm gear arrangement of the base facilitates rotational motion of the Spoon base.

A worm gear arrangement facilitates the rotational movement of the Spoon base (1). A 4mm pitch worm screw (2) couples with the gear designed into the fixed base (3). The fixed base is statically fixed to the Perspex base of the RatBot enclosure using a bolt (4) and any rotational force created by the rotation of the worm gear translates into rotational motion of the Spoon base.

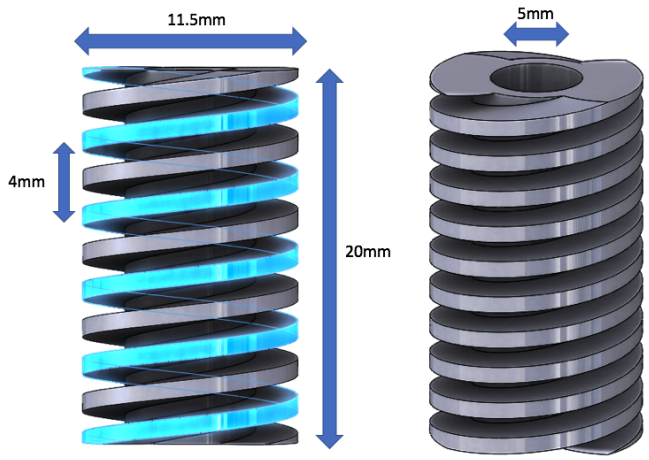

Figure 3.15 - A worm screw is used to facilitate rotational movement of the device.

A dimensional overview of the worm screw in the worm gear assembly that facilitates rotational movement of the RatBot. A 4mm pitch provides 4mm of translated linear motion for each rotation of the gear. A 5mm bore was machined into the gear to allow for a custom printed shaft to be inserted.

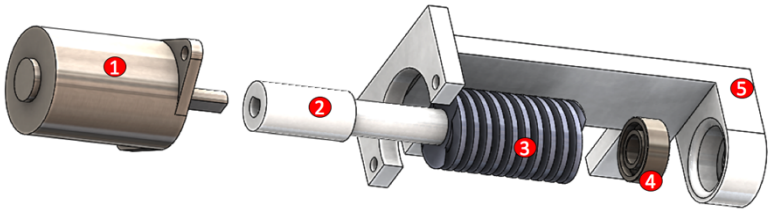

Figure 3.16 - Exploded view of the worm and drive assembly.

1. The driving stepper motor with a 20:1 gearbox (Goot Motor - PG15S-020-01/20).
2. A 5mm 3D printed nylon axle couples the worm screw with the stepper motor and support bearing.
3. A 4mm pitch worm screw machined with a 5mm bore to allow the insertion of the axle.
4. A 4mm ID 9mm OD bearing is used to stabilise the opposing end of the axle.
5. The 3D printed worm screw assembly housing that is attached to the underside of the spoon base.

To allow for accurate positioning, a known home location is required. This is accomplished by using an Omron DF02-D micro switch (Figure 3.17) with a homing sequence (Figure 5.7). The worm gear is rotated to move the base in the home direction (Figure 3.17b-2) until the microswitch is triggered high. At that point the driving motor reverses direction and moves in the opposite direction until the micro switch reverts to a low state. This step off action ensures that the device was not always pressing against the flexible reed of the micro switch. If the initial movement to the home position does not trigger the home sensor high within 20 seconds of initiating the homing sequence, then the firmware progresses to an error state and sends a notification email to the end user. This is done to prevent the motors from continually running and overheating.

a.

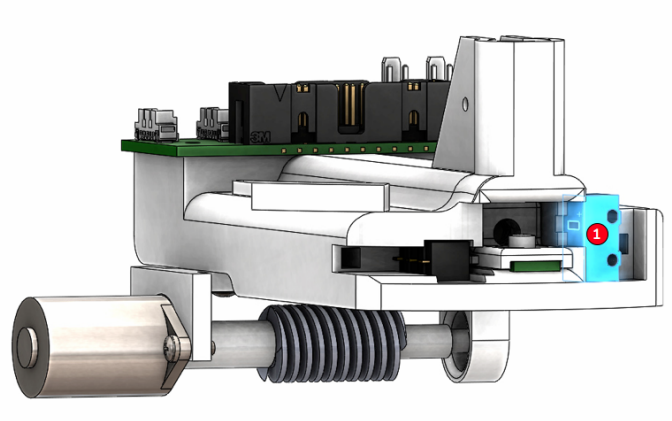

b.

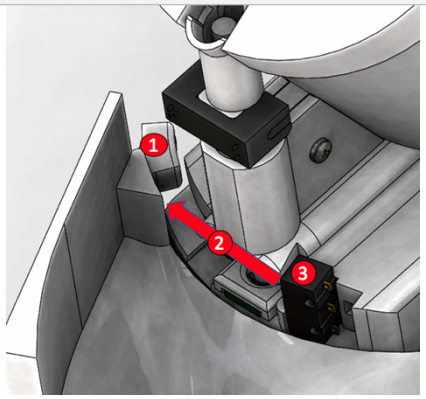

Figure 3.17 - Rotational home sensor microswitch location and trigger operation.

An Omron DF02-D micro switch (a-1,b-3) is used as a home positioning sensor. When the RatBot is rotated towards (b-2) the home position, the micro switch is depressed by the pellet guard (b-1) and a homing event is captured by the firmware. The pellet guard also serves as retention mechanism to prevent the pellet from bouncing off the spoon during the dispensing procedure.

3.3.7 Radial Motion

A pellet is dispensed onto a spoon (80mm (l) x 9.5mm (h) x 11.5mm (w)) (Figure 3.18, Figure 3.19) and the spoon is then moved to a programmable location (Figure 3.21) during the normal execution of a reaching trial. The linear motion of the Spoon is accomplished by implementing a lead screw configuration (Figure 3.20). A 3.5mm diameter trapezoidal lead screw (Haydon Kerk LSSSSR-014-0394-FY12) with a lead of 10mm is used to translate rotational into linear motion (Figure 3.20). The lead screw is driven by a 20:1 18º/step stepper motor (Goot Motor - PG15S-020-01/20) and is attached by a keyed coupling (Figure 3.20). A 10:1 thread has been designed into the spoon (Figure 3.20a) to mate with the lead screw.

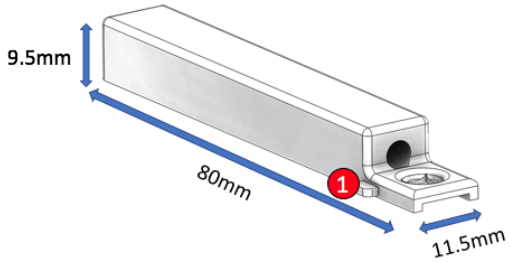

Figure 3.18 - Overview of the custom designed spoon used to position pellets.

The spoon 80mm (l) x 9.5mm (h) x 11.5mm (w) facilitates the radial movement of the pellet. The spoon contains a VCNL4000 proximity sensor (Figure 4.23) as well as a protruding feature (1) to trigger the home sensor (Figure 3.17b-3).

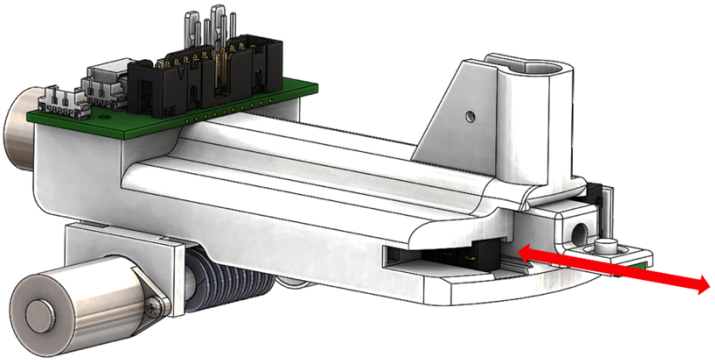

Figure 3.19 - Partially assembled right view of the spoon base indicating the direction of movement.

A partial assembly of the spoon base component with rotational worm gear and spoon components is presented here. The spoon can move linearly in the directions indicated by the arrows thereby allowing the pellet to be presented closer or further from the rat executing the trial.

Due to space restrictions, a standard lead screw nut was not used and instead a matching helix thread pattern was designed into the spoon (Figure 3.20b) to serve the purpose of mating with the lead screw to translate rotational motion into a linear movement. The spoon is constrained to move linearly through the rectangular slot in the spoon base (Figure 4.19); it cannot rotate.

a.	b.
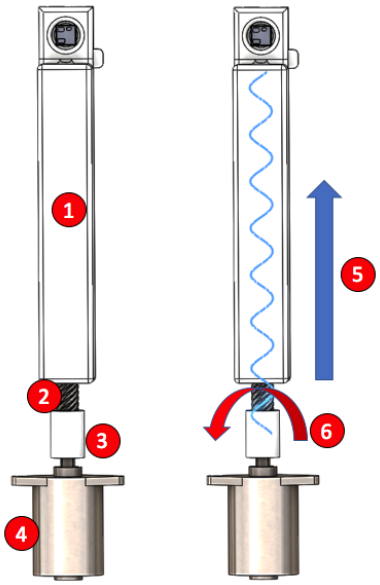	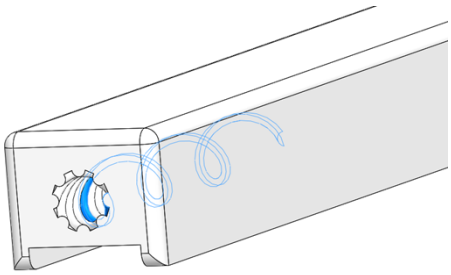

Figure 3.20 - The linear motion of the spoon is achieved using a lead screw feature designed into the spoon.

a. The spoon (1) is coupled to a 10mm pitch lead screw (2) (Ametek) which, when rotated by the motor (4) translates the rotational motion (6) into linear motion (5). This allows for the extension and retraction of the spoon during the operation of the RatBot.
b. Due to space constraints, a typical lead screw nut could not be used. Instead, a helical thread has been designed into the spoon to mate with the 10:1 Ametek lead screw. This translates the rotational motion of the screw into linear motion of the spoon.

3.3.8 Grasping success determination

After a pellet is presented at a programmable location (Figure 3.21), a combination of sensors determines if the pellet was grasped or dropped (Figure 3.22). A proximity sensor (VCNL4000) is integrated into the design of the spoon (Figure 3.23) and provides feedback on the presence of the pellet on the spoon. A through-beam slit sensor (Omron EE-SX 1140) (Figure 3.24) incorporated into the slit detects if there was interaction by rat through the slit, either by its snout or forelimb. Two through-beam drop sensors (Omron EE-SX 3070) (Figure 3.22; Figure 3.25) determine if the pellet was dropped.

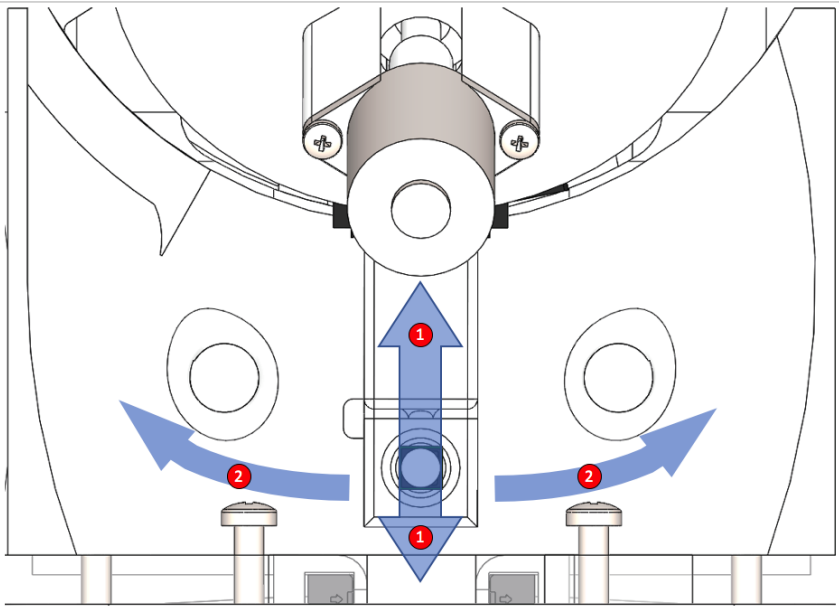

Figure 3.21 - Top view of RatBot CAD rendering showing direction of motion that can be achieved during pellet positioning.

The RatBot can programmatically position a pellet by moving the spoon along the radius indicated by 1, and by rotating the device as indicated by arrows 2. This allows the device to position the pellet near the slit during acclimation, and then progressively distance the pellet from the slit eventually requiring the rat to reach for the pellet with its forepaw instead of licking it with its tongue.

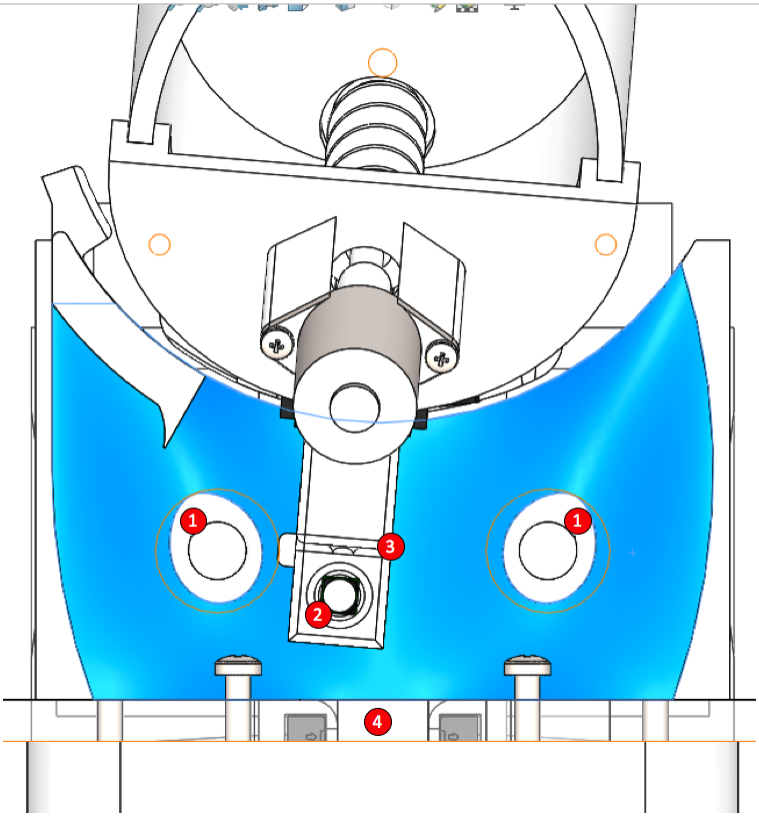

Figure 3.22 - Top view of RatBot CAD rendering indicating drop and proximity sensor arrangements

1. Two drop chutes with embedded through beam sensors (Omron EE-SX 3070). Each drop chute consists of a sloped funnel (in blue; see also Figure 4.26) which guides dropped pellets past a sensor which records the pellet drop. Each chute opens into a pellet drop box for storage of the dropped pellets until manually removed. This prevents access to the pellets by the rats.
2. A 45mg sucrose pellet.
3. The spoon, which moves a pellet to a programmable location.
4. The 11mm slit through which the rat reaches for a presented sucrose pellet. The slit contains on Omron EE-SX 1140 through beam sensor to determine if any interaction has occurred.

Trial Result	Dropped Sensor	Slit Sensor	Spoon Sensor
Grasped	False	True	False
Dropped	True	True	False
DroppedButSpoonSensed	True	True	True

Table 3.3 - Trial result truth table based on sensor input

a.	b.
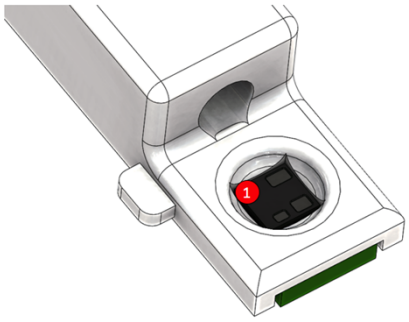	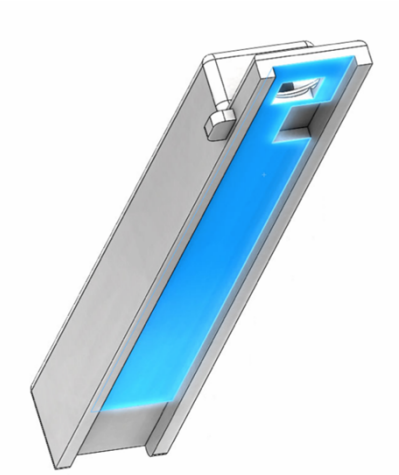

Figure 3.23 - The Spoon with an embedded proximity sensor.

a. A VCNL4000 proximity sensor (1) is designed into a custom PCB (Figure 4.9).
b. The PCB is recessed into the base of the spoon such that the sensor is positioned at the front of the spoon below a hole through which pellets can be detected.

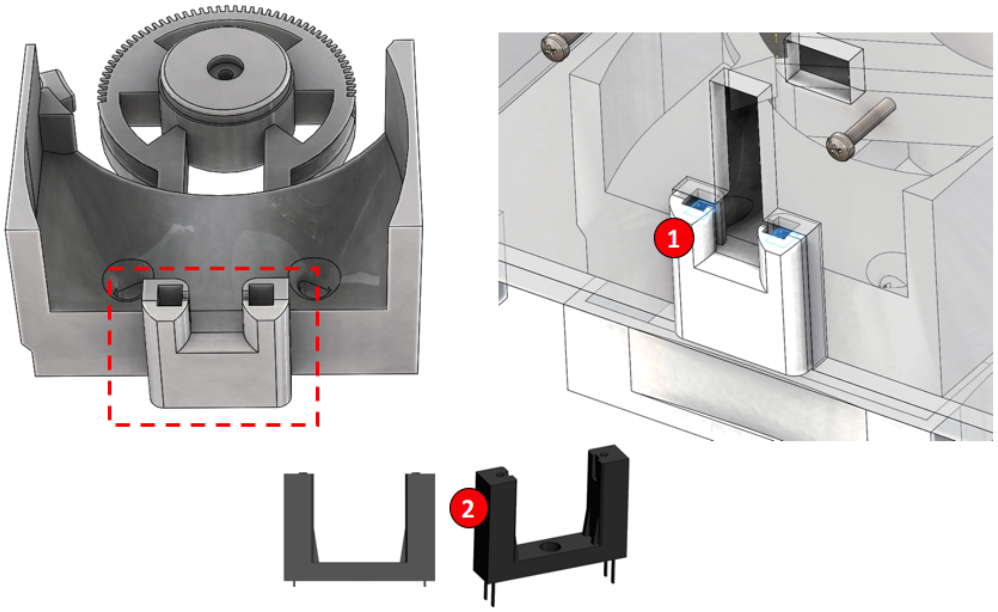

Figure 3.24 - The slit through-beam sensor provides animal interaction information.

1. The slit with a through beam slit sensor contained within. This sensor detects rat interaction with the device. It is also used to detect obstructions in the slit.
2. The Omron EE-SX 1140 through beam sensor embedded into the slit.

Two through beam sensors are designed into the fixed base to detect pellets being dropped. The sensors are arranged in a logical OR configuration so that the trigger of either side sends a signal to the firmware indicating that a pellet (or other item, e.g., wood chip from bedding) has dropped into the drop box. Dropped pellets are securely contained within a drop box. This is required to prevent the rats from accessing the dropped pellets. It has been observed that rats will develop an alternative pellet acquisition strategy if no drop box was present i.e. the rat will knock the pellet off the spoon and retrieve it from underneath the device.

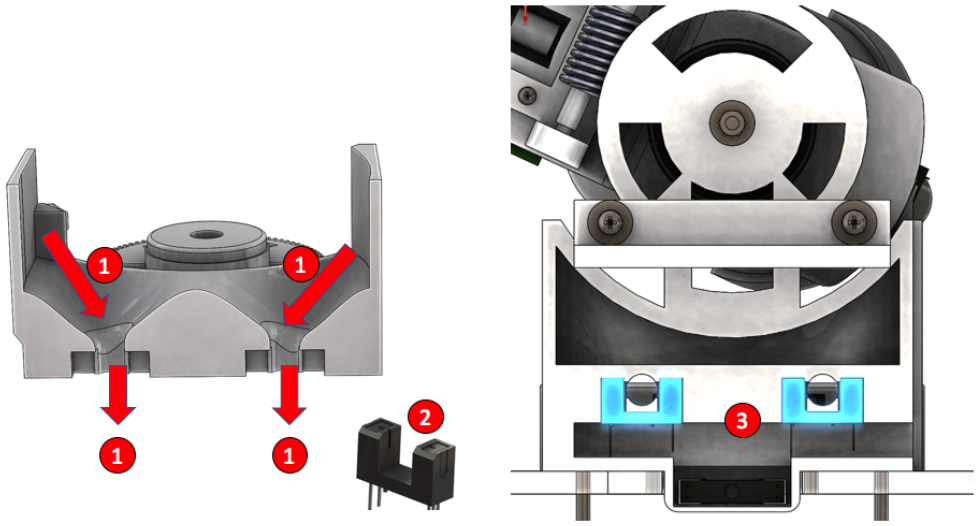

Figure 3.25 - Drop sensor arrangement in the base of the device.

1. The dropped pellets are guided towards two drop chutes designed into the base of the RatBot. The dropped pellets flow through the drop chute and into a drop box.
2. Two through-beam sensors (Omron EE-SX 3070) are used to detect pellet drops. A beam break is an indication of a pellet drop (Table 4.3).
3. The two sensors (2) are installed in appropriate cut-outs designed into the underside of the RatBot

The drop box is magnetically secured to the underneath of the acrylic enclosure. This allows the user to quickly remove, empty and replace the drop box during the daily maintenance schedule.

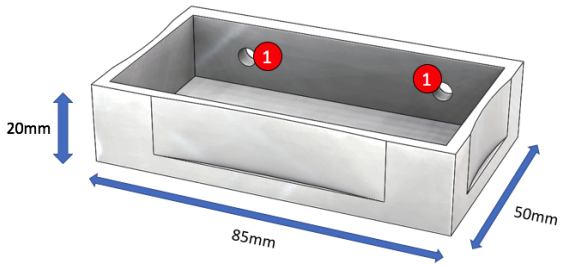

Figure 3.26 - A dimensional representation of the drop box.

A magnetically attached (1) drop box (85mm(w) x 50mm(d) x 20mm(h)) was designed to be easily installed and removed to facilitate daily cleaning. All pellets dropped through the drop chute, fall into the drop box and preventing access by the rats.

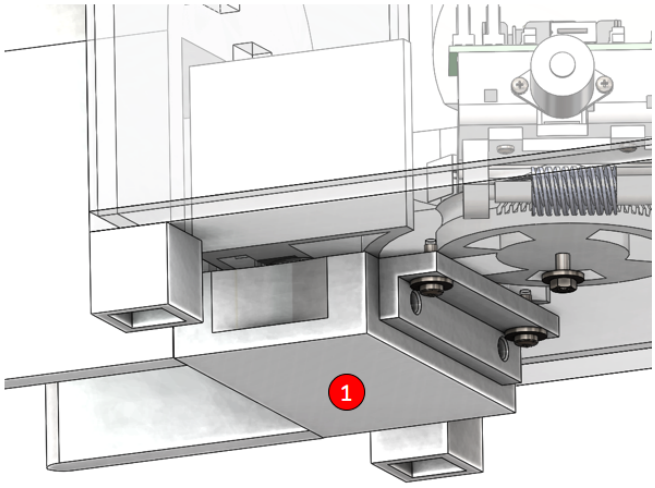

Figure 3.27 - The drop box is magnetically coupled to the underside of the RatBot.

The drop box (1) is magnetically coupled to the bottom of the RatBot for secure storage of dropped pellets. This feature allows the user to quickly remove, empty and replace the drop box during the daily maintenance regime.

A custom designed LED strip consisting of 3 warm white LEDs (CLM3C-MKW-CWAXB233) was introduced to provide artificial lighting into the cage. This was done to account for the lack of light during the trial during the night cycle within the behavioural services unit.

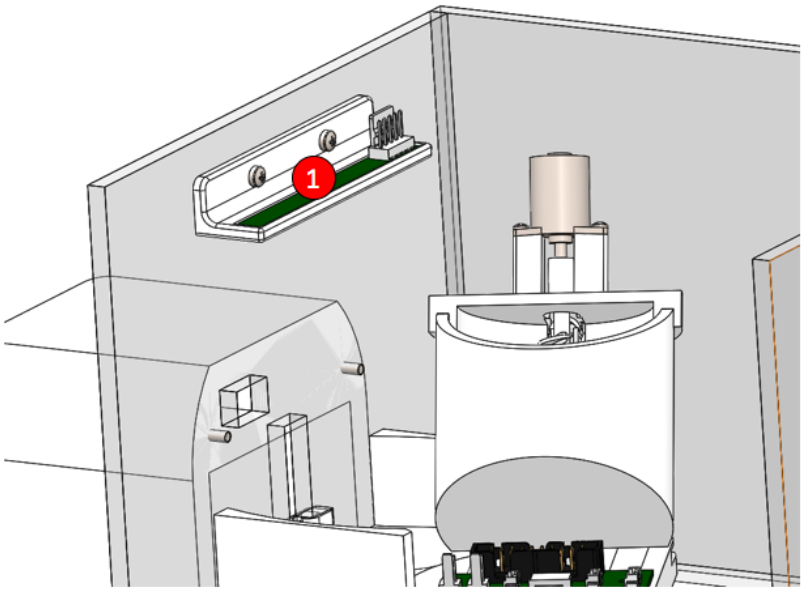

Figure 3.28 - The LED strip positioned at the front and inside of the device ensures pellet visibility in the dispensing zone.

An LED strip (1) consisting of 3 warm white LEDs, provides consistent lighting in pellet dispensing zone. The intensity of the LED array can be programmatically controlled.

The mechanical device described thus far incorporates custom developed electronics as well as off-the-shelf equipment to facilitate the coordinated motion, pellet delivery and result determination required for correct operation. The next chapter details the electronic components, architecture and custom designed circuit boards that have been implemented to facilitate the execution and assessment of the SPRT.

Chapter 4

RatBot™ control electronics

Acknowledgements:

Lawrence Moon and Sotiris Kakanos assisted with the assembly of printed circuit boards.

4.1 Introduction

The RatBot comprises of a multitude of sensors and electromechanical components. An embedded control solution was required to integrate with and control each of these components. To guide the choice of embedded controller and related infrastructure, a set of high-level electronic objectives were defined as follows:

1. The device power requirements should be kept to a minimum to avoid excessive heat dissipation and thereby to ensure safer operation in the cage.
2. Infrastructure requirements to install, operate and maintain the device should be kept to a minimum to allow for larger experiments using a higher number of devices and test subjects.
3. The infrastructure must support suitably high-speed communications to persist captured data, monitor devices and receive instructions by an array of devices.
4. The footprint of the electronics inside the cage must contain features to reduce the likelihood of shock and fire.
5. The electronics must be modular and easily replaceable or upgraded.

Large, off-the-shelf programmable logic controllers (PLC) exist to fulfil such a purpose but unfortunately, higher associated costs, size and power requirements excluded their use. A custom embedded solution is a viable option but the increase in upfront development overhead (cost and time) would not make this a viable option during the prototyping process. This approach will be taken closer to the commercialisation point when a prototype has fully proven the concept. The controller would need to strike a balance between size, power consumption and out-of-the-box functionality.

4.2 Methods

Printed Circuit Boards (PCB) were designed using CadSoft Eagle PCB design software. To reduce the overall cost and accelerate the development of the electronic components, PCBs were initially prototyped in-house using standard exposure and chemical etching techniques. A CNC 6040Z Router was used to drill PCB holes and cut the circuit boards into the desired shapes. Subsequent design iterations were outsourced for manufacture to PCBTrain (Newbury Electronics, UK) and PCB Pool (Beta Layout, Germany). PCBs were assembled in-house using a combination of hot air and hot iron soldering techniques. Cable harnesses were custom constructed based on the connectivity requirements between various device modules. Full details of all PCB designs and components are included in Appendix A - PCB.

4.3 Results and Discussion

During the prototyping of this device it was decided that a Raspberry Pi 2 B+ would serve as the main logical controller (at that time the Raspberry Pi Zero and Raspberry Pi 3 was not released). The benefit is that it contains the core hardware required to facilitate the rapid prototyping process. Custom PCBs to facilitate device and component interconnectivity would be the key items requiring development, hence accelerating the electronic controller development process.

The RatBot is controlled by a Raspberry Pi 2 B+ along with a series of custom designed electronic printed circuit boards (Figure 4.1). The control electronics were designed in a modular fashion to allow for simplified connectivity and maintenance. Power extraction, motor control and logical control components were intended to reside outside the rat cage for safety purposes. The remaining electronic components and connectors were designed to be integrated within the RatBot hardware and hence reside inside the RatBot acrylic enclosure.

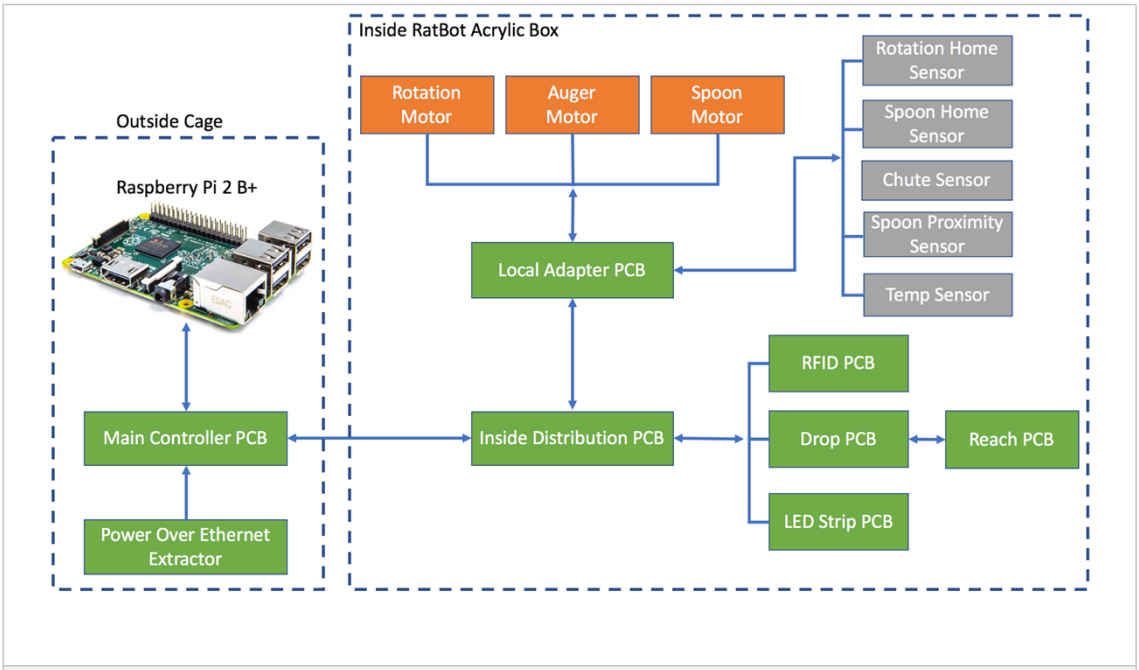

Figure 4.1 - High-level electronics overview of the RatBot.

The electronics comprises of two core segments. Firstly, a main controller residing outside the rat cage and secondly, a set of components residing inside the RatBot acrylic enclosure. This allows for quick connection, disconnection and/or replacement of various components. Multi-way connectors (rather than soldered wires) were used where possible to ensure simplicity of connectivity. A Raspberry Pi 2 B+ formed the core logical component on which the firmware was loaded and executed.

4.3.1 Main controller board (MCB)

The MCB (version 39) (Figure 4.2, Figure 4.4, Appendix A - PCB) was designed to expand the functionality and connectivity of the Raspberry Pi to interface with the RatBot hardware. It was designed to be easily interchangeable during the iterative design process with the inclusion of a 40-way connector to mate with the Raspberry Pi in a Pi-Hat fashion. A 30-way connector allowed for quick connectivity via a 30-way ribbon cable between the external-to-cage components to the internal RatBot electronics.

A two-stage fuse configuration was used as overcurrent protection to the device. A polyswitch (MICROSMD150F-2, Raychem connectivity) with a 1.5A holding current and a 3A trip current was selected to allow for current variations up to 2A. The polyswitch is a resettable fuse that will temporarily cut current flow to the electronics when the current starts to rise above the 1.5A holding current and will fully trip out at 3A. However, under

normal operation, the system should not draw more than 1A at peak usage. If the current usage rises to the 2A level, it indicates that there is an electronic fault in the system and in this case power should be cut to the device. To accomplish this, a 2A fast blow fuse (Shurter, PN: 0034.1519) is designed into the MCB as a secondary master blowout.

Three stepper motor drivers (Pololu DRV8834; Figure 5.3) were configured in full step mode (Table 4.1). This ensured that the motors could be driven at a faster RPM compared to that of any micro-step mode.

The Raspberry Pi General Purpose Input Output (GPIO) pins are not 5v tolerant. A 3v3 to 5v bi-directional level shifter was designed into the main controller board, to adjust the serial communications voltage levels for communication between the Raspberry Pi and the RFID reader (Priority 1 Designs, RFIDREAD-mRW-134).

Inputs and outputs for limit switches, 5v & 3v3 supplies, as well as I^2C and serial communications are directed through the 30-way connector.

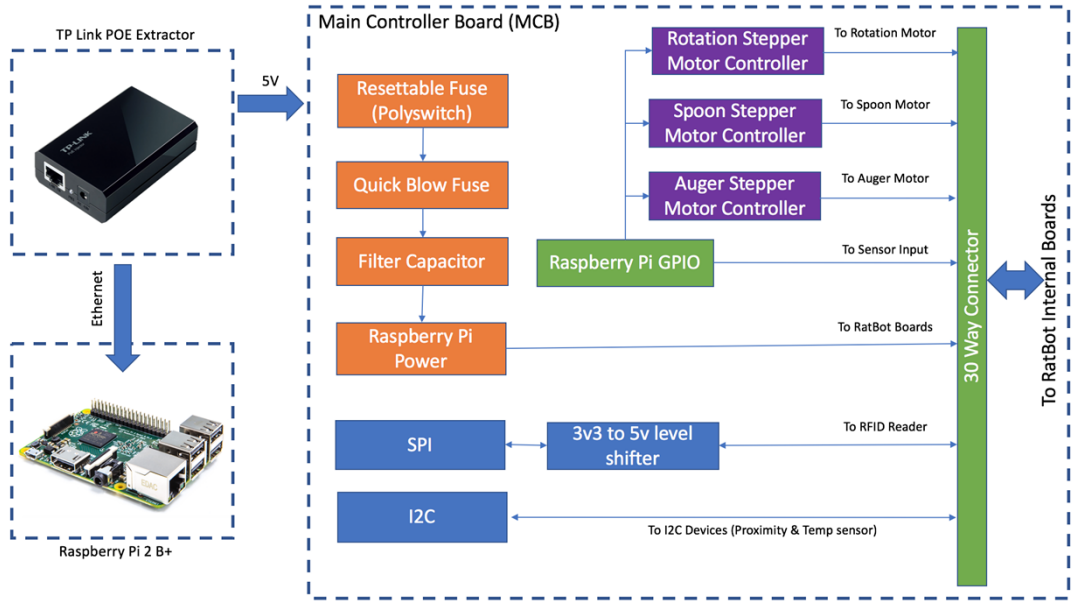

Figure 4.2 - Main Controller Board Block diagram

A TP-Link POE extractor extracts power (5v) delivered by a Netgear POE switch. This 5v supply powers the Raspberry Pi, custom electronics, motors and sensors.
The custom Main Controller Board (MCB) was designed in a modular fashion to house power filter and current safety components, serial communication voltage-shifting circuitry and stepper motor controllers. The internal RatBot electronics is connected to the core RatBot electronics via a 30-way ribbon cable.

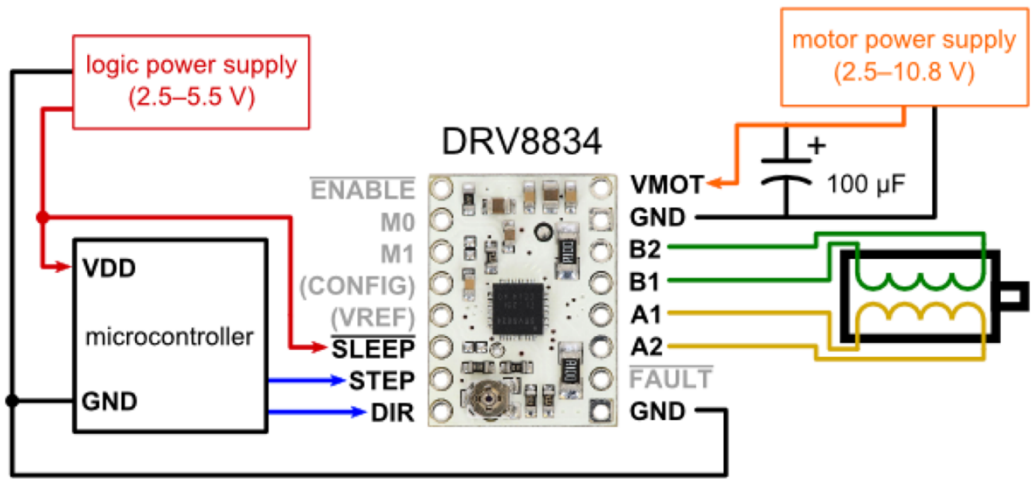

Figure 4.3 - Pololu Stepper Motor Driver Usage

The Pololu low-voltage stepper motor was configured to run in full step mode allowing for the maximum possible stepper motor speed with the Raspberry Pi.
(Image: pololu.com)

M0	M1	Micro-step Resolution
Low	Low	Full step
High	Low	Half step
Floating	Low	1/4 step
Low	High	1/8 step
High	High	1/16 step
Floating	High	1/32 step

Table 4.1 - DRV8344 Micro stepping configuration.

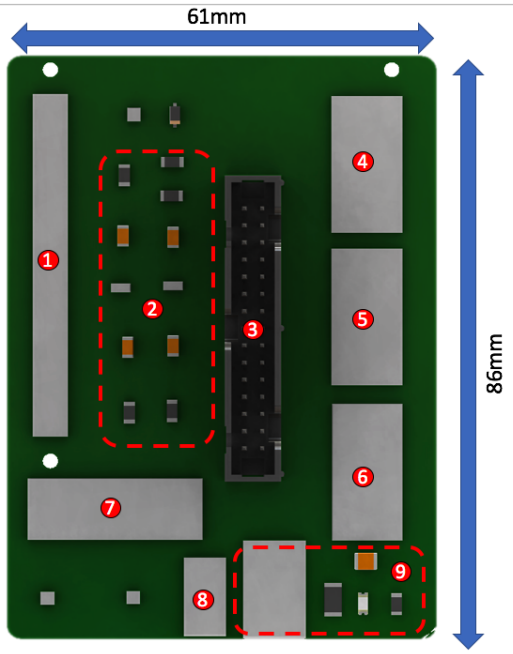

Figure 4.4 - Main Controller Board (version 39) overview.

A modular overview of the main controller board.

1. 40-way connector which connects (in a Pi-Hat style) directly to the 40-pin header on the Raspberry Pi.
2. A MOSFET voltage level shifting circuit to convert 3v3 to 5v and vice versa when communicating via serial communications with the RFID Reader.
3. 30-way connector to connector to the internal electronics of the RatBot via a 30-way ribbon cable.
4. Rotation stepper motor driver configured in full step mode.
5. Spoon stepper motor driver configured in full step mode.
6. Auger stepper motor driver configured in full step mode.
7. Fast blow 2A fuse that will cut power to main controller board and connected electronics in the event of a short circuit or current draw beyond 2A.
8. DC-DC Converter to isolate noise from the stepper motors from the serial communications to the RFID reader
9. 5v DC connector, filter and resettable polyswitch fuse to mitigate the random current spike that may occur below 2A. If the current spike is sufficiently large (>2A) then the fast blow fuse will trip out, cutting power to the unit.

4.3.2 Intermediate distribution board (IDB)

The IDB (version 5) (Figure 4.6, Appendix A) was designed as an internal-to-RatBot junction board that would allow the electronic components outside the cage to be easily connected to or disconnected from the components inside the RatBot enclosure. This board also provides pluggable connections for the RFID sensor, Drop/Slit sensor and LED strip. Ribbon cables and flexible stranded multi-core cables were used to reduce the effects of cable strain and retarding torque on the motion of the RatBot (Figure 4.5).

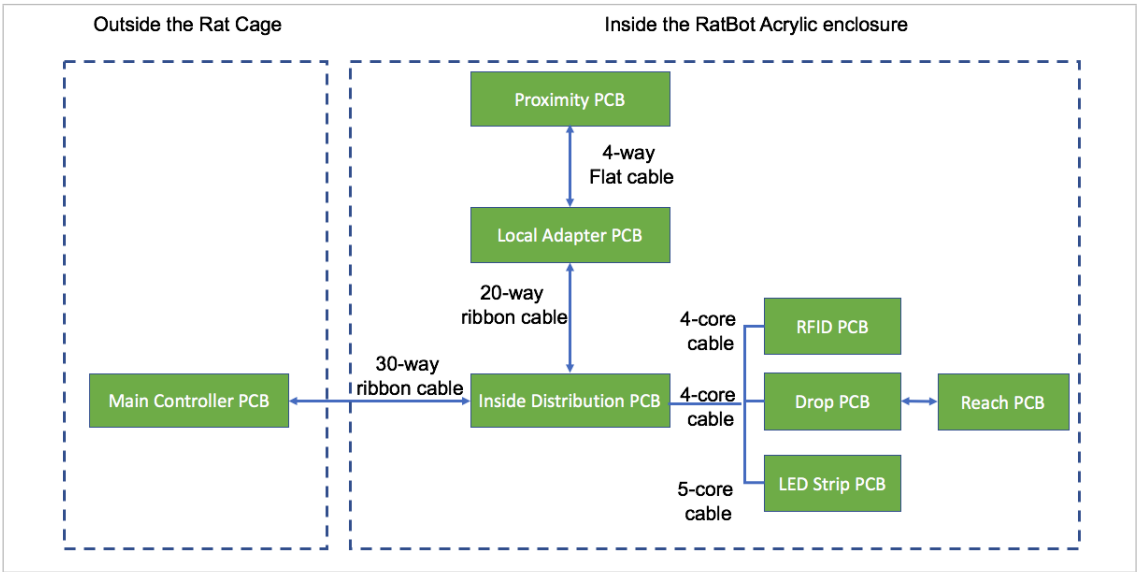

Figure 4.5 - Intermediate Distribution Board Block diagram

The main distribution board located on the outside of the rat cage is connected to the internal RatBot electronics via a 30-way ribbon cable.

The inside distribution board splits the incoming 30-way connection into separate connection points for the local adapter (motion connections & proximity sensor), RFID reader, drop sensor, slit sensors and the LED strip. This connection architecture ensures that maintenance and/or replacement of the modular components can take place without replacing the entire wiring harness or other modular components.

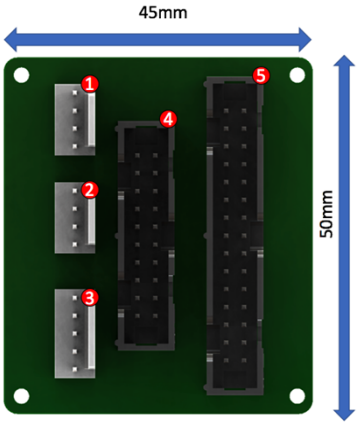

Figure 4.6 - Intermediate distribution board (version 5) overview.

Dimensioned 3D top view of the intermediate distribution board

1. RFID Connector (4 way).
2. Drop Reach connector (4 way).
3. LED Connector (5 way).
4. Local Adapter connector (20 way). Connects via a 20-way ribbon cable to the local adapter board.
5. Main Board connector (30 way). Connects via a 30-way ribbon cable to the Main controller board that is directly attached to the Raspberry Pi.

4.3.3 Local Adapter board (LAB)

The LAB (version 7) (Figure 4.7, Figure 4.8, Appendix A) has been designed to easily connect and disconnect the stepper motors, home and chute sensors and the proximity sensor. This board also houses the TMP102 temperature sensor so that device temperature can be obtained closer to the core of the device where heat radiating components such as the stepper motors reside. The LAB PCB connects to the Intermediate Distribution Board via a 20-way ribbon cable to reduce the rotational retarding force that comes with large cable looms. This allows for the use of a lower powered, low torque stepper motor to rotate the device.

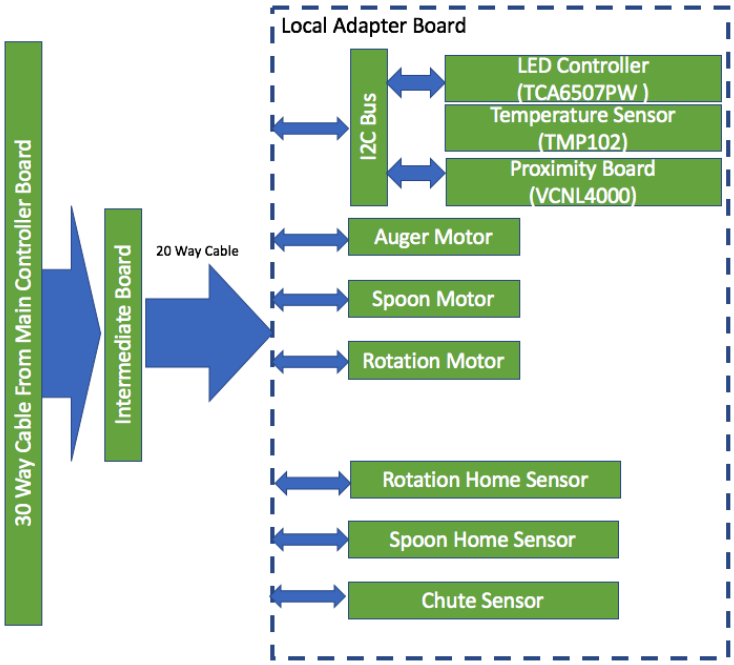

Figure 4.7 - Local Adapter Board Block diagram

The local adapter board (LAB) provides connectivity for all stepper motors via 3 connection points. Connection points for the home and chute sensors have also been designed into the board. An I^2C bus enables communication between the Raspberry Pi, the TMP102 temperature sensor, the LED controller (TCA6507PW) and the VCNL4000 proximity sensor. The LAB connects to the intermediate distribution board via a 20-way ribbon cable. This single connection point serves two purposes: 1. Simple connection or disconnection of the core device from the acrylic enclosure, 2. Reduced retarding torque that would ordinarily be introduced by a larger gauge cable harness, which allows for smaller lower torque stepper motors to be used for the rotational motion of the device.

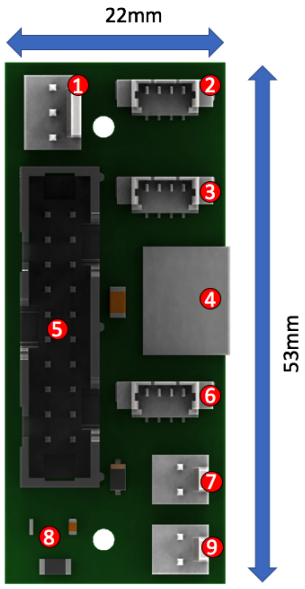

Figure 4.8 - Local Adapter Board (version 7) overview.

Dimensioned 3D top overview of the local adapter board.

1. Chute Sensor connector.
2. Rotation stepper motor connector.
3. Spoon stepper motor connector.
4. Spoon proximity sensor connector.
5. 20-way connector that interfaces with the Intermediate Distribution Board via a 20-way ribbon cable.
6. Auger stepper motor connector.
7. Rotation home sensor connector.
8. Spoon home sensor connector.
9. Temperature IC and supporting components.

4.3.4 Proximity Sensor board (PSB)

The proximity sensor was designed onto a PCB (Appendix A - PCB, *Figure 4.9*) that is embedded in the spoon. This board forms the base of the spoon providing a smooth gliding surface for the linear motion. A VCNL4000 proximity sensor is capable of reading both the ambient lighting conditions as well as object proximity using reflective infra-red.

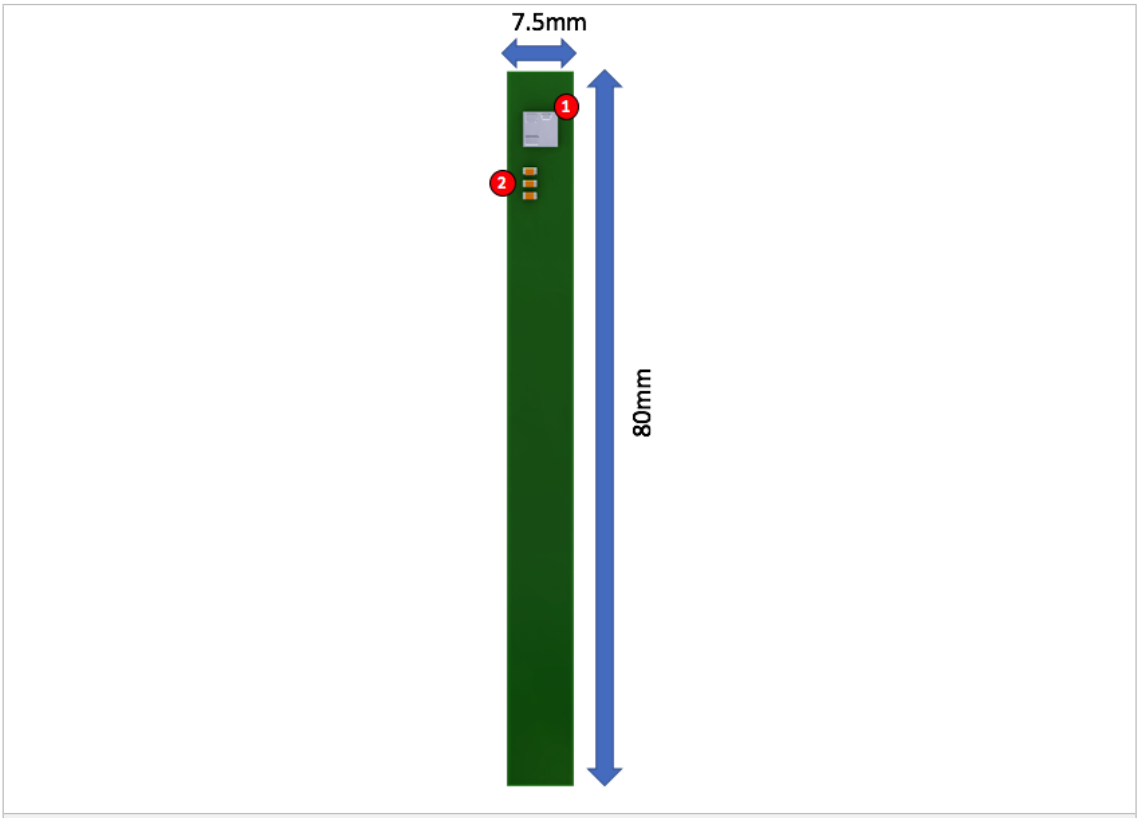

Figure 4.9 - Proximity Board (version 8) overview.

Dimensioned 3D top view of the proximity board.

1. VCNL4000 Proximity sensor.
2. Manufacturer recommended filter capacitors.

4.3.5 Slit Sensor board (SSB)

The slit sensor board (Figure 4.10, Appendix A - PCB) integrates an Omron EESX1140 transmissive photo micro sensor. This sensor provides feedback about slit obstructions and rat interaction, either via the snout or forepaw. The EESX1140 is active low but an active high signal was required. To accomplish this, a single channel logic inverter (Figure 4.11) was integrated into the circuit.

a.	b.
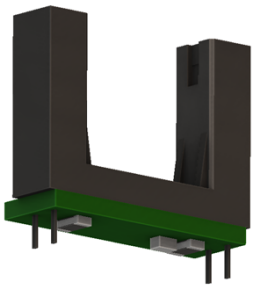	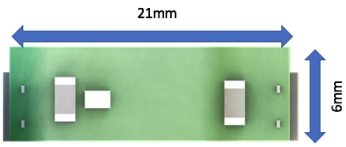

Figure 4.10 - Slit Sensor Board (version 3) overview.

a. 3D rendering of the printed circuit board.
b. Dimensioned 3D bottom view.

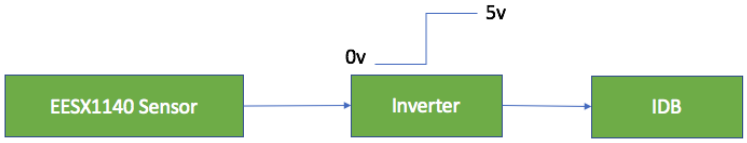

Figure 4.11 - Slit Sensor Block Diagram

The EESX1140 provides an active low output i.e. when the beam is obstructed, the output signal is 0v and 5v when no obstruction is present. The firmware continuously monitors for a rising edge of this input line and thus the output from the EESX1140 should be inverted. This is achieved by using a single gate CMOS Schmitt-trigger.

4.3.6 Drop Sensor board (DSB)

The drop sensor board (Appendix A, Figure 4.12) consists of a pair of EE-SX-3070 photo micro sensors, used to detect the drop of a pellet through either of the drop chutes located in the base of the device (Figure 3.25). To ensure that a triggered event of a falling pellet was captured by the non-real time polling of the Raspberry Pi, capacitive delay logic was implemented. The photo micro sensors are active low and to facilitate a capacitive delay, the output signals were inverted. To reduce the overall wiring, logic from the two sensors were combined into a logical OR gate so that the firmware could identify the triggering of either the left or right sensor (Figure 4.13).

a.

b.

Figure 4.12 - Drop Sensor Board (version 3) overview.

a. Dimensioned 3D bottom view. 1 – EESX3070 through beam sensor.
b. 3D top view.

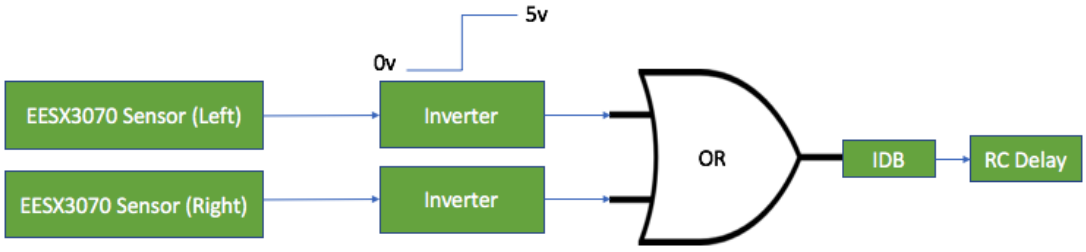

Figure 4.13 - Drop Sensor Block Diagram indicating inverter logic.

The EESX3070 is an active low component. To minimise wiring, the left and right sensors are each coupled to an inverter (single gate CMOS Schmitt-trigger inverter) and a 2-input positive OR gate before being sent to the MCB. The signal's high state duration is extended using an RC delay circuit, before being sent as a single signal to the Raspberry Pi. The firmware then monitors just a single input line instead of two and a single transmission line is required instead of two.

4.3.7 RFID board (RFIDB)

An interface board (Figure 4.14, Appendix A - PCB) was designed to be directly attached to the RFID reader (Priority1Designs Model: RFIDREAD-mRW-134). The board was designed to optionally allow the installation of an LED indicator used to determine if a successful RFID read had taken place. This was used primarily during development for debugging purposes and was later removed during the execution of overnight studies.

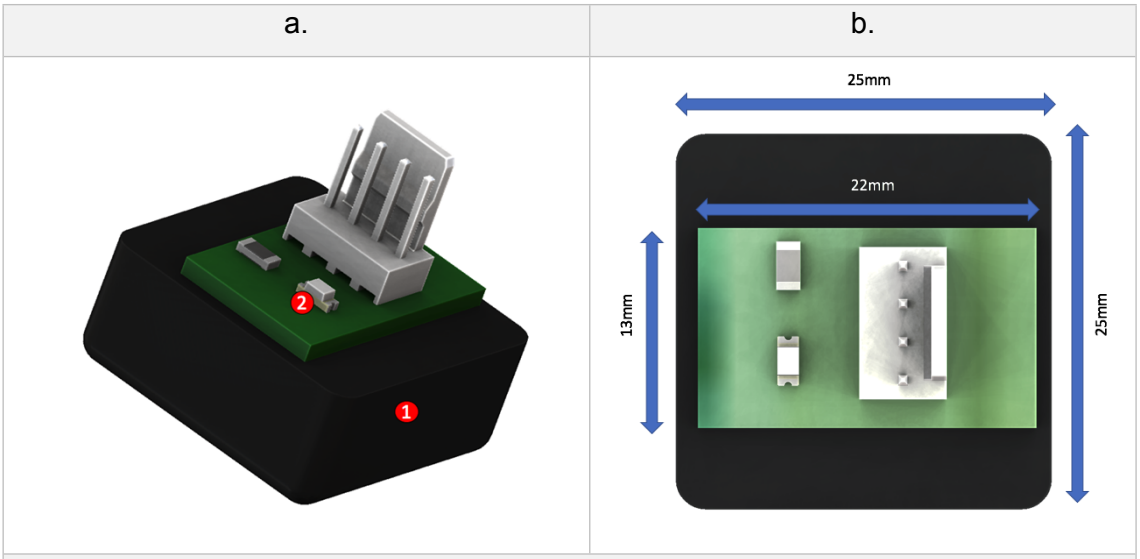

Figure 4.14 - RFID Interface Board (version 3) overview.

a. 3D rendering of the RFID interface Board.
    1. RFID Reader (Priority 1 Design RFIDREAD-mRW-134).
    2. LED RFID Read indicator.
b. Dimensional overview of the RFID board.

4.3.8 LED Strip board (LEDB)

Artificial lighting was introduced into the cage to remove the lighting variable from the study. An LED controller (Texas Instruments TCA6507PW) was used to control the intensity of the LEDs and is controlled via I^2C communications. A custom PCB was designed to house an array of 3 LEDs and the controller logic (Appendix A - PCB, Figure 4.15)

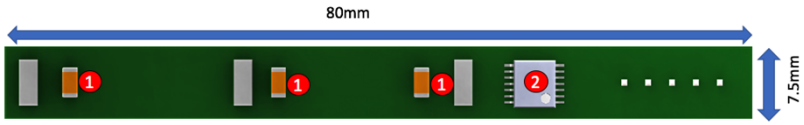

Figure 4.15 - LED Strip Board (Version 3) overview.

Dimensioned 3D bottom view of the LED strip board

1. Warm white LED. PN: CLM3C-MKW-CWAXB223
2. LED Driver (Texas Instruments TCA6507PW)

4.3.9 Chute Sensor board (CSB)

A chute sensor board (Appendix A - PCB, Figure 4.16) comprising of a photoelectric microsensor (Omron EE-SX3070) was designed to detect the falling of a pellet through the pellet chute attached the reservoir (Figure 3.8-4). The active low operation of the sensor was inverted to simplify monitoring by the firmware, so that all triggers were treated as rising edge signals (Figure 4.17).

a.	b.
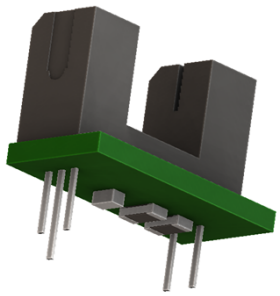	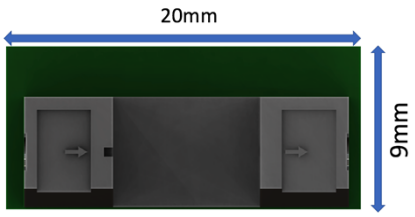

Figure 4.16 - Chute Sensor Board (Version 1) overview.

a. 3D rendering of the printed circuit board.
b. Dimensioned 3D top view.

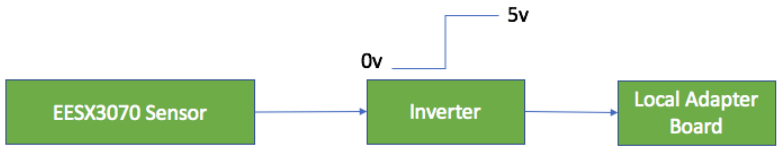

Figure 4.17 - Chute Sensor Block Diagram

The EESX070 through beam sensor is used to detect a pellet falling through the pellet chute. The signal is inverted so that a high (0-5v) trigger may be used to indicate the pellet presence.

The sensors, custom boards and electronic components described in this chapter facilitate the motion control and information feedback capability of the device. The software and firmware (described in the next chapter) allows us to programmatically utilise these electronics to control the mechanical hardware and logically interpret and persist the device feedback in the form of trial results.

Chapter 5

RatBot™ software and firmware

5.1 Introduction

One of the objectives of this project is to have an array of RatBots running on a programmable schedule, overnight. This introduces a potentially large management overhead if each RatBot™ were to be manually controlled. At the same time, running larger numbers of trials will increase the amount of data generated introducing a data management overhead. To streamline the process and execution, three core pieces of software (Figure 5.1) are required to fulfil the device control, experiment and data workflows:

1. Firmware which is installed on each Raspberry Pi, which will coordinate the motion control as well as the data acquisition from the various sensors and embedded devices contained within. This software is also responsible for programmatically executing the trials and recording the trial data to a database.
2. A management application (*e.g.*, on a single PC) is required to control, monitor and maintain an array of RatBots as well as provide structured access to the data generated by the devices.
3. A database server to allow for the persistence of trial results, diagnostic data and device instructions queued for execution by each RatBot.

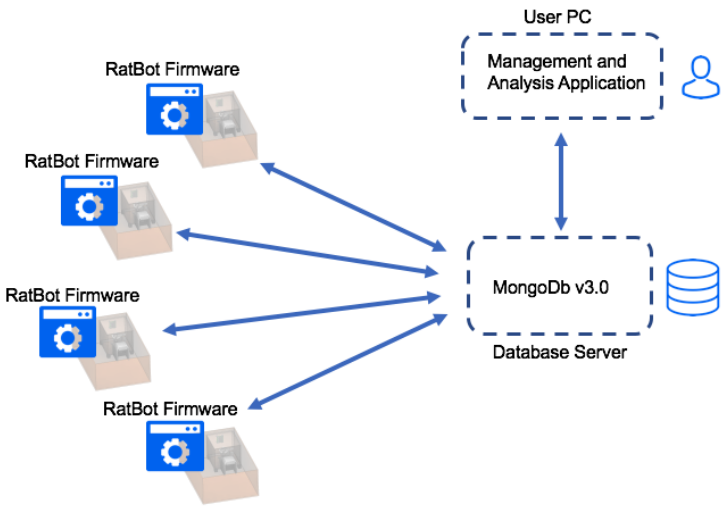

Figure 5.1 - High level architecture of key software components

An instance of the firmware is installed on each RatBot's Raspberry Pi and is responsible for the device operation and persistence of data obtained. The database server hosts a MongoDb database which stores instructions sent to RatBots, trial results and diagnostic data. A user management application interacts with the database server to send device instructions and read back trial results.

5.1.1 Software Objectives

1. The firmware must be able to communicate with all sensors and devices attached to the Raspberry Pi and execute the logical steps required to perform a reaching trial.
2. The firmware must perform read and write operations on a database.
3. The control and monitoring software must be centralised allowing end users to control, maintain and extract data from a large array of devices.
4. Data must be persisted to a database that allows for evolving data formats, and must be able to scale and cope with large data sets exceeding hundreds of gigabytes.
5. The device must be able to communicate errors, alarms and other notifications to the end user so that a quick appropriate response can be made, minimizing experimental downtime.
6. The configuration of the control and monitoring software must be simple and transparent to the end user. The control software must automatically detect devices within the study ensuring easy access to control and extract data.
7. The firmware that controls the device should be a lightweight program, which prevents the need for excessive logic to be contained within the embedded level.

5.2 Methods

The Raspberry Pi runs a Linux operating system (OS) Raspbian. This would further accelerate the software development process as a variety of Open Source software modules are available to control the various electronic components in use, and software may be written at a high level rather than an embedded level due to ease of debugging and unit testing (Liggesmeyer and Trapp, 2009).

Firmware prototypes were created using Python 3 using the Open Source RPi library. The latest version of the firmware was developed in C Sharp (C#) using Microsoft Visual Studio 2013-2015 and the Microsoft .Net Framework version 4.5. The firmware runs using the Mono Framework within the Raspbian variant of the Linux Operating System (OS).

A desktop management application was developed using Visual Studio 2015, Windows Presentation Foundation (WPF) & C#. Data is stored in a document format in a NOSQL database (Mongo DB).

The following freely available libraries were used for core operational and data persistence functionality:

a. Raspberry Pi Sharp (https://github.com/raspberry-sharp/raspberry-sharp-io)
b. MongoDB CSharp driver (https://docs.mongodb.com/ecosystem/drivers/csharp/)

5.3 Results and Discussion

5.3.1 Raspberry Pi configuration steps

Each Raspberry Pi requires configuration prior to being connected to its RatBot's electronics and infrastructure. The set of commands described in Table 5.1 outlines the preparation process.

Command	Description
apt-get update	Update the list of available packages and their versions.
apt-get upgrade	Install newer versions of installed packages.
apt-get install mono-complete	Install the mono framework on which the .Net software will be executed
sudo raspi-config	Enable SSH, Enable SPI, Enable I^2C, Disable output to COM port
apt-get install python-smbus i2ctools python-serial	Install python tools to assist during debugging processes

Table 5.1 - Raspberry Pi setup commands

The list of commands required to configure the Raspberry Pi so that it may run the firmware described in this section and provide access to features such as serial ports, remote SSH access and I^2C communications.

5.3.2 Firmware Overview

The firmware executes reaching trials (Figure 5.8) and persists the associated results to the database. The firmware is written in an object orientated fashion, comprising of multiple reusable software modules (Figure 5.2) that facilitate communication with the hardware components required for normal device operation. Instructions are created by the RatBot management application and are executed by each RatBot (Figure 5.3).

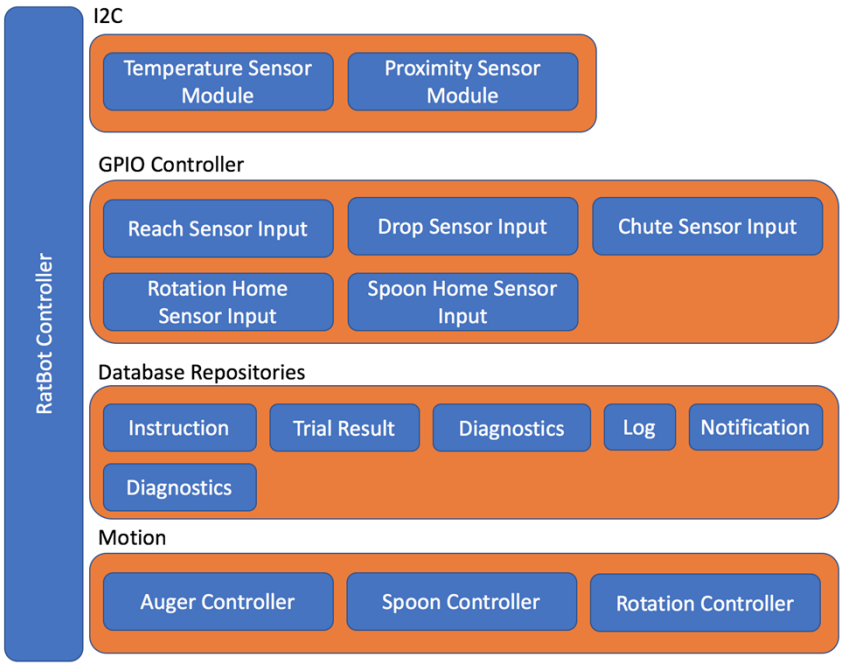

Figure 5.2 - Firmware module overview.

An I2C bus controller was extended to create temperature sensor and proximity sensor modules.

A GPIO Controller was created to read the statuses of the IO required for device operation. Home sensor feedback is required during homing of the device. Reach, drop and chute sensor feedback is required during the dispensing and positioning of pellets for reaching trials.

A repository pattern was adopted for database interaction whereby a repository was created for each document type.

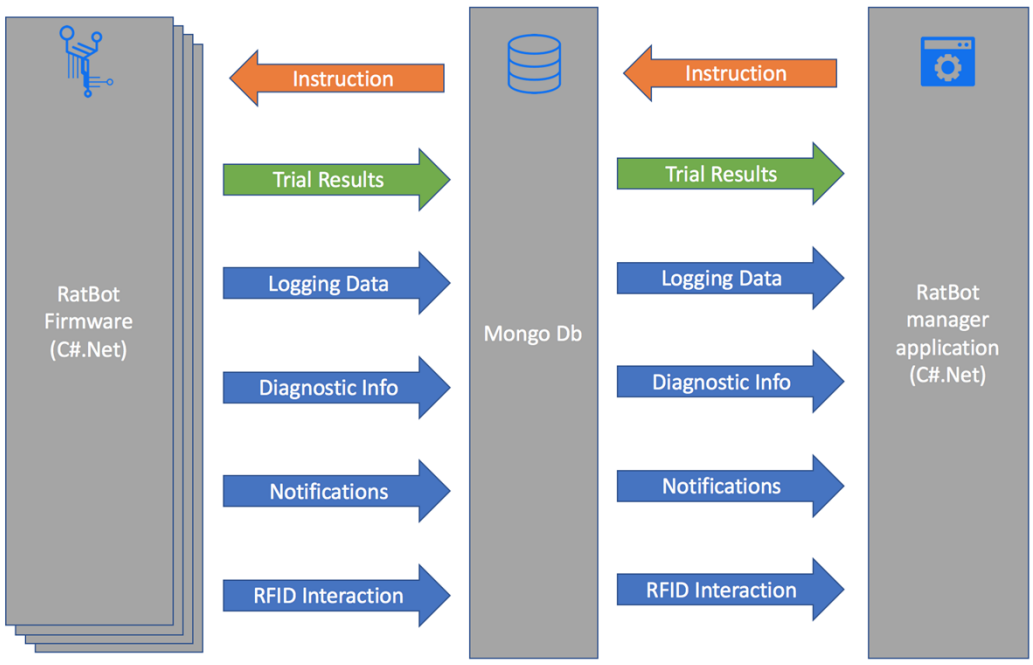

Figure 5.3 - High level overview of control software data flow.

A high-level representation of the flow of data and instructions between the firmware and the management application. The database is the intermediary for instructions and a long-term persistence mechanism for generated trial and diagnostic data.

Trial results (Table 5.2) are then stored within the NOSQL database (MongoDB). Trial results comprise of the RFID of the rat that executed the trial, a unique session ID, the trial result state (Table 5.3), the date and time of the trial execution. In addition to this, proximity data captured from the VCNL4000 sensor embedded in the spoon is persisted in the database with the trial result.

Property	Description
Animal Id	The RFID number of the rat that executed the task.
DroppedTime	The time at which the drop sensor was triggered during the trial.
EndTime	The end time of the trial.
Error	Any error that occurred during the trial.
PelletDispenseProximityData	All the readings from the proximity sensor that were taken during the trial.
PelletPosition	The XY coordinate at which the pellet was placed during this specific trial.
RatBotId	The unique identification number of the RatBot. The MAC address of each Raspberry Pi was used as its unique identifier.
ReachAttempts	A date stamped list of all the triggers recorded by the through beam sensor embedded into the 11mm slit.
RFID Reads	An array of all the RFID tags that were read during the execution of the trial.
SessionID	A unique identifier that could be used to group individual trials into sessions.
TrialID	A unique identifier of the trial.

Table 5.2 - Structure of the trial result stored within the database

Trial Result States	Description
Dropped	Only the drop sensors were triggered.
Grasped	The proximity sensor indicated that pellet was no longer present. The drop sensors did not record a drop event. The slit sensor recorded an interaction event.
FirstAttemptTimeout	The time allowed (12 minutes) for the rat to engage with the device elapsed. If no events were recorded by the slit sensor within the specified amount of time, then this result is reported.
MaxAttemptsReached	The slit sensor was triggered more than 10 times during a trial without a success report by the pellet proximity sensor or a dropped report.
DroppedButSpoonSensed	The drop sensor was triggered but the spoon proximity sensor still detected a pellet present.

Table 5.3 - Trial result states.

Instructions	Description
Reboot	Reboots the Raspberry Pi.
Initialise	Initialises the RatBot to the following defined position: Rotation and Spoon axes are homed and the spoon is cleaned automatically. Chute, Slit and Drop sensors are tested for obstructions.
Start Trial (Position array)	Start trials with the RatBot using the specified dispense positions.
Stop Trials	Stop any currently running trials

Table 5.4 - Instructions supported by the RatBot firmware.

5.3.2.1 Motion Control Module

A stepper motor module (Figure 5.4) was developed to control the individual stepper motors (auger, spoon, base) using standard step and direction control typically used for stepper motors. The module was designed to accept position, speed and sensor information with methods exposed to allow for homing, and positioning of the various components. With this module, dispensing and precise positioning of a pellet is made possible.

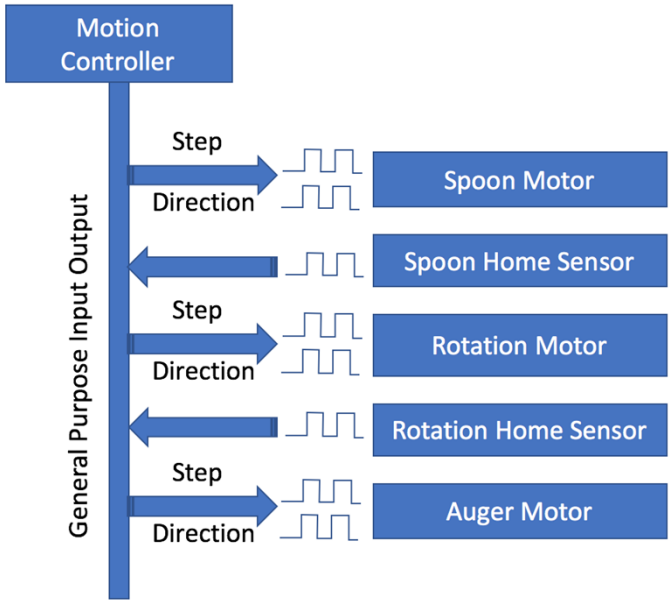

Figure 5.4 - Motion control overview

The custom written motion controller software module encapsulates the coordinated movement of the RatBot allowing for the dispensing and positioning of pellets. Typical step and direction stepper motor control has been implemented to control the movement of the 3 stepper motors (Auger, Rotation & Spoon) and bring the device to a known position with the use of home limit switches.

5.3.2.2 RFID reader module

The RFID module (Figure 5.5) runs as a background process to communicate with the Priority 1 Design RFID reader. Communication between the RFID reader and the RFID module is via the Serial Peripheral Interface (SPI) (baud rate 9600) available on the Raspberry Pi. The RFID reader automatically relays the identification number of the RFID tag that was read. This information is then stored in a date-stamped list of RFID tag readings. When a trial is completed, all RFID tags read during the single trial are stored with the trial result. This allows us to track the interaction of multiple rats during a single trial. The date-stamped RFID list is cleared at the start of every trial.

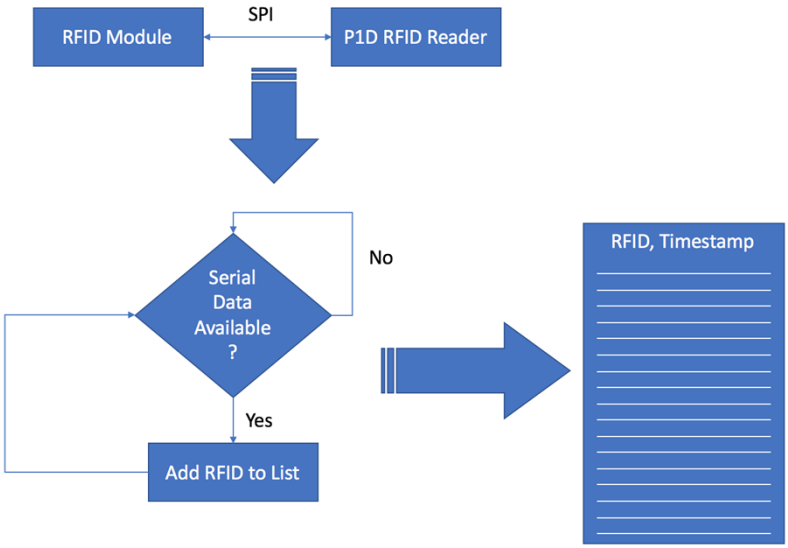

Figure 5.5 - RFID data recording workflow.

The RFID module transmits the identification number of the RFID tag read when the rat enters the RFID tunnel. The identification number is stored in a timestamped list and this list is included with the trial result stored in the database. This allows us to identify the animal that executed the task as well as determine whether other animals were present at some point during the execution of the task.

5.3.2.3 Diagnostics module

The diagnostics module periodically reads the temperature from the TMP102 temperature sensor, memory and CPU usage and the IP address, and stores this information within the database. This diagnostics information allowed us to more easily debug software and device issues during the development phase.

5.3.3 Start-up and Initialisation Sequence

During the start-up and initialisation sequence (Figure 5.6), the device tests connectivity with the database, initialises sensors, moves the device to a known state and cleans the spoon.

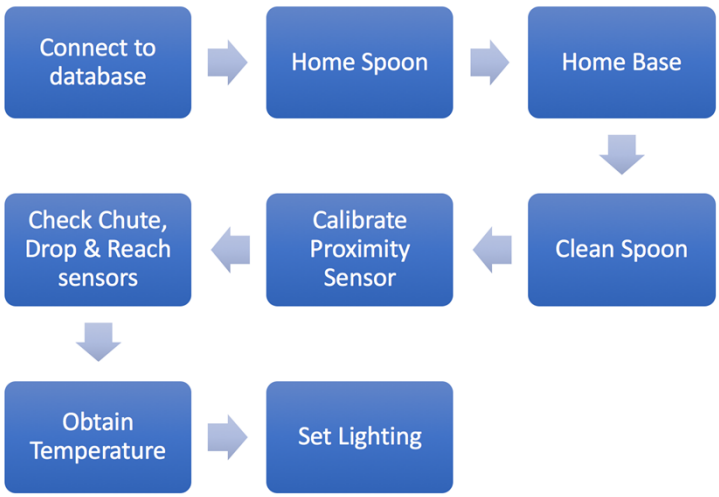

Figure 5.6 - Initialisation sequence of the RatBot.

During initialisation, the RatBot connects with the database (Mongo DB), carries out a time synchronisation and attempts to initialise the device as presented in the flow chart. The device is moved into a known home state. Reach, chute and drop sensors are checked for jams. The proximity sensor is calibrated. The spoon is cleaned. Diagnostic logging is initiated and lighting is set.

5.3.3.1 Database Connectivity

During the initialisation sequence (Figure 5.6), the firmware of each Pi attempts to connect to the Mongo Db instance (on the database server) to retrieve the current system time. This is necessary because the Raspberry Pi does not have an on-board battery required for the persistence of the system clock. Further, the private LAN (Figure 8.1) does not have access to the internet to execute a time synchronisation with a Network Time Protocol (NTP) server. Thereafter the RatBot registers itself in the database with its IP and MAC addresses. This data is used by the management application during device discovery and management.

5.3.3.2 Homing Sequence

During the homing sequence (Figure 5.7), the Spoon and Base are homed to a known position by moving the spoon and base until the respective home sensors are triggered. The spoon is homed first, to ensure that no collision will occur during the rotational homing movement. The base is then rotated towards the home position.

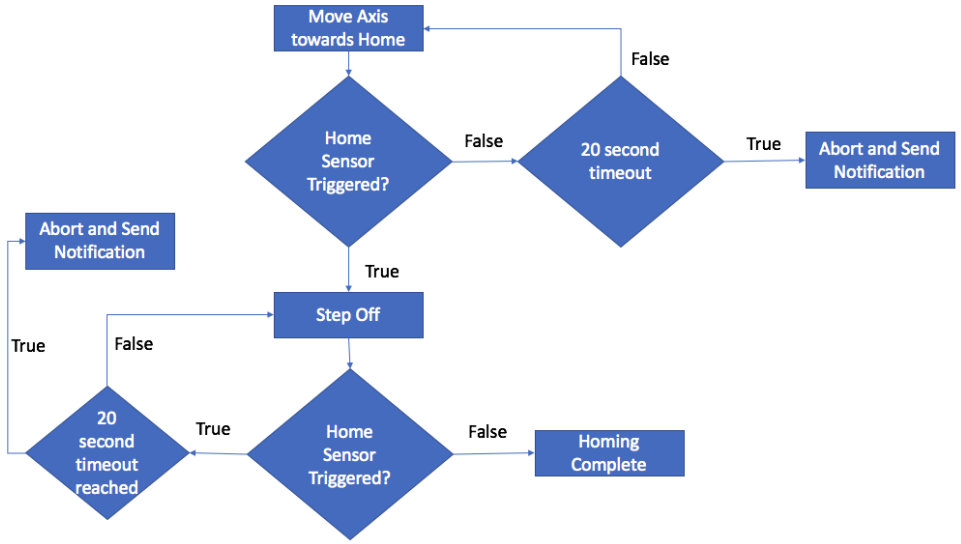

Figure 5.7 - Homing logic used for the spoon and rotational base.

The process of homing the rotational base and spoon. The axis is moved towards the home location until the home sensor is triggered. When the sensor is triggered, the axis reverses direction and steps off so that the sensor is not depressed persistently. If the home sensor is not triggered high within 20 seconds, the device stops, goes into an error state and sends an email notification to the user.

5.3.3.3 Cleaning

After homing, the spoon executes a sequence of movements to clean the proximity sensor. This is necessary because of the accumulation of dust and debris on the sensor over time. The sensor is passed under a brush (Figure 3.3-2) laterally in multiple directions to maximise the cleaning efficiency.

5.3.3.4 Calibration

Upon completion of the cleaning cycle, the firmware executes a calibration process that has been developed to calculate the optimum thresholds (Figure 3.23) required to determine if a pellet is present on the spoon or not, as follows. The spoon moves to its home position and records an average of 1000 proximity readings from the proximity sensor. This is regarded as the internal proximity threshold without a pellet. The spoon then extends to an external position (X=5, Y=5) and takes an average of 1000 proximity reads. This value is regarded as the external proximity threshold without a pellet. To detect if a pellet is present on the spoon when it is fully extended, the outside threshold is applied. Initially, the internal proximity threshold was used to determine if the pellet

was dispensed from the reservoir, but this proved unreliable and was replaced by the chute sensor.

5.3.4 Trial execution module

A firmware module was written to coordinate the execution of a single trial. This included the motion and sensor coordination required to dispense a pellet (Figure 5.9), and detect if a consumption, drop or timeout had occurred. A flow chart describing the trial logic is described in Figure 5.9.

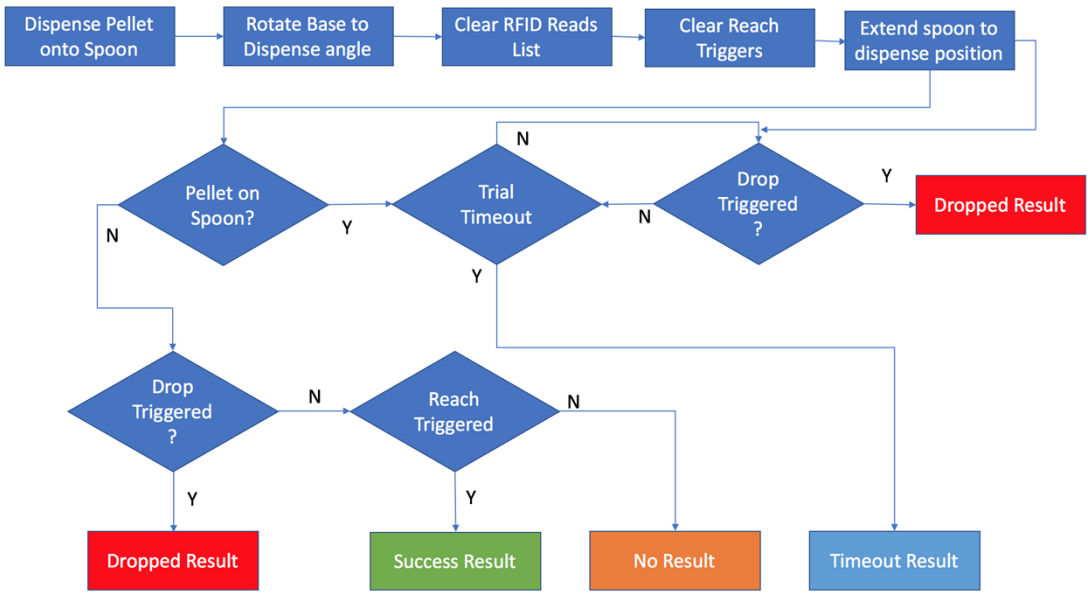

Figure 5.8 - Trial workflow and result logic, executed by the firmware.

The Trial execution module coordinates the motion control and sensor modules to dispense a pellet, position it at the required location and determine the success rate. This module also generates the data that is persisted to a database using a Trial data repository module.

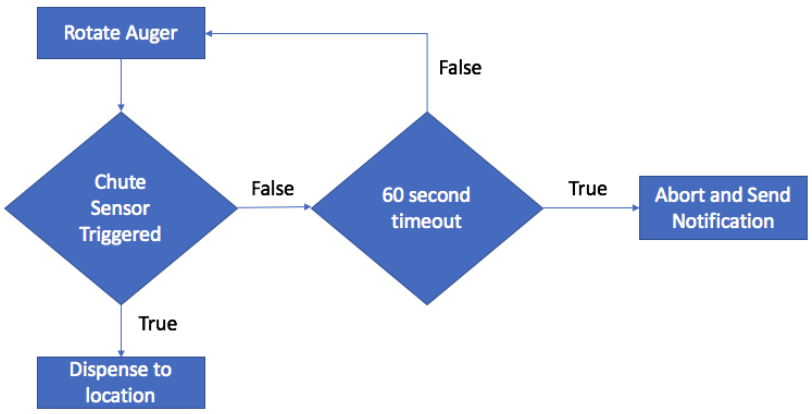

Figure 5.9 - Flow chart of the dispensing logic.

The Auger is rotated until a pellet is detected passing down the chute by the through beam chute sensor. If a pellet is not detected by the chute sensor within 60 seconds of starting the dispense, a timeout occurs and generates a notification that is emailed to the end user. This is usually an indication that the reservoir requires refilling, or possibly that the motor has failed due to an electrical or mechanical reason.

5.3.5 Management Application

A custom RatBot management application was designed and developed to manage a typical RatBot installation. The software allows users to view and manage RatBots and the data generated by the RatBots. The software was written in a modular, plugin pattern to allow other software modules to be created to introduce new functionality into the application. The management application interacts directly with the Mongo database and not directly with the RatBots. The database is used as an intermediate proxy to relay data and instructions between the management application and the RatBots.

5.3.5.1 Device Manager

The Device Manager user interface (Figure 5.10) enables the user to manage RatBots installed and operating within the system. The user may select any specific RatBot listed to control its operation and view status information. The user may initialise, reboot, start trials, stop trials and specify the trial position.

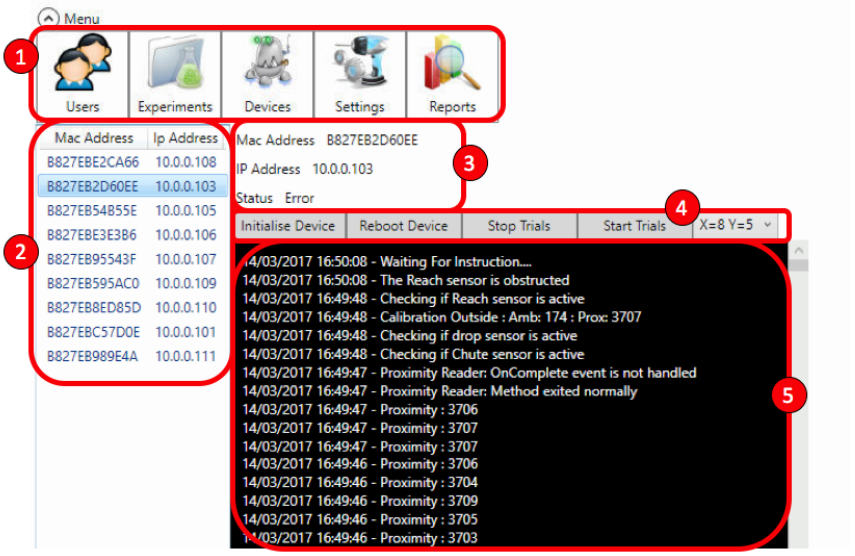

Figure 5.10 - RatBot management application device manager overview.

The RatBot device manager allows the user to view, control and manage all RatBots in a study.

1. A menu bar, which allows the user to switch context between Device Settings and Reports. Other menu items provide for future development of the application.
2. A device list is presented with the list of RatBots in the system. The Media Access Control (MAC) and Internet Protocol (IP) address is displayed for a given RatBot. Selecting a specific RatBot provides access to its logs and allows the user to control the device.
3. Status information about the selected RatBot is provided.
4. An operation toolbar allowing the user to Initialise, Reboot, Stop Trials, Start Trials and specify the trial testing position for the RatBot selected in (2).
5. A log history for the selected RatBot is presented to the user.

5.3.5.2 Trial Results

The trial results module provides a simple, summarised view of the selected RatBot results (Figure 5.11). A detailed and organised view of the trial data is exported to a comma separated variable (csv) file and is described in the next section.

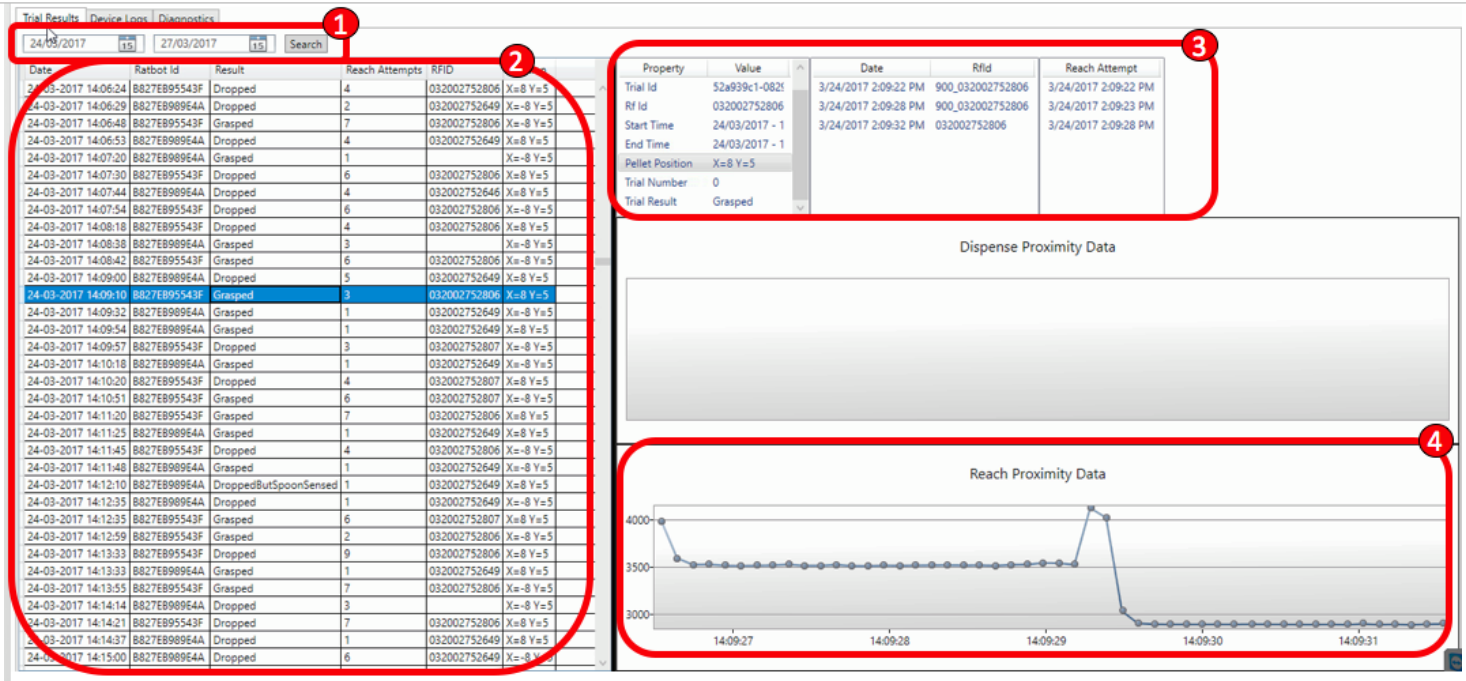

Figure 5.11 - RatBot management application Trial Result overview.

1. A search bar allows the user to search for trial results within a date range.
2. A list of the trial results is presented to the user containing the following information. Trial Date, RatBot Id, Trial Result, Reach Attempts, RFID & Position.
3. Summarised trial result information is presented here when a single trial is selected. RFID tags scanned during the trial as well as the timings for the reach attempts made during the trial is presented to the user.
4. The proximity data captured from the VCNL4000 embedded into the spoon is presented to the user in a graphical format.

5.3.5.3 Exported data

When the user retrieves data from within the Trial Result user interface (Figure 5.11) data is automatically collated, reformatted and exported to a comma separated variable (CSV) file for offline analysis. The following files are exported:

a. ReachAttemptsRaw.csv - A summary of the slit sensor trigger events in a day for a given rat described in Table 5.5.
b. TrialResultRaw.csv - A summary of every trial result stored in the database in a specified date range described in Table 5.6.
c. RfidInteraction.csv - All RFID readings taken whilst the device is running as described in Table 5.7.
d. SummaryResult.csv - A summary of all trial results on a specific date for a specific RFID as described in Table 5.8.

Property	Description
Date	The date on which the results were summarised for a specific rat.
RFID Number	The RFID of the rat that executed the trial.
Total Reach Attempts	The total number of triggers of the slit sensor recorded for this specific RFID.
Position	The position to which the pellet was dispensed.

Table 5.5 - ReachAttemptsRaw.csv export description.

Property	Description
Date & Time	The date and time of the trial result.
RatBot Id	The ID of the RatBot that the trial was executed on.
Result	The result of the trial. (Table 5.3)
RFID	The RFID number of the rat that executed the trial
Position	The position at which the pellet was dispensed during this specific trial.

Table 5.6 - TrialResultRaw.csv - The individual trial results recorded.

Property	Description
Date & Time	The date and time at which the RFID was recorded.
Device Id	The ID of the RatBot where the RFID was recorded.
RFID	The RFID number of the that triggered the RFID read.

Table 5.7 - RfidInteraction.csv - The RFID numbers recorded as the rat enters the RFID tunnel.

Property	Description
Date & Time	The date on which the summary was created for.
RFID	The recorded RFID number of the rat.
Position	The XY position to which the pellet was dispensed.
Dropped	The total number of drops recorded for the specific date for the specific rat.
DroppedButSpoonSensed	The total number of drops recorded but the proximity sensor still recorded a pellet presence.
Grasped	The total number of successful grasps detected on a given date for a specific rat.
FirstAttemptTimeout	The total number of occurrences of the FirstAttemptTimeout detected on a given date for a specific rat.
MaxAttemptsReached	The total number of occurrences of the MaxAttemptsReached detected on a given date for a specific rat.

Table 5.8 - SummaryResult.csv - A collated summary of the trial results.

The software and logical workflow described in this chapter allows us to programmatically control the electromechanical device and obtain trial results that may be analysed. The next phase of this iterative device development process is to assess the device operation in-cage using a small cohort of rats and is described in the next chapter.

Chapter 6

System Validation

6.1 Introduction

The development of the Ratbot was an iterative prototyping process which encompassed a continuous design, build, test and iterate workflow for all components. Each feature was tested in isolation, and as a unified device to verify correct operation. In this section, I will present a series of validations, both in-cage (with rats performing the tasks) and standalone (with a human simulating the rats' behaviour), of the various device components and functions. Sixteen videos are provided in Appendix A that show (in real-time) sensor output for each of the different operations and functions carried out by the device. These include initialisation, pellet dispensing and sensing, RFID sensing, pellet drop and successful retrieval of a pellet, both manually and in-cage by rats.

6.2 Methods

Standalone desktop validation techniques (with a human simulating the rat's behaviour)

During the standalone validations of the device, the component or function of interest was video recorded in High Definition (HD) using an Apple iPhone 6 at 30fps. Log information generated by the device was captured via screen recordings using QuickTime Player within OSX El Capitan. The captured log information was then overlaid using iMovie 10 onto the original video and time synchronised to demonstrate the success or failure of the validation of interest.

In-cage validation techniques (with rats performing the tasks)

During the in-cage validation, video of the interactions between the rats and the device was recorded in HD at 30fps and 120fps slow motion (where appropriate) using an Apple iPhone 5 or an Apple iPhone 6. Log data was persisted to a text file and a custom application (*Figure 6.1*) was developed (Visual Studio 2015, C# .NET) to visualise previously generated log information in a time synchronised fashion. The application was screen recorded using QuickTime Player and overlaid onto the original video using iMovie 10 to provide visual feedback of sensor and animal activity.

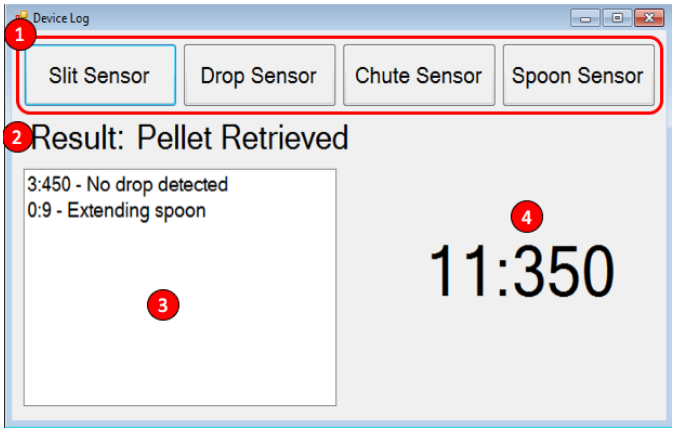

Figure 6.1 – Log visualisation application.

An application was developed to visualise historically generated log information. The application displays key sensor activity and log information in a time synchronised fashion.

1 – Sensor activity for the Slit, Drop, Chute and Spoon sensors are displayed.

2 – The result determined by the RatBot is shown here.

3 – Key log information is presented here. This includes information about mechanical actions and RFID tag data acquisition.

4 – A timer (seconds:milliseconds) provides a time reference.

This application enables the overlaying of previously captured log information on videos captured at that point in time.

6.2.1 Pellet dispenser validation

To verify the correct functioning of the pellet dispenser, a standalone pellet dispenser was mounted on a worktop above a waste container (*Figure 6.2*) and filled with approximately 1000 45mg sucrose pellets (Sandown Scientific, TestDiet 5TUT, dust free). Custom firmware was configured to automatically start-up and execute 250 dispense cycles using the chute sensor (*Figure 3.8* - 5) as positive feedback of a successful dispense. The dispense process was observed and instances of single and multi-pellet dispenses were recorded. Further validation of the pellet dispensing mechanism was achieved by simultaneously video recording the dispensing process, and capturing log information generated by the device.

Figure 6.2 – Standalone pellet dispenser mounted above a waste container.

The device setup used to validate the dispense functionality. 250 dispense operations were carried out and recorded to assess the reliability of dispensing single pellets.

6.2.2 Pellet positioning validation

It was important to validate that the pellet was dispensed to the intended locations. First, as described below, I verified that a pellet could be delivered immediately adjacent to the slit (position $0,0_{device}$) and that the rat could reach these pellets with its tongue or its forepaws. Next, I verified that a pellet could be delivered to positions that can only be retrieved with one or the other forepaw. As described previously (section 1.4), work by Ian Whishaw et al (Whishaw et al., 1986a; Iwaniuk and Whishaw, 2000; Alaverdashvili and Whishaw, 2010; 2013) has shown convincingly that if a pellet is dispensed to locations sufficiently to the left of the slit (e.g. $-6,13_{device}$ (Whishaw and Pellis, 1990b)), then the rat can only retrieve the pellet with its right paw (and *vice versa*).

Pellet positioning validation was achieved by placing a standalone RatBot on a worktop and running trials whilst being video recorded. A grid (Chartwell graph paper with 1, 5 and 10mm divisions) was overlaid with 30% opacity onto the original video recording using iMovie 10 in OSX El Capitan, and was used to determine the actual position vs the requested position for the specific trial. Trials were executed for the 5 positions specified in *Table 6.1*. The grid was used as a measurement reference and the positioning point of interest is the centre of the proximity sensor embedded into the spoon (*Figure 3.23*). Still images (*Figure 6.4*) were extracted from the video recordings (Appendix A – Videos

1,2 and 3) and markers were superimposed to highlight and assess the actual position of the point of interest. Red markers were used to indicated the XY_{device} (0,0) position and green markers were used to indicate the actual position of the centre of the proximity sensor that is embedded into the spoon.

Position (X_{rat},Y_{rat})	**Position (X_{device},Y_{device})**
(0,15)	(0,0)
(±4,19)	(±4,4)
(±8,20)	(±8,5)

Table 6.1 – Dispense positions used during pellet positioning verification

6.2.3 Sensor validation

A version of the RatBot firmware was developed specifically for validating the correct operation of the array of sensors contained within the device. To demonstrate this, the device was placed on a benchtop and all sensors were manually triggered to ensure that the firmware captured all inputs and reads data from sensors correctly. The VCNL4000 proximity sensor was tested using a vendor provided development kit (*Figure 6.5*) by placing a 45mg sucrose pellet directly onto the sensor and capturing the sensor readout using the provided test application. The integrated sensor (i.e. within the spoon) was tested in a similar fashion with a 45mg sucrose pellet over many place-remove cycles (Appendix A – Video 5). The chute sensor was tested by manually dropping pellets, one at a time down the pellet chute and verifying that the sensor changed state appropriately (Appendix A – Video 6). The drop sensors were prototyped and assessed in a standalone fashion using the drop sensor electronics (*Figure 3.25*, *Figure 4.12*) and an LED which served as a trigger indicator (Appendix A – Video 7). The integration test of the drop sensor was carried out using the assembled device along with the test firmware which displayed the drop sensor activity. 45mg sucrose pellets were manually dropped down each of the left and right drop chutes to ensure that the sensors triggered correctly (Appendix A – Video 8). The slit sensor was validated using the test firmware by placing an obstruction within the slit to mimic a limb of a rat reaching (Appendix A – Video 9). Sensor feedback from the test firmware application was used to confirm their correct operation.

6.2.4 Manual validation of integrated operation

Standard operating firmware was loaded onto the device and trials were run and recorded. Videos of various segments of the device operation were isolated and presented alongside time synchronised logs. This includes the following sequences:

1. Initialisation (Appendix A – Video 10).
2. Trial execution at position $(\pm 4,4)_{Device}$ simulating drop and retrieval scenarios (Appendix A – Video 11).
3. Automated cleaning after a pellet remained on the spoon between trails (Appendix A – Video 12).

To assess the performance of a RatBot during a continuous sequence of trials, video footage (Appendix A – Video 13) was obtained of a run of approximately 55 minutes that was executed manually whereby pellets on the spoon were randomly retrieved or dropped down the drop chute using a tweezer. The pellet reservoir was filled to approximately two thirds capacity with the aim of avoiding double dispenses. An RFID tag (900_032002752798) was manually moved into the scanning zone of the RFID reader within the tunnel. These manually executed trial actions were then compared to the results determined by the device.

6.2.5 In-cage validation with rats performing the tasks

The RatBot was placed in cage with two adult Lister Hooded female rats that were acclimated to the automated task and the 45mg sucrose pellet reward. Video interaction was recorded to demonstrate licking, drop, grasp and RFID read events of the device in cage and is presented with video using the techniques described above (Appendix A – Videos 14,15 and 16).

6.3 Results and Discussion

First I validated the correct stand-alone operation of each of the component parts of the final version of the RatBot (sections 6.3.1 to 6.2.3). Next, I validated the correct operation of the RatBot as an integrated device on the benchtop (section 6.3.4) and finally I validated the correct operation of the RatBot using adult rats (section 6.3.5).

6.3.1 Pellet dispense validation

In a run of 250 consecutive pellet dispenses, the pellet dispenser exhibited a 98.9% average success rate. A dispense anomaly, where 2 pellets are simultaneously dispensed (*Figure 6.3*) was observed, accounted for 1.1% of dispenses. It was noted that the double dispense events occur near the beginning of the test session when the reservoir was filled with approximately 1000 45mg sucrose pellets, and after a 'settling' period, the dispenser consistently dispensed single pellets. This early double dispense anomaly may be due to the organisation of the pellets and the height to which it is filled within the reservoir. It must also be noted that double dispensing was not observed when using polished augers manufactured from stainless steel, whereas the devices that exhibited this double dispense behaviour were manufactured using SLS 3D printing technologies which does not yield as smooth a surface. The next iteration of the device will make use of the polished stainless steel augers which may fully eliminate this observed anomaly.

The representative video recording (Appendix A – Video 4) of the dispense action confirmed that the device only proceeds to the pellet presentation step after a pellet has been detected by the chute sensor.

Further validation of pellet dispensing was performed when integrated into the RatBot on the benchtop and using adult rats (see section 6.3.4 and 6.3.5).

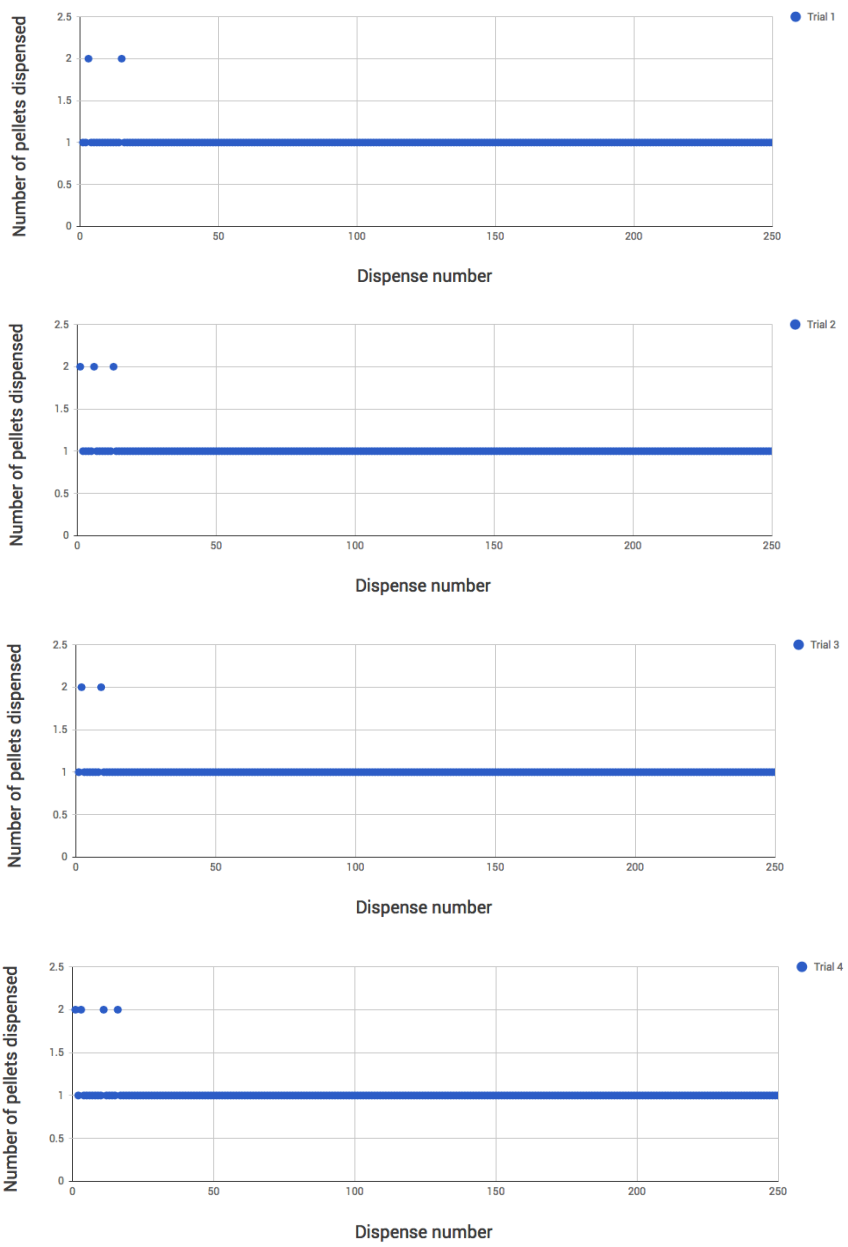

Figure 6.3 – Number of pellets dispensed per dispense cycle.

A >98% success rate in single pellet dispensing was observed when dispensing in 4 batches of 250 consecutive trials. The dispense data indicates that the double dispenses occur only rarely and typically at the start of a dispense cycle, directly after the pellets have been loaded into the device. Later dispenses consistently delivered single pellets.

6.3.2 Pellet positioning validation

Observation of a large number of trials during device development and testing confirmed that pellets were dispensed consistently to the desired locations. For example, it can be seen in videos (Appendix A – Videos 1,2 and 3) that the distance between the XY_{Device} (0,0) indicated by the red marker, and the centre of the presented proximity sensor (green marker) was within 0.5mm of the target position. Pellets were dispensed consistently to the desired locations. It was observed that the centre of the pellet could be up to 1.5mm from the centre of the spoon. This variation in the position of the pellet on the spoon is due to the size of the recessed cut-out in which the proximity sensor resides (which may be reduced in future) after being dropped from the top of the pellet chute in the reservoir. However, this small amount of the positioning variability may have minimal impact on reaching studies due to the broad range of rat reaching capabilities determined in Chapter 2 and because we selected final positions for reaching that are sufficiently to the left and right of the slit. Variation in positioning of the spoon may be accounted for by backlash in the rotation worm gear (*Figure 3.15*) and spoon leadscrew (*Figure 3.20*) mechanisms. Minor variations in the fabrication and assembly quality of the device may also account these positioning variations. In future, a combination of linear and rotary encoders, along with higher quality manufacturing processes may remove the positioning variability within the spoon movement.

Further validation of pellet positioning was performed when integrated into the RatBot on the benchtop and using adult rats (see section 6.3.4 and 6.3.5). This includes a video (Appendix A – Video 13) of a 55-minute set of consecutive trials which demonstrates that a pellet can be delivered consistently to one of four pre-programmed positions $(\pm 4,4; \pm 8,5)_{device}$.

In Chapter 7 and Chapter 8, I describe experiments in which I observed that the rats were able to retrieve pellets presented to one side of the slit only with their contralateral paw and not their ipsilateral paw (or with their tongue), as has been shown before by Prof. Ian Whishaw et al (Whishaw et al., 1986a; Iwaniuk and Whishaw, 2000; Alaverdashvili and Whishaw, 2010; 2013).

a.	b.	c.
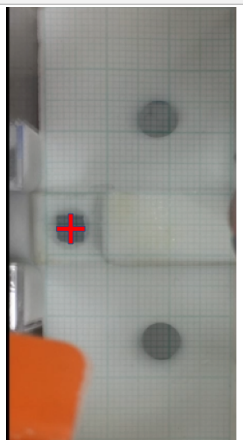	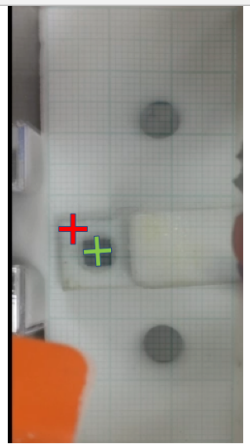	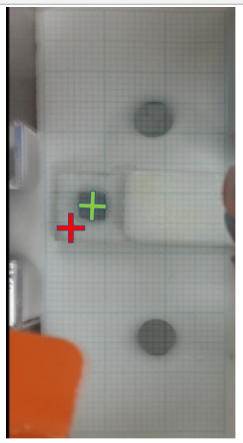
d.	e.	
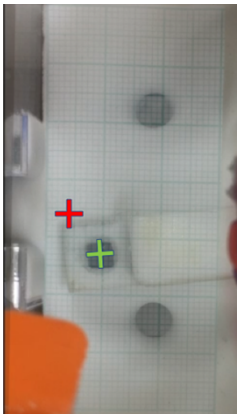	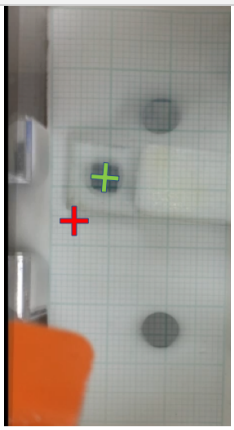	

Figure 6.4 – Pellet Position validation.

Still images of the positioned spoon were extracted from captured videos (Appendix A – Videos 1,2 and 3) and markers were superimposed to verify correct positioning. Positioning was found to be correct to within 0.5mm. Variation in positioning between trials was not discernible. The red cross indicates the XY_{Device} (0,0) position. The green cross indicates the actual position of the centre of the proximity sensor embedded into the spoon.

a. XY_{Rat} (0,15) → XY_{Device} (0,0)
b. XY_{Rat} (4,19) → XY_{Device} (4,4)
c. XY_{Rat} (-4,19) → XY_{Device} (-4,4)
d. XY_{Rat} (8,20) → XY_{Device} (8,20)
e. XY_{Rat} (-8,20) → XY_{Device} (-8,20)

6.3.3 Sensor validation

Proximity Sensor

The VCNL4000 proximity sensor was able to detect the presence of a 45mg sucrose pellet during all test cycles, when tested with the vendor supplied evaluation kit by applying a detection threshold to the proximity readout. Due to variations in lighting and environmental conditions, an automatic calibration described in section 5.3.3.4 was implemented to determine the appropriate thresholds to be applied for pellet detection for each RatBot separately. A video (Appendix A – Video 5) of the integrated proximity sensor (*Figure 3.6*) confirms that the proximity sensor functions similarly to the evaluation kit and that thresholding is a viable method for pellet presence detection.

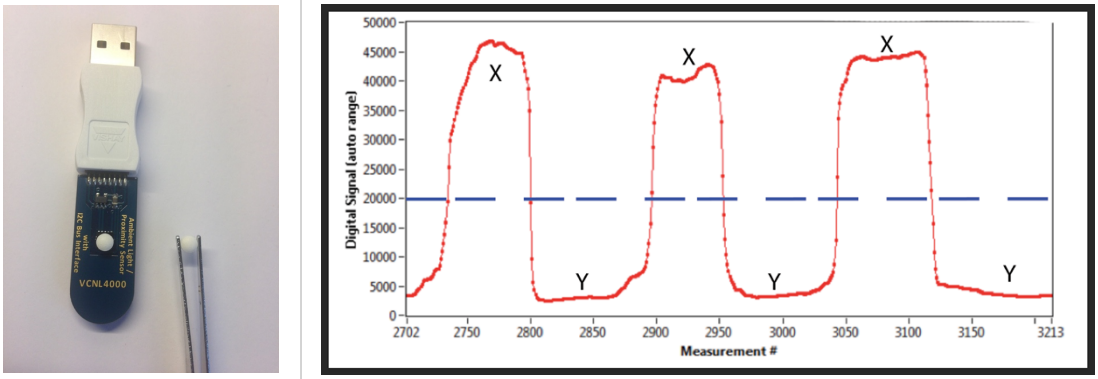

Figure 6.5 - Proximity data acquired using a VCNL4000 USB Sensor Kit by Vishay Electronics.

A VCNL4000 sensor evaluation kit was used to capture proximity recordings with pellets on and off the sensor. A capture of the recordings made by the supplied software is presented here. A pellet was placed on (X) and subsequently removed from (Y) the VCNL4000 proximity sensor. A shift in proximity readings is observed, allowing for the use of thresholding (at a reading of 20000 units) as a possible pellet presence determination algorithm.

Chute Sensor

The chute sensor (*Figure 3.6*) function was validated by observing the correct sensor states when a pellet was dropped down the chute (Appendix A – Video 6, *Figure 6.6* – two trials are presented). Further validation of the chute sensor was performed when it was integrated into the RatBot on the benchtop and using adult rats (see section 6.3.4 and 6.3.5).

a.	b.
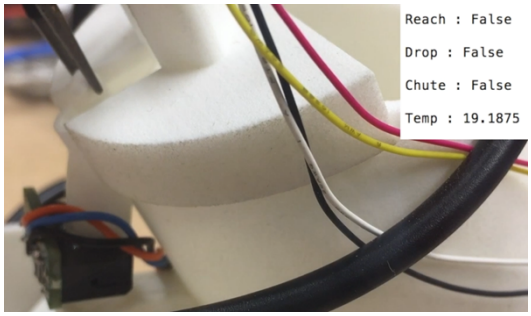	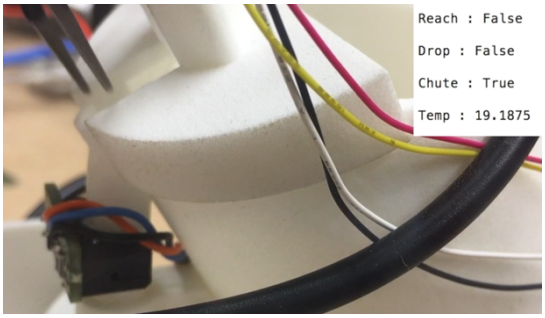

Figure 6.6 - Chute sensor validation through video confirmation

Before and after images extracted from Appendix A – Video 6, taken during the validation of the chute sensor operation.

a. Before the pellet was dropped down the chute. A pellet can be seen in the tweezer at the top left of the image. Chute = False.
b. After the Chute Sensor detected the pellet that was dropped. The empty tweezer can be seen in the top left after the pellet has been released. Chute = True.

Drop Sensor

The drop sensor (*Figure 3.6*) function was validated in standalone mode during the development of the device (Appendix A – Video 7 – Four trials are presented). Correct detection of a dropped pellet was further observed when operating as part of an integrated device with test firmware (Appendix A – Video 8).

Further validation of the drop sensor was performed when it was integrated into the RatBot on the benchtop and using adult rats (see section 6.3.4 and 6.3.5).

a.	b.
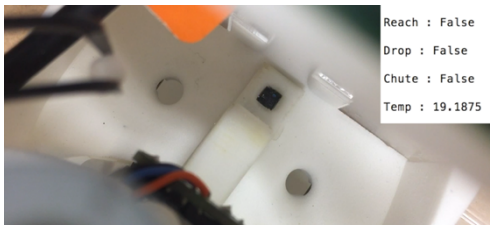	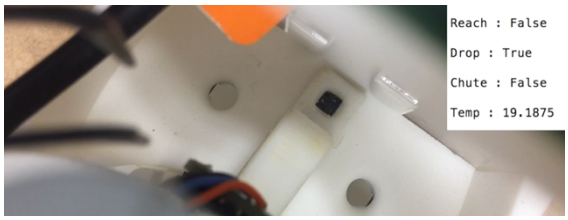

Figure 6.7 - Drop sensor validation through video confirmation

Before and after images extracted from Appendix A – Video 8, that were taken during validation of the drop sensor operation.

a. Before the pellet was dropped down the drop sensor. A pellet can be seen in the tweezer at the top left of the image. Drop = False.
b. After the Drop Sensor detected the pellet that was dropped. An empty tweezer can be seen at the top left after the release of the pellet. Drop = True.

Slit Sensor

The slit sensor (*Figure 3.6*) (also referred to as the Reach sensor) was validated as part of the integrated device operation whilst in test mode (Appendix A – Video 9 – Three trials) which confirms that an object within the slit is detectable by the device.

Further validation of the slit sensor was performed when it was integrated into the RatBot on the benchtop and using adult rats (see section 6.3.4 and 6.3.5).

a.	b.
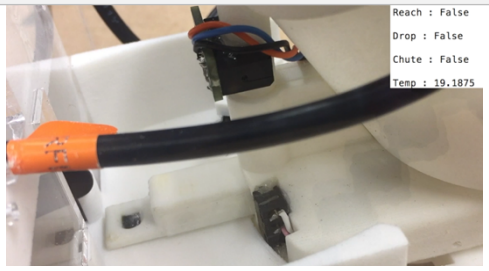	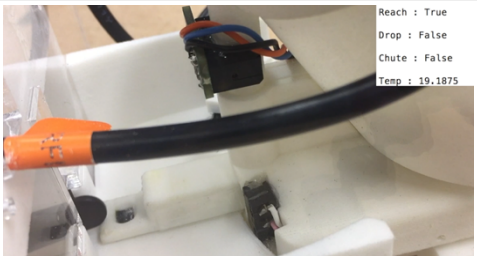

Figure 6.8 - Slit sensor validation through video confirmation

Before and after images extracted from Appendix A – Video 9, that was taken during validation of the slit sensor operation.

a. Before the obstruction was introduced. A black spatula can be seen protruding through the slit above the sensor. Reach = False.
b. After the Slit Sensor detected the obstruction. A black spatula can be seen protruding through the field of view of the slit sensor. Reach = True.

6.3.4 Manual validation of integrated operation of the entire device

Video 10 (Appendix A) shows the log output during the initialisation routine. The RatBot moves to a home position, cleans the spoon and its sensor, and then calibrates the proximity sensor in the spoon. Proximity readings of ~11000 can be seen when the spoon is retracted and, as expected the reading changes to ~3000 when the spoon is extended. The threshold values of 11857 and 3137 obtained during calibration in this instance are used to determine if a pellet is on the spoon when retracted or extended respectively.

Video 11 (Appendix A) shows the log output during reaching trials at position $(4,4)_{device}$ and $(-4,4)_{device}$. A pellet is dispensed onto the spoon at the home position. After extending the pellet to the target position, the proximity sensor reading changes from ~6800 to ~3000 indicating that the pellet has been displaced from the spoon. The log file shows that RatBot correctly judges that this represents a successful retrieval because the drop sensors were not activated. The spoon then returns to the home position and a new pellet is dispensed. In the second trial, the log file shows that the RatBot correctly judges that that pellet is removed but is dropped down the drop chute.

In some trials, a pellet is dispensed but no rat attempts the task for a configurable period of time. This scenario is determined by the software to be a timeout. Video 12 shows that under these circumstances, the pellet that remains on the spoon is cleaned off so that it falls down the drop chute. A new trial is commenced at a later time, according to the training or assessment schedule.

Video 13 (Appendix A) shows a 55-minute set of consecutive trials. This video shows that a pellet can be delivered consistently to one of four pre-programmed positions $(\pm4,4; \pm8,5)_{device}$. The RatBot correctly judged in 100% of these trials whether the pellet was retrieved or dropped. 15 trials were carried out at position $(4,4)_{device}$ and 62 trials at position $(8,5)_{device}$. Of the 77 trials, only a single dispense anomaly (8min:38s) was observed whereby the pellet dropped off the spoon prior to reaching its target position. The drop sensor was triggered, the proximity sensor detected a pellet removal, and zero reaches were recorded. The RatBot management software handles this kind of rare dispensing anomaly because it excludes from analysis any trials in which the reach sensor fails to detect a reach and yet the pellet is removed from the spoon and falls down the drop chute. Accordingly, this single instance of a dispensing anomaly was appropriately handled by the software. For all the other trials, the RatBot drew the correct conclusions: i.e. whether the pellet had been manually retrieved or dropped. This accounts for a 1.29% anomaly rate during this test. Moving forward, a tighter guarding

mechanism may be added to ensure that the pellet is dispensed directly onto the centre of the proximity sensor that is embedded into the spoon.

6.3.5 In-cage validation with rats performing the task

The performance of the RatBot sensors was also validated by monitoring their output during reaching by rats.

Video 14 (Appendix A) shows a rat entering the RFID tunnel and the corresponding output of the RFID sensor showing that the RatBot detected the rats' unique identification code. The RatBot is seen to have positioned a pellet correctly next to the slit such that the rat can retrieve it with its tongue.

Video 15 (Appendix A) shows a rat retrieving a pellet with its paw; the log shows that the reach sensor was activated and that the spoon sensor detected removal of the pellet and, because the drop chute sensors were not activated, the RatBot correctly concluded that the pellet had been retrieved.

Video 16 (Appendix A) shows a rat reaching for a pellet with its forepaw but it displaces it from the spoon. The reach sensor detected the reach and the pellet sensor detected the displacement of the pellet and, because the drop chute sensors were activated, the RatBot correctly concluded that the pellet had not been retrieved but had been dropped.

With these videos, it has been demonstrated that the array of sensors are capable of detecting slit interaction, drops and successful retrievals by rats, in their home cage.

6.4 Conclusion

In this chapter, a series of validations has been presented to confirm the correct functioning of the device, both in-cage and in standalone mode with manual operation. Several enhancements have been identified to improve the reliability of the dispensing and positioning system and these features will be improved in subsequent versions of the RatBot. The results obtained from these validations demonstrate that the device is suitable for use in in-cage stroke studies to further validate its ability to train and identify a reaching deficit in rats after CNS injury. In subsequent chapters, in-cage experiments will be carried out using an array of devices within a standard animal holding room. Visual inspection in these experiments contributed to the validation of the performance of the RatBots.

Chapter 7

The In-cage training and assessment of a cohort of rats before and after stroke

Acknowledgements:

Photothrombotic surgery training and assistance was provided by Lawrence Moon and Sotiris Kakanos. The end of study termination of rats, fixing and extraction of brains was carried out by Claudia Kathe.

7.1 Introduction

This study was designed to provide further insight into the functioning of the various features, software and electromechanical components of the RatBot in a networked, multi-cage environment outside of the animal holding rooms. We also sought to gain insight into whether the device could reliably detect a motor deficit after stroke in a smaller cohort of rats, allowing us to develop the analysis techniques required to interpret the generated data correctly.

The device would be used to acclimate and train naïve rats on the single pellet reaching task using their left forepaw. The rats will then be given a cortical stroke on the right hemisphere. An assessment period will follow to understand if the device could detect a reaching deficit.

Issues relating to improper device operation would be identified and rectified on an ad-hoc basis throughout the study as part of the iterative development process.

7.2 Methods

Animal procedures were carried out in accordance with the guidelines and regulations provided by the United Kingdom Home Office (Home Office, 2014) and the Animals (Scientific Procedures) Act 1986. Rats had access to standard chow and water ad libitum and were housed in a standard 12-hour day/night cycle.

10 Female Lister Hooded rats (18-month-old, 240g) were implanted with Radio Frequency Identification (RFID) tags (SmartChip, FDX-B, ISO 11874/11785) under anaesthesia (induced at 5% Isoflurane, O_2 1 L/min, maintained at 2% Isoflurane) one week prior to the commencement of the study. Rats were originally housed as a litter (2 x groups of 4 and 1 group of 2) and subsequently split randomly into pairs, in 5 large rat cages (Techniplast 1354G). This communal housing strategy was adopted with the outlook that a greater probability of even interaction between the device and each animal may be observed with two rats.

Rats were introduced to the 45mg sucrose pellets (Sandown Scientific, TestDiet 5TUT, dust free) by sprinkling approximately 3-5g of the pellets into a cage daily for 3 days prior to the introduction of the RatBot™. Daily, at approximately 9am, the 5 cages of rats were transported from an animal holding room to an animal behaviour room and placed on a workbench. A single RatBot™ was placed inside each cage (Figure 7.1, Figure 7.2) and attached to a private network (Figure 7.3). The private local area network (LAN) was setup to facilitate communication between the RatBots, a Mongo database (v3.0) server (MacBook pro, late 2011, core i5), a DHCP server (MacBook Pro, late 2011) and an 8-port Ethernet router (Netgear GS110TP-200EUS ProSAFE) with Power over Ethernet (POE) capability.

a.	b.
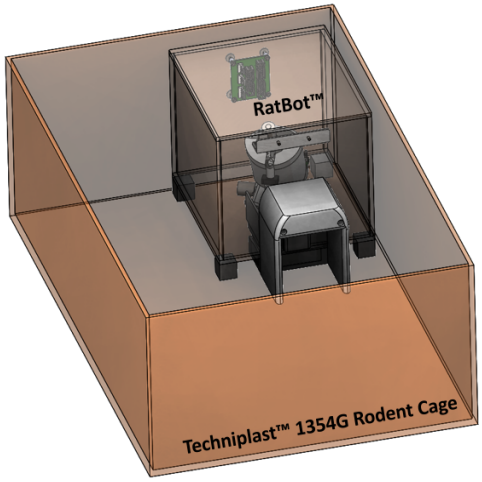	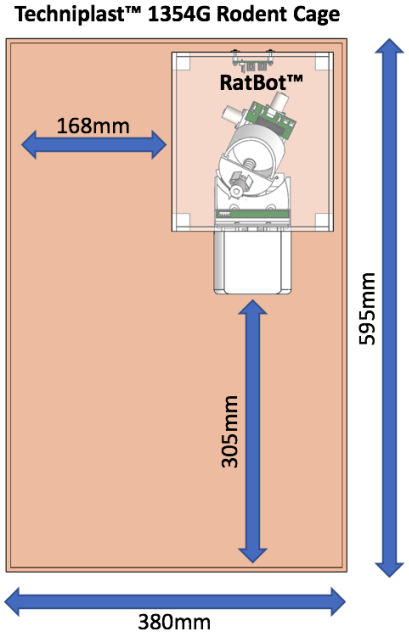

Figure 7.1 - Position of the RatBot™ inside a Techniplast 1354G series -117/-120 rodent cage.

a. A 3D rendering of the RatBot inside the Techniplast cage.
b. A top view indicating the available space inside the Techniplast cage with the device present.

a.

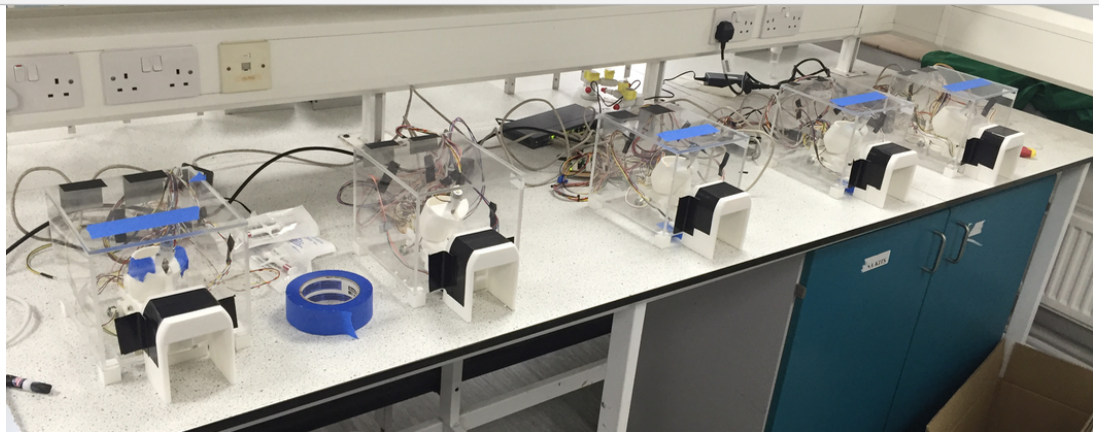

b.

Figure 7.2 - Workbench arrangement of in-cage RatBots.

a. RatBots being prepared for installation into the cages. Devices were connected and tested on the benchtop outside of the cages prior to installation.
b. An array of cages with RatBots installed and executing trials.

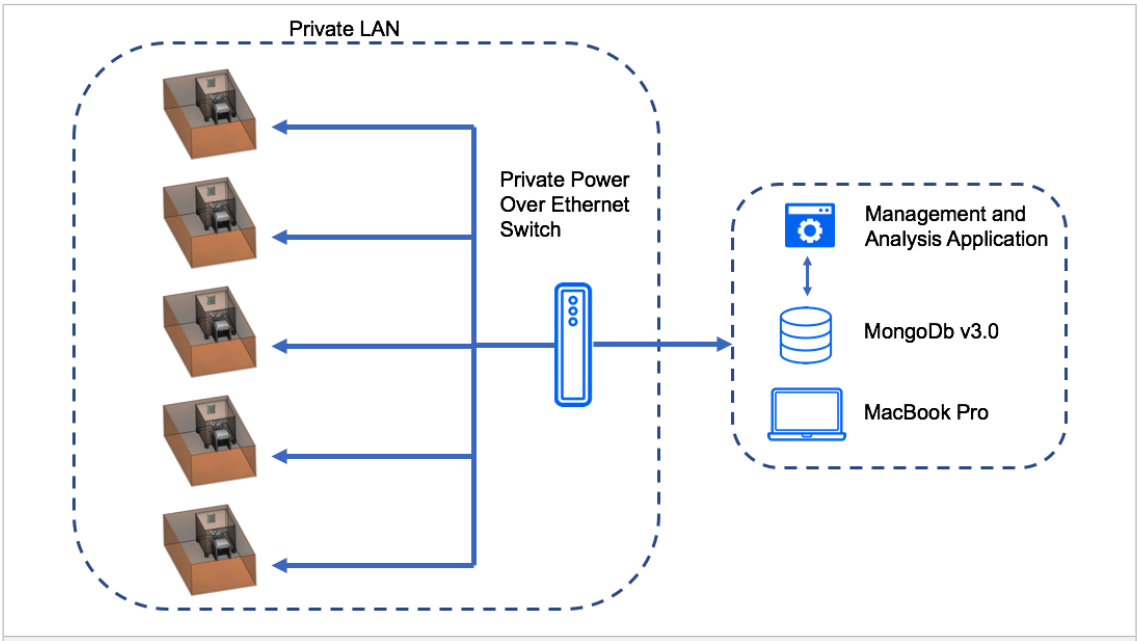

Figure 7.3 - Ratbot network architecture during workbench operation.

An array of 5 devices in-cage were connected to a Netgear POE switch that facilitated communications and power delivery. A MacBook pro (late 2011, Core i5) served as a DHCP and a Mongo database server. The management and analysis application was hosted within a Windows 7 Pro, Parallels Virtual Machine on the MacBook pro.

Trials were run at various dispense positions for varying time periods (Table 7.1) to understand how positions should be altered during training. Trials were run for up to 3 hours a day and devices were run in parallel. All positions used (Table 7.1) required use of the left forepaw for grasping. As part of the ongoing validation of the RatBot hardware, firmware and software, hundreds of trials were inspected visually in real-time for correct dispensing and positioning of the pellet. Any minor problems were corrected as part of the ongoing iterative improvements in the device.

X_{rat}	Y_{rat}	Duration (days)
0	15	4
5	20	3
7	20	1
9	21	9

Table 7.1 - Trial positions and duration acclimation and training.

The device was run in acclimation mode at position XY_{rat} = (0,15) for 4 days while device operation was analysed. This was followed by 3 days at position XY_{rat} = (0,20). A short attempt at position XY_{rat} = (7,15) was attempted before progressing to the final position of XY_{rat} = (9,21). After 9 days of training at the desired reach position of XY_{rat} = (9,21), the rats were given a cortical lesion in the right motor cortex using the photothrombotic model of stroke.

7.2.1 Photothrombotic Stroke Procedure

(Stutzmann et al., 2002; Lindau et al., 2014; Wahl et al., 2014; Becker et al., 2016).
Rats were anesthetised using 5% isoflurane in O_2 at a flow rate of 1L/min, and maintained at 2% isoflurane in O_2 at 1L/min. Each rat's weight was recorded and the head was shaved from between the eyes to ahead of the ears. The intraperitoneal injection site was shaved. Both shaved areas were disinfected using ethanol swabs. Analgesia (Carprieve 20:1 2.5ml/kg) was administered prior to any incision. The rat was then placed on a heated blanket (Harvard Instruments) to maintain a 37°C body temperature using a rectal thermometer. The rat was then mounted on a stereotaxic frame using ear bars to stabilise the animal's skull during surgery and to correctly position the cold light source. A sterile drape was placed over the animal as part of the aseptic technique and to prevent any effect of the ambient room lighting on the Rose Bengal that would be administered later. After checking that hind limb and forelimb withdrawal reflexes and corneal blink reflexes were absent, the skin was incised from ahead of the eyes to between the ears. Bulldog clamps were used to keep the skin laterally tensioned and away from the working area. The periosteum was scraped from the skull using the scalpel on the contralateral side to the rat's tested paw. A foil template with a 5mm x 6mm window was used to focus the light source was placed in position above the sensorimotor cortex (±5mm symmetrically across Bregma and 0.5 to 5.5mm laterally) (Figure 7.4).

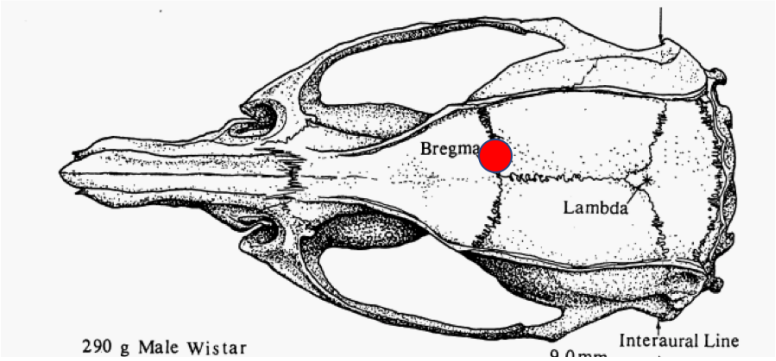

Figure 7.4 - Skull diagram showing positioning of the light source.

A 9mm-diameter fibre optic light guide connected to a cold light source (Schott KL 1500) was placed at the area (±5mm symmetrically across the bregma and 0.5 to 5.5mm laterally) indicated by the red circle above during the exposure period to activate the rose Bengal.
(image: Paxinos and Watson Rat Brain Atlas, 4th edition)

The fibre optic end of a cold light source (Schott KL 1500) was positioned over the window of the foil template but not turned on. The rat was covered using a blanket to prevent any ambient light exciting the Rose Bengal. An IP injection of Rose Bengal (30mg/kg) was administered and left for 13 minutes to circulate. After 13 minutes, the cold light source was turned on 3300K, full aperture (setting E). After 10 minutes, the cold light source was turned off. The exposed skull was rehydrated using saline, the skin was sutured using 3-0 absorbable sutures and the rat was placed in an incubator set at 32ºC. Rats were placed back in their cages after recovering from the anaesthesia and provided with a soft diet. Cages were placed back in the animal holding room and were covered to prevent possible activation of the Rose Bengal due to light exposure. Analgesia (Carprieve 20:1 2.5ml/kg) was given 24 and 48 hours post-surgery to prevent any postoperative discomfort.

7.2.2 Trials resumed

The rats were allowed between 4 and 7 days to recover before resuming the in-cage reaching trials. All remaining sutures were removed on day 5 after stroke. On days 1 and 2 of post stroke trials, the RatBot™ was run in acclimation mode which dispenses pellets at position XY_{rat} = (0,15). Subsequent trials were executed at the previously taught position XY_{rat} = (9,21).

7.2.3 Histology

Rats were euthanized at the end of the study on day 20 and perfused with phosphate buffered solution (PBS) and then fixed with 4% paraformaldehyde (PFA) in PBS (pH 7.4). Brains and RFID tags were extracted and stored individually in 30% sucrose in PBS (pH 7.4). The RFID tag of the rat was attached to the storage container for later identification. 2mm-thick coronal cross sections (Figure 7.5) were later taken using a rat brain matrix with 1mm slice spacing, to measure the infarct volumes.

a.

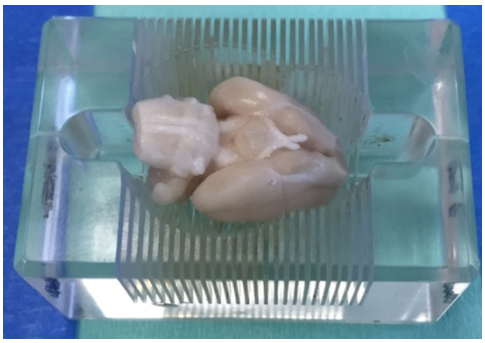

b.

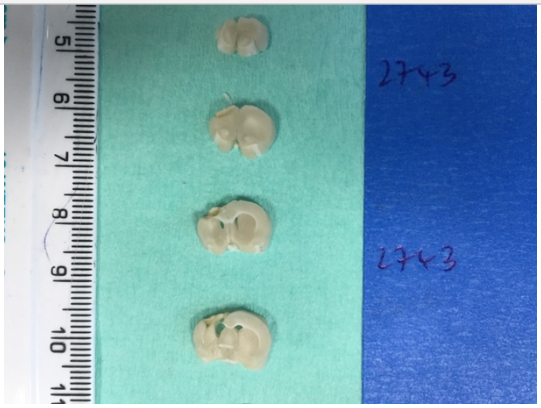

Figure 7.5 - Rat brain slices used to determine lesion volume.

Rat brains were extracted and sliced into 2mm slices to approximate the lesion volume. This would be used correlate lesion volumes with grasping deficits.
a. Brains were placed into a Rat Brain Matrix with 1mm section spacing.
b. 2mm cross sections were taken in the coronal plane over the length of the brain.

Intact portions of the left and right hemispheres of each slice were highlighted using Photoshop Creative Cloud (CC) 2016 in red and blue, respectively. Images were then calibrated to real world dimensions and the overall lesion volume was calculated as follows:

Approximate infarct volume of each slice =

(Area intact hemisphere - area lesioned hemisphere) x slice thickness

Total lesion volume = ∑ *slice lesion volume*

a.	b.
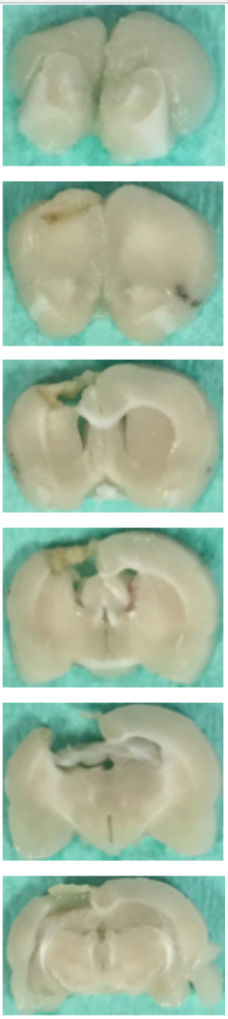	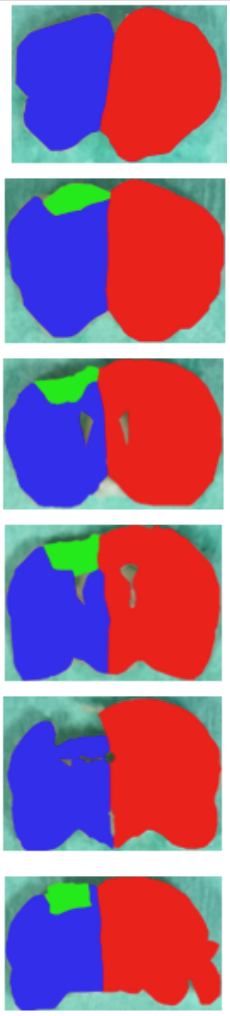
Not to scale	Not to scale

Figure 7.6 - Left and right hemisphere section images and analysis.

The 2mm brain slices were outlined and lesion areas were calculated for each calibrated image using Photoshop CC 2017.

a. Brain slices before highlighting in Photoshop.

b. Brain slices after highlighting in Photoshop. Red: Non-lesioned hemisphere, Blue: Lesioned hemisphere, Green: Lesioned Area.

7.2.4 Noise measurement

Sound measurements were taken using a Dr Meter MS10 digital decibel sound level meter at 1cm from the outside of the RatBot™. Measurements were taken during normal RatBot initialisation and dispensing operation when placed outside of the rat cage in a non-anechoic room.

7.2.5 Results analysis

Reach results generated by each RatBot was stored inside the system database and the RatBot management application described in section (Chapter 5) provided a facility to export data for offline analysis. Results were analysed using Microsoft Excel, Prism 7 (Graphpad) and Statistical Package for the Social Sciences (SPSS) v24 (IBM).

Paired two-tailed t-tests were calculated in Prism 7 using pellet reaching data to determine if a reaching deficit was observed between reaching data at two time points or the means of two groups of time points (Figure 7.7). This was also used to evaluate participation differences before and after stroke. All paired t-tests were two-tailed. Means of consecutive days were used because of the day-to-day variabilities in the rats' motivation to undertake the task.

One sample t-tests were calculated with Prism 7 using pellet reaching data to determine if a non-zero difference in average daily trial counts were observed between cohabitating rats.

Pellet reaching data was analysed in SPSS using linear models and Restricted Maximum Likelihood estimation to accommodate data from rats with any missing values (Duricki et al., 2016). Akaike's Information Criterion (AIC) showed that the model with best fit for the data before and after stroke from the preferred paw had a First-Order Autoregressive covariance structure. Degrees of freedom were expressed to the nearest integer. Days were regarded as covariant. A $p <= 0.05$ is regarded as statistically significant. M and SD represents the Mean and Standard Deviation respectively. Results were presented with 3 significant figures.

7.3 Results

Two rats were excluded due to lack of interaction with the device and a further two were excluded due to post stroke complications. The excluded animals were humanely euthanized due to observed nose bleeds and seizures. Average daily grasping success rates of the rats pre-stroke and post-stroke at position XY_{rat} = (9,21) was calculated and analysed. A further rat was humanely put down post stroke resulting in a post stroke n=5.

Stroke caused a rapid decrease in grasping success (Figure 7.7; comparing mean of days -1 and -2 with mean of days 1 and 2; M=-26.6, SD=14.5; paired t-test; t_4=4.1; p=0.015). This deficit persisted at least one week (comparing means of days -1 and -2 with mean of days 8 and 9; M=-30.6, SD=17.1; paired t-test; t_4=4.0, p=0.016) and was maintained until the end of the study at day 20.

A training effect was observed in pre-stroke reaching success rates (Figure 7.7, linear model analysis - First-order autoregressive; n=6; $F_{1,23}$=6.9; p=0.015). No recovery in reaching success was observed post stroke (Figure 7.7, linear model analysis - First-order autoregressive; n=5, $F_{1,21}$=0.013, p=0.911).

Infarct volumes (Figure 7.8a) ranged from 23.1mm^3 to 135.1mm^3 (M=64.6mm^3, SD = 41.3mm^3). No relationship between infarct volume and the decrease in grasping success rates after stroke (Figure 7.8b) was observed r=0.74, p<0.15 (Pearson's correlation coefficient).

A difference in trial participation of cohabitating rats was observed pre-stroke (Figure 7.9; one sample t-test; M=43.6, SD=24.5; t_3=3.56, p=0.0378).

There was no observable difference in trial participation when comparing trial data before and after stroke for individual rats (Figure 7.10; M=-15.4, SD=33.6; paired t-test; t_6=1.22, p=0.27).

Rats were weighed daily post stroke for 10 days and then weekly as part of the health and wellbeing monitoring. No noticeable weight loss (Figure 7.11) was observed over this period.

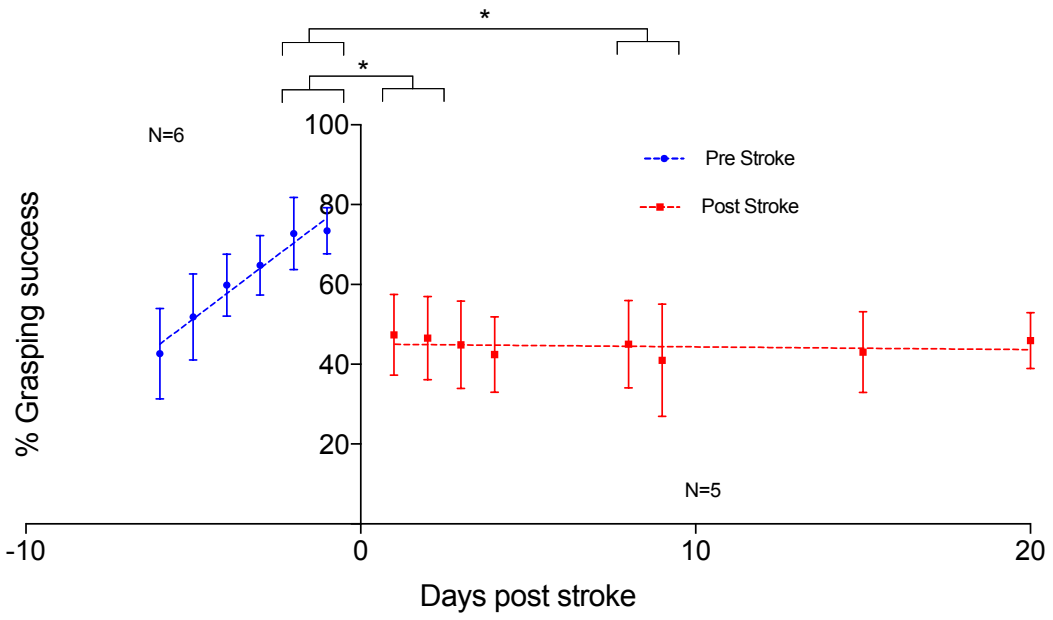

Figure 7.7 - Average daily grasping success across the cohort of rats at XY_{rat} = (9,21) indicates a deficit is observed.

A decrease in grasping success was observed after stroke (M=-30.4, SD=15.9; paired t-test; t_4=4.276, p=0.0129).

A training effect is observed pre-stroke (Linear Model Analysis - First-Order autoregressive; n=6, $F_{1,23}$=6.9, p=0.015).

No recovery effect was observed post-stroke (Linear Model Analysis - First-Order autoregressive; n=5, $F_{1,21}$=0.013, p=0.91).

Error bars indicate ±SEM

a.

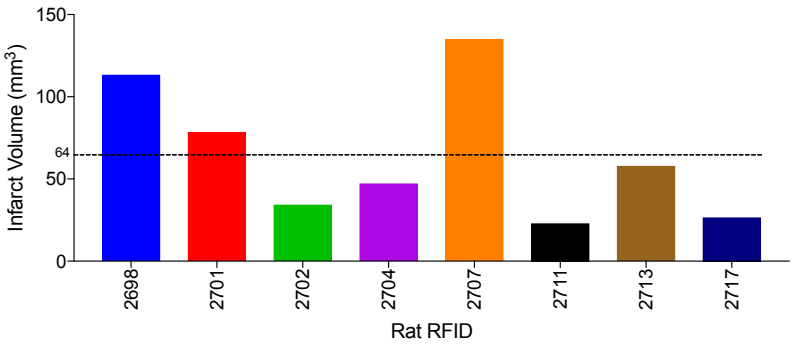

b.

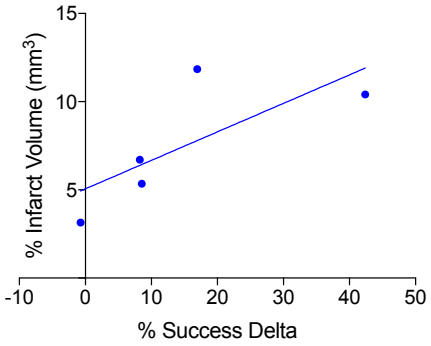

Figure 7.8 - No relationship between infarct volume and reaching deficit was found.

a. Lesion volumes varied between 23.1mm^3 and 135.1mm^3 (M=64.6mm^3, SD=41.3mm^3)

b. No relationship between infarct volume and the decrease in grasping success rates post-stroke was observed r=0.742, p=0.151 (Pearson's correlation coefficient).

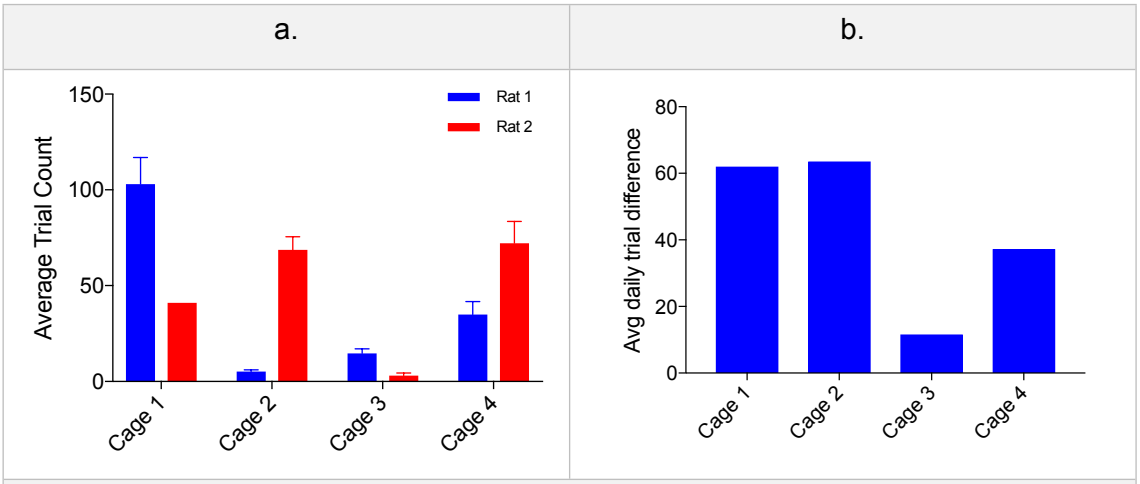

Figure 7.9 - Cohabitating rats have different participation levels in the task pre-stroke.

a. The average daily trials per cohabitating rat.
b. The difference between average daily trials of cohabitating rats.

A participation difference between rats in the same cage was found pre-stroke (M=43.6, SD=24.5) t_3=3.56, p=0.0378 (one sample t-test comparing sample data to a theoretical population mean of 0).

Error bars indicate ±SEM.

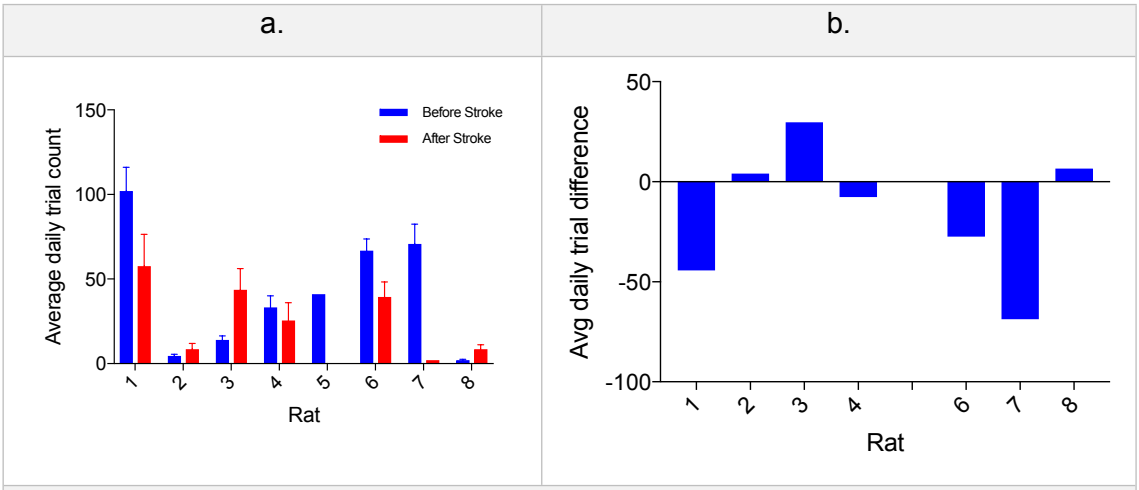

Figure 7.10 - Trial participation before and after cortical stroke.

a. The average daily trail count before and after stroke.
b. The difference between average daily trials before and after stroke. Negative values indicate a decrease in participation.

There was no evidence of a difference in average daily trial participation after stroke compared to before stroke (M=-15.4, SD=33.6; paired t-test; t_6=1.22, p=0.27).

Error bars indicate ±SEM.

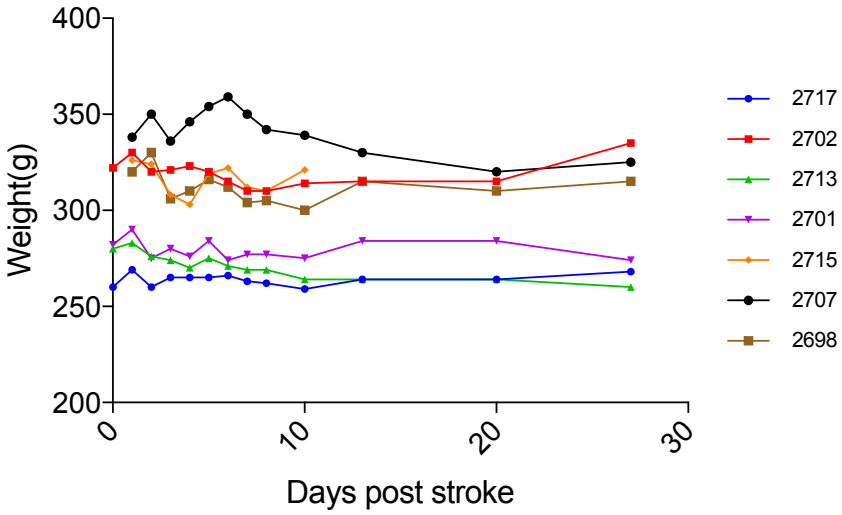

Figure 7.11 Rat weight was monitored post stroke over the study.

No noticeable weight loss was observed post stroke.

During the design and development of the device, we aimed to keep the operating noise low. The sound level was measured to be 41.8dB during the dispensing and 52.6dB during initialisation 1cm from the outside of the RatBot (Figure 7.12).

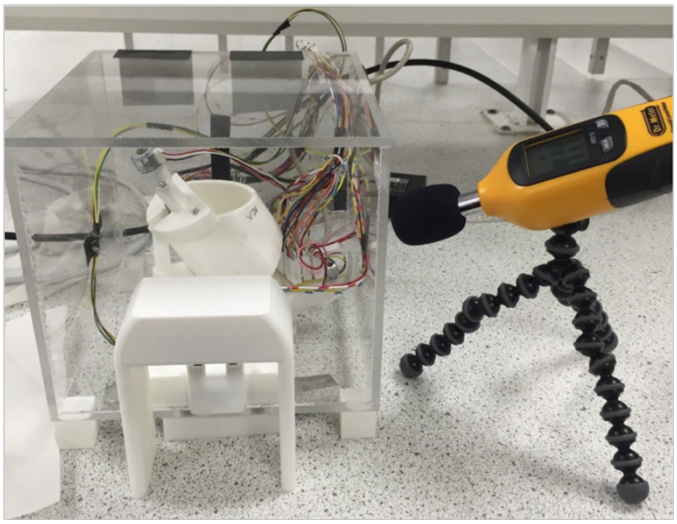

Figure 7.12 - Operating sound levels of the RatBot™

Noise measurements were taken 1cm from the outside of the RatBot™ enclosure. During dispensing noise was measured to be 41.8dB. During the initialisation sequence when motors were active, noise was measured to be 52.6dB.

7.4 Discussion

The study has demonstrated that a RatBot™ can successfully automate the training and assessment of forelimb reaching ability before and after cortical stroke. An array of RatBots in a networked configuration, operating for short daily sessions (up to 3 hours) has been shown to be able to detect a deficit after a unilateral cortical stroke.

7.4.1 General device operation

Here we have shown that the RatBot can automatically dispense a 45mg sucrose pellet from a pellet reservoir and position it at a programmable location. We have also shown that the RatBot can determine if the rat has consumed or dropped the pellet hence providing insight into its motor skills and forelimb motor coordination.

7.4.2 Lesion Volume

We had found no evidence of a correlation between lesion volume and reaching performance. This study may have been underpowered to detect a relationship. The next study will incorporate a larger cohort of rats and this relationship will be re-examined.

7.4.3 Post stroke complications

Two rats were humanely euthanized post stroke due to a nose bleed in one rat and seizures in a second rat. The causes of these observed symptoms is not known but similar seizures (barrel rolling) have been linked in other stroke studies to damage to the ventricles in the endothelin-1 model of stroke (Soleman et al., 2010). It may be possible that the same is true for the photothrombotic model of stroke.

7.4.4 Interaction with the RatBot™

In this study, a networked set of RatBots operated during the light cycle in a well-lit environment. Once acclimated to the task, in daily sessions, rats actively participated at the start of the session but it was observed that the rats seemed disinterested after 2 to 3 hours of executing trials and were not engaging towards the end of the session, preferring to rest or sleep. This may be due to the timing of the trials being carried out in the day cycle when the rats are less active (Whishaw et al., 2013). This reinforces the need for studies to be carried with trials executed in the night cycle (as I have done in Chapter 8).

It was also noted that the average number of trials executed by rats in the same cage were unevenly distributed. This may be as a result of social dominance (Ramirez, 2013; Jupp et al., 2016; Moneo et al., 2017) and opens up the possibility of this device not simply being used for reach related assessments but to understand social dominance of a cohabitated cage, and possibly a mixed gender in-cage assessment. It also requires investigation in to how the device and/or its control software may be designed to attempt to evenly distribute trials between rats in the same cage, for example, a gate that prevents access to specific rats based on historical interaction data.

It is also possible that some rats simply did not learn the task adequately even though they had adequate opportunity to interact with the RatBot, and based on visual observations, were not actively excluded by a dominant partner. The interaction of rats in cage 3 (Figure 7.9) were the lowest of all cages throughout the study. This would indicate that there may be a requirement to motivate the rats to interact with the device further by food restriction or increase task difficulty more gradually. Further, it is possible that the lack of interaction is due to the daytime execution of the task, as well as taking place outside of their holding rooms after a brief transit which may have increased stress levels.

Visual inspection of hundreds of trials confirmed that when a pellet was dispensed to the right of the slit ($9{,}6_{device}$) then it could be retrieved by only the left paw. There were no instances where the rat could use its right paw to retrieve pellets from this location. This is consistent with work by Prof Ian Whishaw (Whishaw and Pellis, 1990b; Whishaw et al., 2008c).

7.4.5 Acclimation and device jamming

During the initial acclimation phase of the study, the rats responded cautiously to the presence of the RatBot and pushed cage bedding through the reaching slit (Figure 7.14), clogging the drop zone (Figure 7.13), which obstructed the drop and slit sensor. The size of the drop chute is not sufficiently large to allow the bedding to fall through, and the current choice of sensor precludes us from making the hole larger. However, other sensors may be compatible with a larger drop chute and will be considered when developing the device further. Further bedding sizes and types will be investigated at a later stage (Chapter 8) as a possible option to reduce jamming. Jams due to bedding in this study were not a hindrance as they were cleared as soon as they occurred allowing the task to continue. This will not be as convenient during overnight in-cage studies.

Figure 7.13 - Top view of a drop sensor jam due to cage bedding.

During the initial acclimation phase, when the RatBot is first introduced into the cage, rats actively push bedding through the slit and into the device jamming the drop and slit sensors.

Figure 7.14 - Slit sensor and slit jam due to cage bedding.

When the RatBot was first introduced into the cage, rats actively pushed bedding into the RFID tunnel which obscured the entrance preventing task execution. This behaviour had resulted in the jamming of the through beam sensors incorporated into the 11mm slit.

7.4.6 Quality of fabrication

Further device and software refinements are required moving forward to increase ease of use, unattended operation and component reliability. For this study devices were

printed out of PLA using a MakerBot 2 Replicator. The quality provided is more suited to a prototyping process and is dissimilar from high quality machined components. To increase overall reliability and build quality, the device would require different fabrication methods, which are usually achievable with good quality electromechanical fabrication service providers. The devices used in the next study (Chapter 8) were produced by Shapeways using higher quality 3D printing fabrication techniques.

7.4.7 Animal well-being

Throughout the study, rats had access to food and water ad libitum. No noticeable weight losses were observed post stroke and visual inspection of the rats revealed no observable negative disposition. Surgical wounds healed and required no additional attention. This positive post-surgery outlook may allow for longer studies spanning many months without possible welfare concerns. The low noise levels achieved (41.8dB to 52.6dB) is similar to that of a household refrigerator (noisehelp.com) which, from visual observations during device operation, did not have adverse effects (a lack of startle behaviours at the start of a device movement) on the rats. Future development, component choices and fabrication methods may further reduce the sound emitted by the device.

Chapter 8

The In-cage training and assessment of a large cohort of rats before and after stroke

Acknowledgements:

Daily maintenance of devices was assisted by Sotiris Kakanos. Photothrombotic surgery assistance was provided by Sotiris Kakanos. Post-op surgical care was assisted by Sotiris Kakanos. The end of study terminating of rats, fixing and extraction of brains was assisted largely by Aline Spejo and Sotiris Kakanos.

8.1 Introduction

This study was designed to provide further insight into the longer term, overnight operation of the RatBot™ in a networked, multi cage environment inside a standard animal holding room. The RatBot will be used to acclimate, train and assess naïve young adult Lister Hooded rats before and after a unilateral cortical stroke.

With this study, we aim to answer the following questions:

1. Can the RatBot determine a deficit in grasping after a unilateral cortical stroke?
2. What maintenance regimes are required?
3. Is the device reliability sufficient to run longer term overnight studies?

As in the previous study, issues relating to improper device operation would be identified and rectified on an ad-hoc basis throughout the study as part of the iterative development process.

8.2 Methods

Animal procedures were carried out in accordance with the guidelines and regulations provided by the United Kingdom Home Office (Home Office, 2014) and the Animals (Scientific Procedures) Act 1986. Rats had access to standard chow and water ad libitum and were housed in a standard 12-hour day/night cycle.

8.2.1 Animals

24 Female Lister Hooded, 4-month-old (200-220g) rats purchased from Charles River UK were implanted with SmartChip FDX-B RFID tags under anaesthesia 1 week prior to commencing the study, as described in section 7.2. Rats were originally housed as a litter (group of 4) which were then split at random into groups of 3. The rats had access to food and water ad libitum throughout the study.

8.2.2 Infrastructure

The RatBot network (Figure 8.1) consists of a private local area network and a database server running MongoDB v3.0. A standard rodent cage rack (Figure 8.2) was fitted with a Netgear GS724 24-port gigabit switch with POE capability and a Gigabyte Brix Core i3 mini PC with Windows 7 Professional and MongoDB v3.0 installed. Cat6 Ethernet cables were custom assembled and installed to enable connectivity to each RatBot (Figure 8.3)

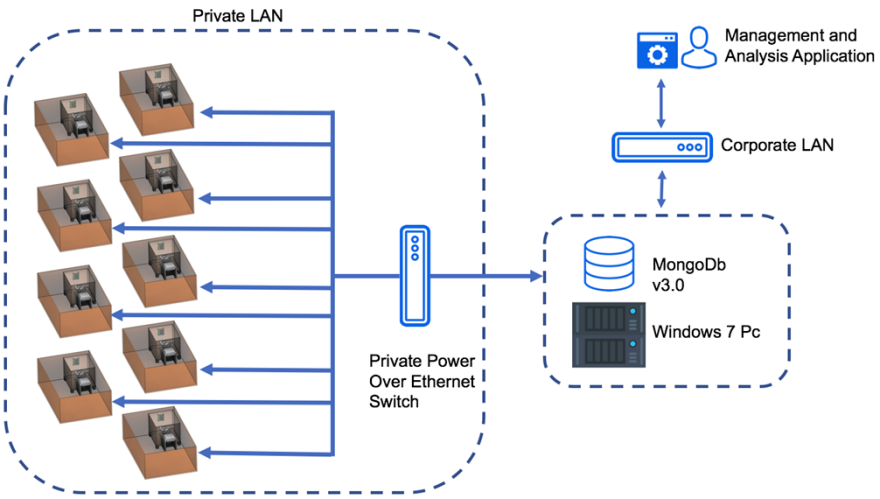

Figure 8.1 - RatBot system architecture implemented during overnight operation.

A typical RatBot network architecture encompasses a private LAN created using a POE enabled Ethernet switch, a local PC serving as a database server (MongoDB v3.0) and a DHCP server to allocate IP addresses to RatBots in the network. The PC is accessible from a corporate network so that instructions and data may be passed between the Management application and the RatBots.

a.

b.

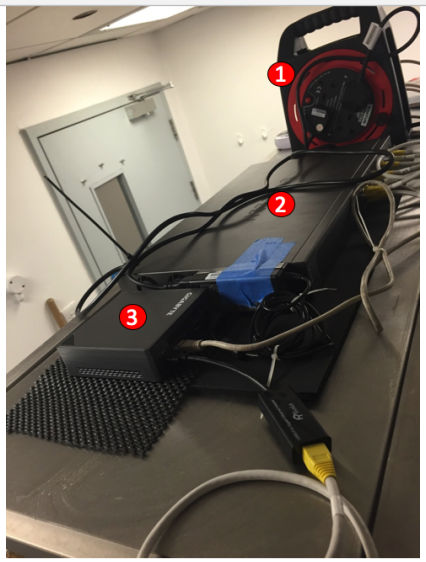

c.

Figure 8.2 - The infrastructure required in a typical RatBot installation.

a. Minimal infrastructure is required to install and operate an array of RatBots. All cages have unobstructed access from the front of the rack. Eight cages located in the top row and left column were used throughout the study. The cage rack was shared with other ongoing studies.

b. The supporting infrastructure is mounted on the top of the cage rack and cabling is routed at the rear of the rack.
   1. A power extension reel with residual current device (RCD) and thermal overload protection.
   2. A Netgear GS724 POE switch.
   3. A Gigabyte Brix i3 small form factor PC.

c. Cat6 cable routing and infrastructure on the top and rear of the cage rack.

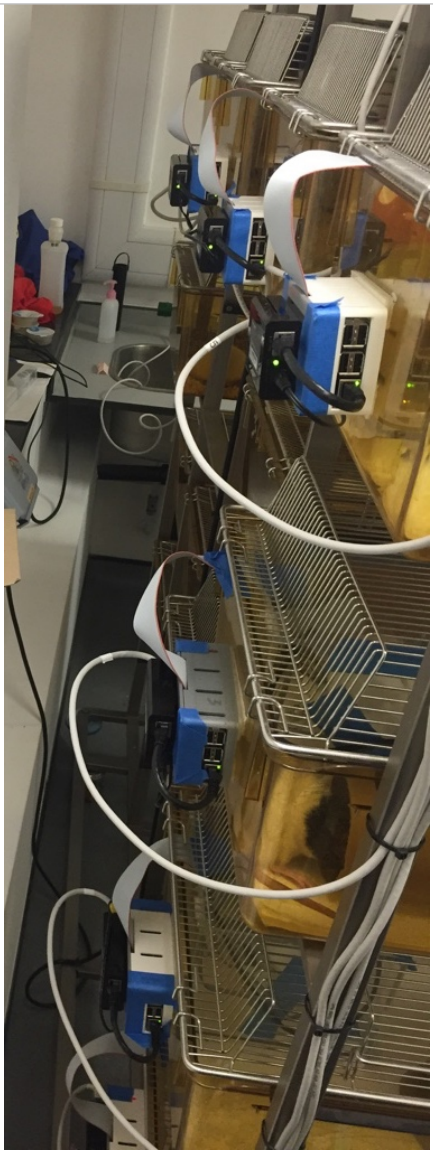

Figure 8.3 - Rear view of a typical cage rack with RatBot infrastructure.

Here the rear view of the cage rack is shown to highlight the installation of the external-to-cage control electronics mounted at the rear of each cage. The electronic enclosures are attached to the cages using Velcro, which endures a standard cage wash (75ºC) and hence, needs not be removed from the cage.

8.2.3 Daily Operation

A single RatBot was installed into each rat cage and was removed once daily to be cleaned and to replenish reservoirs with 45mg sucrose pellets. If a sensor obstruction was reported by the device, it was removed from the rat cage for cleaning and replaced thereafter. RatBots were configured to run trials nightly from 9pm to 7am. Trials were run continuously and all rats had access to the RatBot ad libitum. Rats were not restricted from executing trials. Initially, pellets were dispensed close to the slit XY_{rat}= (0,15) for easy acquisition by the rat using its tongue. The left paw was trained between day -50 (50 days before stroke) and day -32. Training of the right paw was introduced at day -32 up to day 0 (the day of stroke surgery). Pellets were progressively placed further away from the slit, finally alternating symmetrically between the left and right positions as described in Figure 8.4. The symmetric dispensing automated the training and assessing of both the left and right forepaw of each rat. Trial data from the device was automatically persisted to a MongoDB database for later analysis.

Right Paw Position (X,Y)	Duration (Days post stroke)
(-1,16)	[-32 → -22]
(-3,18)	[-22 → -19]
(-5,20)	[-19 → -17]
(-8,20)	[-17 → 42]

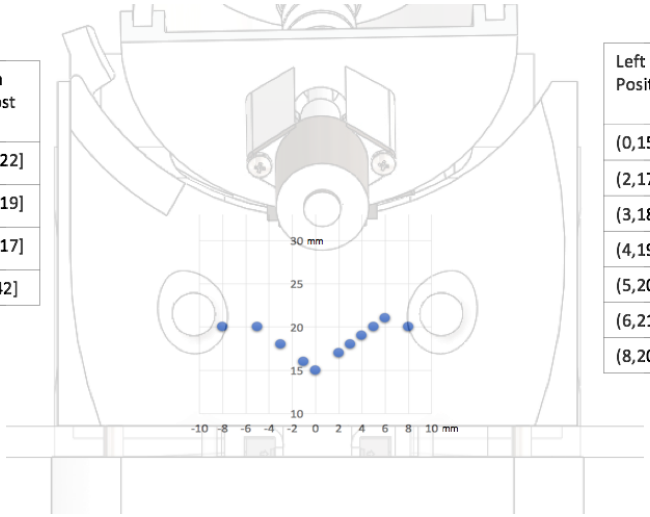

Left Paw Position (X,Y)	Duration (Days post stroke)
(0,15)	[-50 → -49]
(2,17)	[-49 → -47]
(3,18)	[-47 → -45]
(4,19)	[-44 → -42]
(5,20)	[-42 → -40]
(6,21)	[-40 → -30]
(8,20)	[-29 → 42]

Figure 8.4 - Dispense position timeline of a typical training and assessment schedule

An overview of the typical dispense positions and respective durations used during the study. The left forepaw was initially trained from 50 to 32 days pre-stroke, followed by both left and right training from 32 days pre-stroke.

8.2.4 Handedness determination

The handedness of the rat was determined by comparing the median of the mean daily grasping success rate of the left and right forepaw at position XY_{rat}= (8,20). The higher of the two values was regarded as the dominant or preferred forepaw. Ischemic stroke was induced in the cortex contralateral to the determined preferred forepaw.

8.2.5 Photothrombotic Stroke

A photothrombotic stroke was induced as described in section 7.2.1. In this study, the stroke was induced within the cortex contralateral to the determined preferred forepaw. The light source positions are indicated in Figure 8.5.

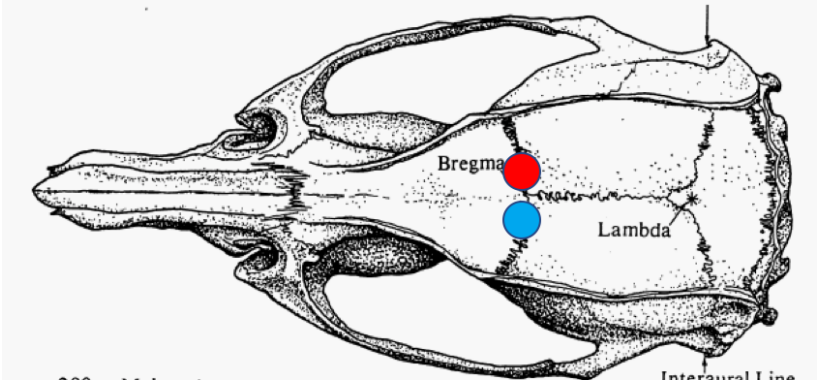

Figure 8.5 - Skull diagram showing positioning of the light source.

A fibre optic light guide connected to a cold light source (Schott KL 1500) was placed at the areas indicated during the exposure period of the stroke procedure to activate the Rose Bengal.

Right hemisphere, left preferred paw (Red): (±5mm symmetrically across Bregma and 0.5 to 5.5mm laterally)

Left hemisphere, right preferred paw (Blue): (±5mm symmetrically across Bregma and -0.5 to -5.5mm laterally)

(image: Paxinos and Watson Rat Brain Atlas, 4th edition)

8.2.6 Temperature and light collection

The control electronics for the RatBot was placed inside of the rat holding room and configured to record ambient lighting (Figure 8.6a) and temperature (Figure 8.6b) readings for a period of 5 days. The VCNL4000 sensor provides ambient light data in the form of a 16bit count that has no unit. Readings were obtained prior to installing the RatBots into the holding room. Readings were stored in a database for later analysis.

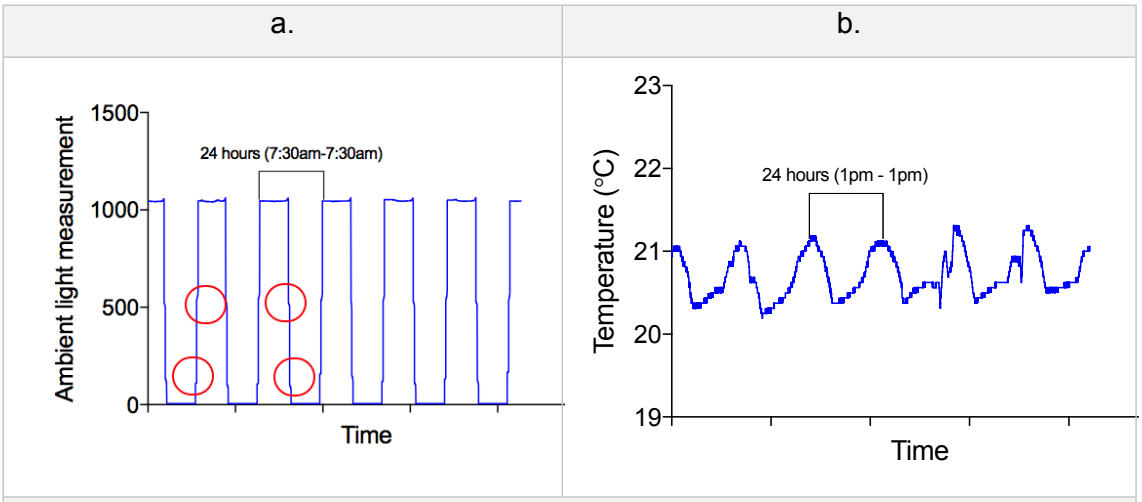

Figure 8.6 - BSU Ambient light and temperature measurements taken pre-study.

a. Measurements were taken at 1 second intervals. The dawn dusk step change in lighting is indicated by the circled areas and occurs over a 30-minute period.

b. A temperature fluctuation of less than one degree was observed with an average temperature of 20.7ºC. This is within the operating temperature of the devices and components in use.

8.2.7 Results analysis

Reach results generated by each RatBot was stored inside the system database. The RatBot management application described in section (Chapter 5) provides the facility to export data for offline analysis. Results were analysed using Microsoft Excel, Prism 7 by Graphpad and SPSS v24.

Paired two-tailed t-tests were calculated with Prism 7 using pellet reaching data to determine if a reaching deficit was observed between reaching data at two time points or two groups of time points for both preferred and non-preferred forelimbs. It was also used to evaluation participation differences before and after stroke. All paired t-tests were two-tailed.

One sample t-tests were calculated with Prism 7 using pellet reaching data to determine if a non-zero difference in average daily trial counts were observed between cohabitating rats. All one sample t-tests were two-tailed.

Pellet reaching data was analysed in SPSS using linear models and Restricted Maximum Likelihood estimation to accommodate data from rats with any missing values (Duricki et al., 2016). Akaike's Information Criterion (AIC) was used to determine the covariance

structure with the best fit for the data before and after stroke from the preferred and non-preferred paw from the following list of models in SPSS:

a. Compound Symmetry
b. Compound Symmetry Heterogeneous
c. First-Order Autoregressive
d. Heterogeneous First-Order Autoregressive
e. Unstructured

Degrees of freedom were expressed to the nearest integer. Time (days) was handled as a covariate in the linear model rather than as a nominal independent variable. A $p <= 0.05$ is regarded as statistically significant. M and SD represents the Mean and Standard Deviation respectively. Results were rounded to 3 significant figures.

8.2.8 Histology

Rats were euthanized at the end of the study on day 42, perfused with PBS and then fixed with 4% PFA. Brains and RFID tags were extracted and stored individually in a sucrose solution. The RFID tag of the rat was attached to the storage container for later identification of the brain. The histological analysis on infarct size was carried out as described in section 7.2.3.

8.3 Results

Rats that had a trial count of less than 3 trials on a given day were excluded from the average grasping success rate for that day only. Rats that exhibited an average grasping success rate difference of <16% were excluded from the final pellet reaching analysis, but were included in the deficit to lesion volume correlation results. One Rat was put down post stroke for welfare reasons and one post-surgery death occurred one day post stroke. Three rats were excluded due to a lack of pre-operative interest in the task. 22 rats were assessed post stroke and 13 were included in result calculations. The 13 included rats generated 51,291 trial results which were included in the analysis between days -48 to day 42. The analysis for days -20 to 20 included 28,259 trial results generated over that period. Over the course of the study inclusive of acclimation and device development periods, a total of 87,882 trials were recorded.

Preferred Paw

Stroke caused a rapid decrease in reaching success for the preferred forepaw post-stroke (Figure 8.7;comparing the mean of days -3 and -4 (1353 trials) with the mean of days 2 and 3 (613 trials); M=-52.1, SD=24.7; paired t-test; t_{11}=7.3, p< 0.0001)

In the last phase of training, after moving the pellet to position XY_{rat} = (±8,20), there was evidence of a training effect in the preferred paw before stroke from days -19 to -3 (Figure 8.7; 20025 trials; n=13; linear model analysis - Heterogeneous First-Order Autoregressive; $F_{1,27}$=9.6; p=0.004) There was no recovery in the success of pellet grasping using the preferred paw after stroke from days 1 to 20 (Figure 8.7;n=13 ;linear model analysis - Heterogeneous Compound Symmetry; $F_{1,77}$=1.23; p=0.27).

There was a decrease in the average daily trial participation post-stroke for the position XY_{rat} =(±8, 20) with the preferred paw (Figure 8.8; M=-25.1, SD=21.7; paired t-test; t_{20}=5.29, p<0.0001)

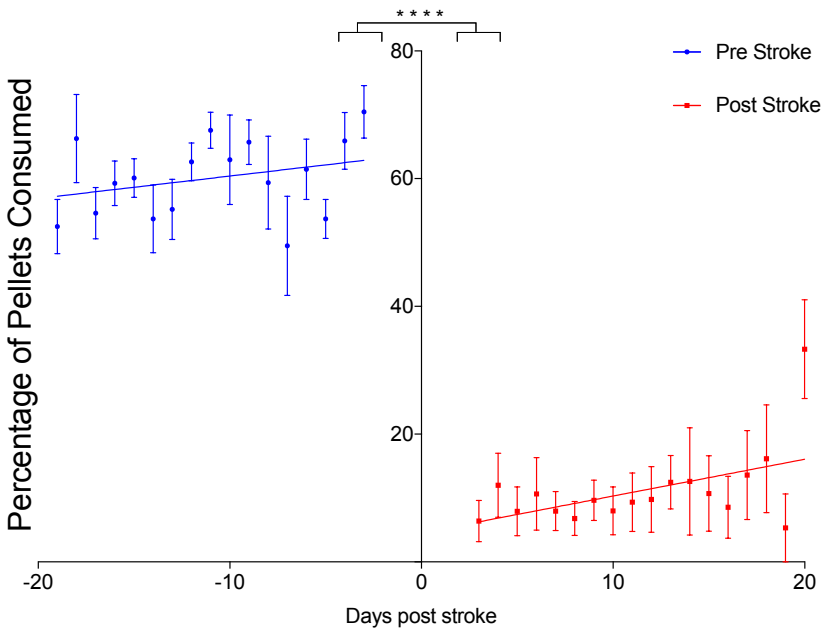

Figure 8.7 - Analysis of pellets consumed before and after stroke reveals a reaching deficit for the preferred forepaw.

A deficit in preferred paw reaching at position XY_{rat} = (±8, 20) was observed after stroke (M=-52.1, SD=24.7; paired t-test; t_{11}=7.3, p< 0.0001)

No recovery in pellet reaching using the preferred paw at position XY_{rat} = (±8, 20) was observed after stroke (linear model analysis - Heterogeneous Compound Symmetry; $F_{1,77}$=1.23, p=0.27). At dispense position XY_{rat} = (±8, 20) there was evidence of a training effect between days -19 and -3 pre-stroke (linear model analysis - Heterogeneous First-Order Autoregressive; $F_{1,27}$=9.6, p=0.004)

n=13.
Error bars indicate ±SEM.

a.

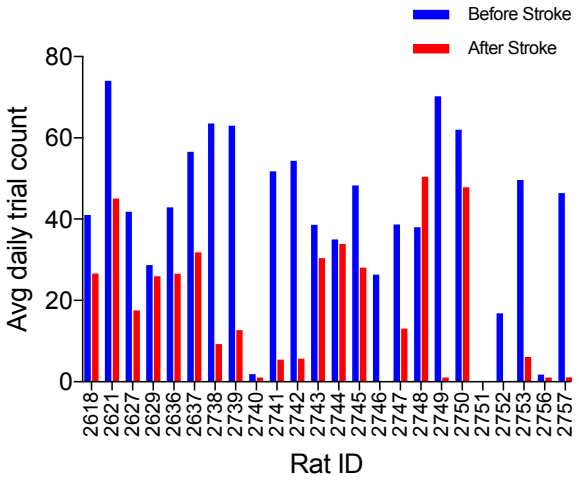

b.

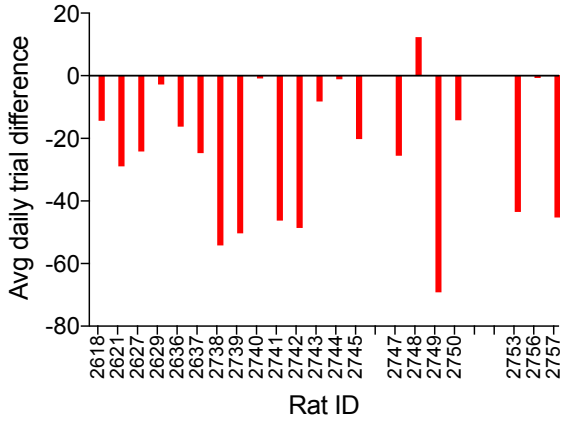

Figure 8.8 - Rats performed fewer trials after stroke than before stroke using the preferred paw.

a. Average daily trial counts before and after stroke at position XY_{rat} = (±8, 20) for pellet retrieval by the preferred paw
b. Difference in average daily trial counts before and after stroke. Negative values indicate a decrease in participation.

There was an observable decrease in trial participation after stroke at position XY_{rat} = (±8, 20) using the preferred paw (M=-25.1, SD=21.8; paired t-test; t_{20}=5.29, p<0.0001). Key data were missing for rats 2746, 2751 and 2752 because they died or were humanely killed before the end of the study.

Non-Preferred Paw

A reaching deficit was observed in the non-preferred paw post-stroke (Figure 8.9; comparing the mean of days -3 and -4 (1353 trials) with the mean of days 3 to 5 (1913 trials); M=-45.7, SD=17.0; paired t-test; t_{12}=9.7, $p < 0.0001$). This was a transient deficit which recovered to pre-stroke reaching success rates in the second week post-stroke (Figure 8.9; calculated between the mean of pre-stroke days -3 and -4 (1353 trials) and the mean of post-stroke days 10 to 14 (2717 trials); M=-8.2, SD=16.0; paired t-test; t_{10}=1.70, p=0.120).

There was evidence of a training effect pre-stroke in the non-preferred paw at position XY_{rat} = (±8, 20) from days -19 to -3 (Figure 8.9; linear model analysis - Heterogeneous First-Order Autoregressive; n=13, $F_{1,34}$=8.1, p=0.007). There was also an observable recovery effect post-stroke in the non-preferred paw at position XY_{rat} = (±8, 20) (Figure 8.9; linear model analysis (Compound Symmetry); n=13; $F_{1,125}$=4.67; p=0.033).
A decrease in average daily trial participation was observed post-stroke at position XY_{rat} = (±8, 20) (Figure 8.10; M=-23.8, SD=24.3; paired t-test; t_{20}=4.49, p=0.0002). A difference in trial participation at position XY_{rat} = (±8, 20), between cohabitating rats was observed (Figure 8.11; using the difference between most and least interactive cohabitating rat; M=30.8, SD=29.3; one-sample two tailed t-test; t_7=2.98, p=0.021).

Lesion volumes varied between rats ranging from 23mm^3 to 251mm^3 (Figure 8.12; M=141mm^3, SD=63.2mm^3). A relationship between infarct volume and the decrease in grasping success rates post stroke was observed (Figure 8.13; Pearson's correlation coefficient; r=0.576, p<0.0154).

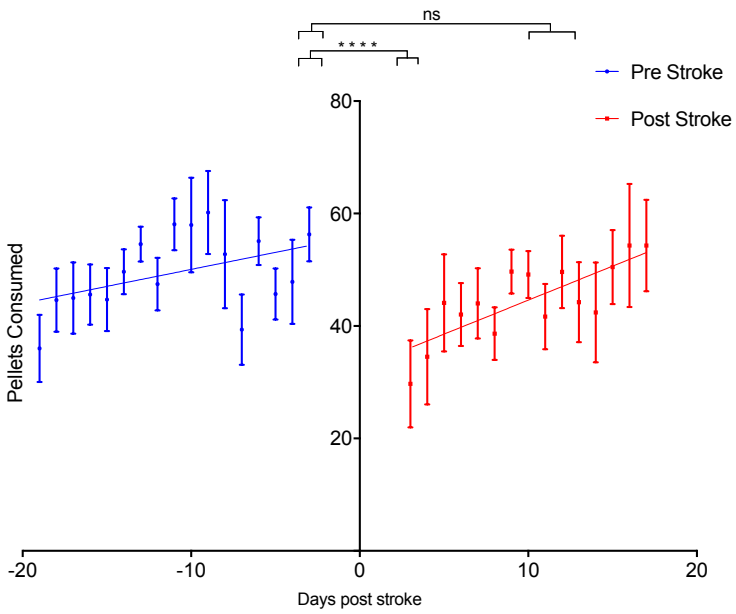

Figure 8.9 - Analysis of pellets consumed before and after stroke reveals a transient reaching deficit for the non-preferred forepaw with subsequent recovery.

A non-preferred paw reaching deficit at position XY_{rat} = (±8, 20) was observed between pre-stroke days -1 and -2 and post stroke days 1 and 2 (Paired t-test; M=-45.7, SD=17; t_{12}=9.7, $p < 0.0001$)

No non-preferred paw reaching deficit at position XY_{rat} = (±8, 20) was observed between pre-stroke days -1 and -2 and post stroke days 10-14 (Paired t-test; M=-8.2, SD=16; t_{10}=1.70, p=0.119).

Evidence of a training effect was observed pre-stroke in the non-preferred paw at position XY_{rat} = (±8, 20) from days -19 to -3 (Linear model analysis - Heterogeneous First-Order Autoregressive; n=13, $F_{1,34}$=8.1, p=0.007). There was an observable effect of recovery in success of pellet reaching using the non-preferred paw after stroke at position XY_{rat} = (±8, 20) (Linear model analysis - Compound Symmetry; n=13, $F_{1,125}$=4.67; p=0.033).

Error bars indicate ±SEM.

a.

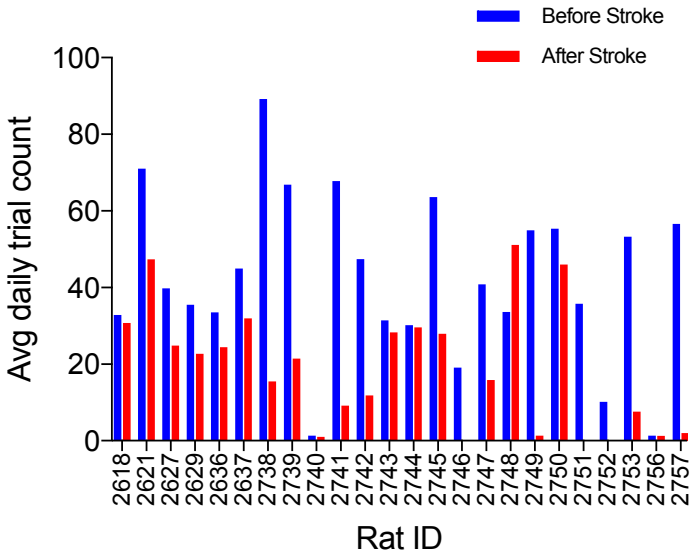

b.

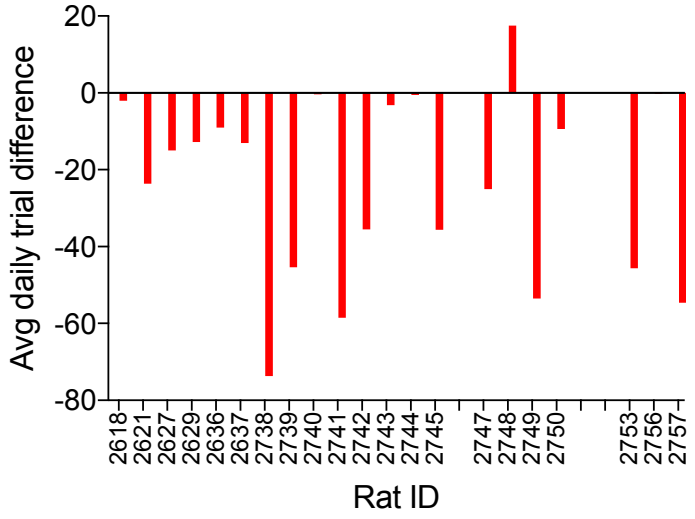

Figure 8.10 - Trial counts decreased post-stroke in the non-preferred paw.

a. Average daily trial counts before and after stroke at position XY_{rat} = (±8, 20) for the non-preferred paw.
b. Difference in average daily trial counts before and after stroke. Negative values indicate a decrease in participation.

There was an observable decrease in trial participation after stroke at position XY_{rat} = (±8, 20) using the non-preferred paw (M=-23.8, SD=24.3; paired t-test; t_{20}=4.49, p=0.0002). Key data were missing for rats 2746, 2751 and 2752 because they died or were humanely killed before the end of the study.

a.

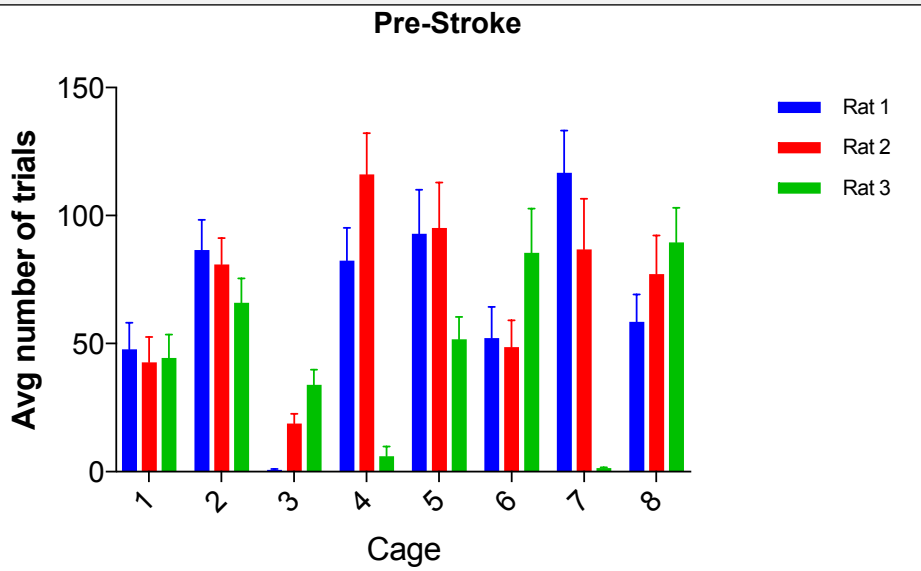

b.

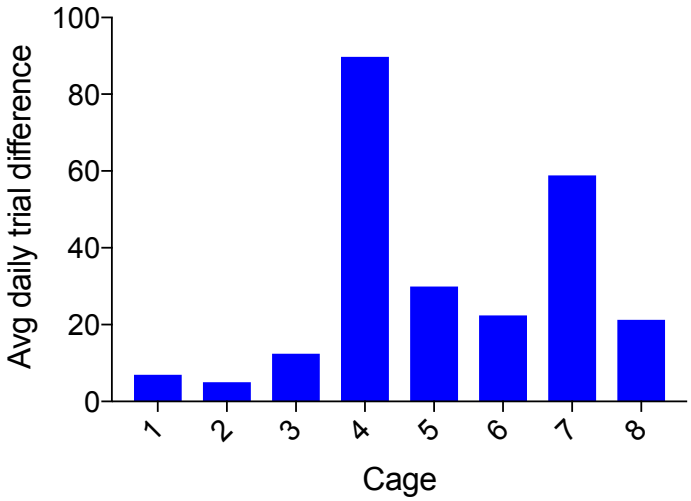

Figure 8.11 - The participation level of cohabitating rats differs.

There is evidence of a difference in trial participation between cohabitating rats that were most and least interactive (M=30.8, SD=29.3; One sample t-test; t_7=2.98, p=0.0205)

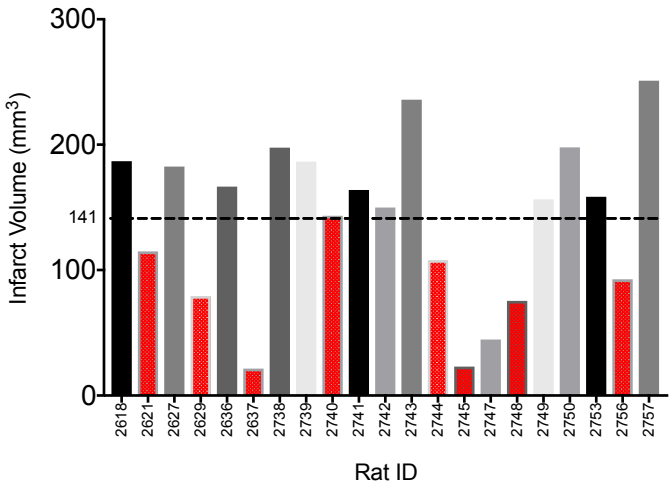

Figure 8.12 - Infarct volume (mm^3) by rat.

Lesion volumes varied between rats ranging from $23mm^3$ to $251mm^3$ ($M=141.1mm^3$,$SD = 63.2mm^3$).

Red bars indicate rats that were excluded from the pellet consumption data analysis based on reaching success rate differences after stroke as described earlier in this section.

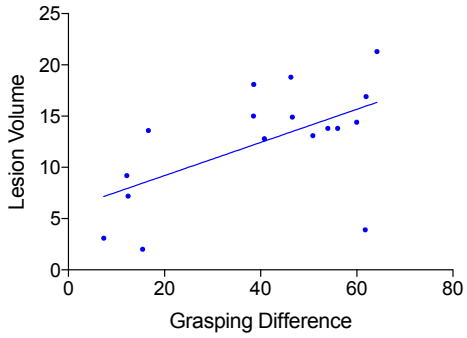

Figure 8.13 - A relationship between infarct volume and deficit is observed.

A relationship between infarct volume and the decrease in grasping success rates (pre vs. post stroke) was observed (Pearson's correlation coefficient; $r=0.576$, $p<0.015$).

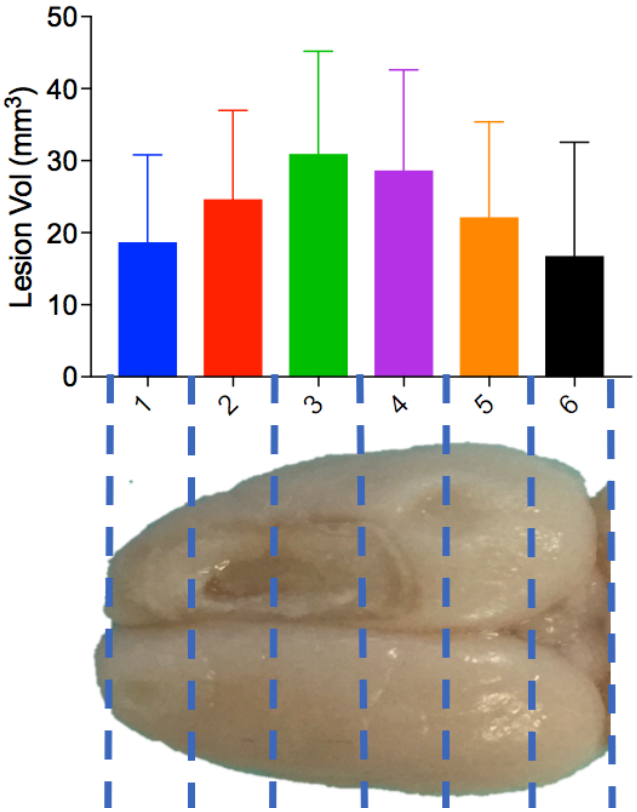

Figure 8.14 - Distribution of lesion volume by section

2mm-thick coronal cross sections were taken using a rat brain matrix with 1mm slice spacing, to measure the infarct volumes. A representation of the distribution of lesion volume by section is presented here.

Error bars indicate standard deviation.

8.4 Discussion

In this study, we have successfully installed an array of 8 RatBots in an animal holding facility and used the devices to automatically acclimate, train and assess 20 young adult female Lister Hooded rats (starting with n=24). The data generated by the array of devices provides evidence that the device is sensitive to the forepaw reaching capability of the rats being assessed. The array of devices successfully identified reaching deficits in the affected forepaws post stroke. Notably, a transient deficit was observed post stroke in the less affected forepaws. This may be attributed to the effects of surgery during the recovery period, or from the lack of balance, or forepaw support that the affected paw might normally provide. Moreover, although the corticospinal tract predominantly supplies the contralateral spinal cord, in the rat 5 to 10% of axons supply the ipsilateral side (Brösamle and Schwab, 2000) and therefore a unilateral cortical lesion affects both sides of the spinal cord. This may form the basis for subsequent investigations into the effect of support and balance, that an affected forepaw may normally provide when reaching with the less affected forepaw.

The baseline reaching success rates achieved pre-stroke presented a mean grasping success rate of 61.7% (SD=13.4) for the preferred forepaw. Although this automated version of the task differs in complexity by design, some comparable data has been observed in other manual and automated versions of the task (Table 8.1). Although the RatBot design raises the task difficulty similar to that of the pedestal variant, it achieves a higher grasping success rate.

Study	Baseline Grasping success mean.	Notes.
(Girgis et al., 2007)	60.9% ±4.5%	6 weeks of training. n=6.
(Adkins et al., 2015)	55-65%.	n=78
(Gonzalez and Kolb, 2003)	65%.	n=8
(Wong et al., 2015)	60.5% ±4.8	n=4. 100 trials per day. An automated station based reaching solution.
(Fenrich et al., 2016)	48.8% ±2.3%.	n=8. An automated station based reaching solution
(Amki et al., 2017)	38.1% ±7.1%	n=18. A slight variation of the task but still assesses forelimb grasping in a similar fashion of reaching for a pellet through a slit.
(Mosberger et al., 2017)	45%	n=121. 40 trials per day for 12 days. Pedestals used instead of standard reaching shelf.
(Buitrago et al., 2004b)	55%	n=14. 25 trials per session for 8 days. Pedestal variant of the task.
(Buitrago et al., 2004b)	58%	n=13. 100 trials per session for 8 days. Pedestal variant of the task.

Table 8.1 - Comparative reach success results from other studies.

8.4.1 General device operation

This study provided the opportunity to assess the functioning of the RatBot in a longer-term study to understand the general dynamics of the system, interaction of parts and reliability of components. The stepper motors were found to degrade over time as shafts would detach from the gear assembly. This was resolved by using a metal bonding (Evo-Stik metal epoxy) agent between the shaft and gear. This seemed to resolve this detaching issue and no further detachments were observed after applying this fix.

The installation of the required cabling infrastructure was carried out whist rats were housed in the same rack to not interrupt other ongoing studies. On one occasion, a rat was able to pull a disconnected Ethernet cable into the cage and within a short period

was able to bite through it (Figure 8.15a). This reveals the need for precise cable routing that is well outside of the reach of the rats, as the rat can reach through the cage lid.

On a single occasion during the study, a rat was able to get access to the rear of the RatBot and had bitten through the 30-way (low power) ribbon cable (Figure 8.15b) that connected the internal RatBot electronics to the outside control and power electronics. Rats were not harmed and fuses were blown which cut power to the device protecting the Rats from shock. This highlights the need for either a cable-free installation or more appropriate internal routing and securing of the RatBot inside of the rat cage.

In addition, it was noted that slit sensor housing was bitten into (Figure 8.16) randomly in various cages. This behaviour may be attributed to the eagerness of the rat to obtain more sucrose pellets, which reinforces its use as a suitable reward. These components were replaced as soon as it was observed. This feature will require redevelopment to either make it easier to replace or fabricated from a different material to be more impervious to damage by the rat.

a.	b.
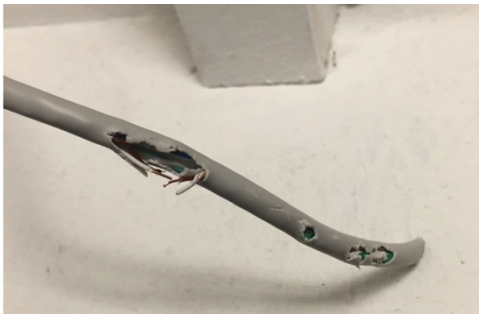	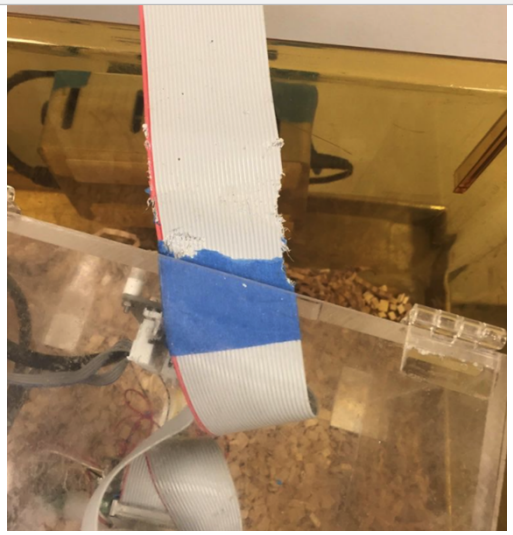

Figure 8.15 - Cables were only rarely bitten through during the 3 month experiment.

a. During installation, a disconnected Ethernet cable was grasped by a rat through the cage lid and was bitten through.
b. On one occasion during the study, a rat was able to gain access to the rear of the RatBot and bitten through the interconnecting 30-way ribbon cable.

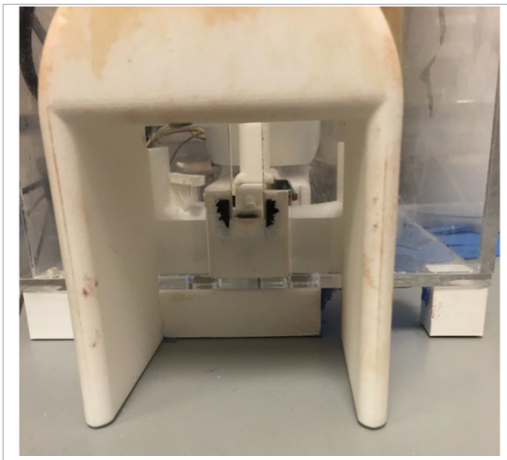

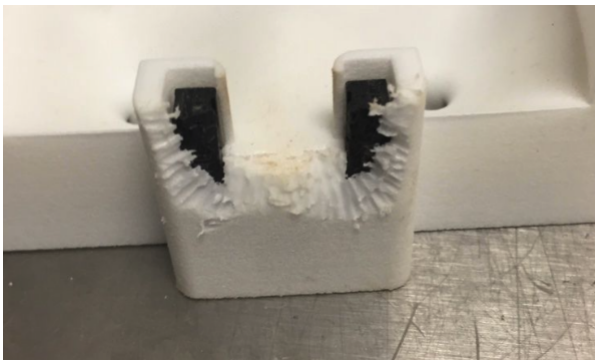

Figure 8.16 - Slit sensor bitten through during normal device operation.

Occasionally the slit sensor housing of random RatBots would be chewed through. When this was observed, the appropriate components were replaced to not interfere with the running of the study and interpretation of results.

8.4.2 Interaction with the RatBot™

As in the previous study a similar uneven distribution of trials between cohabitating rats was observed. This observation may be attributed to the general variable nature of animal behaviour experiments, the effects of social dominance (Ramirez, 2013; Melhorn et al., 2017) or lack thereof, stress or anxiety (Hogg, 1996; Campos et al., 2013) , technician interaction or a variety of other environmental variables. This reinforces this need for a restricting or encouraging mechanism to be introduced to control participation between cohabitating rats. In future, the software could be modified to ensure that rats receive equal numbers of trials. The firmware would read the RFID tag, and based on the number of trials executed by the specific rat on the current day, may decide not to dispense a pellet. In addition to this, visual cues using the LED lighting may be provided to indicate that a rat has exceeded their daily trial execution quota e.g. LED lights turn off indicating that no trials may be carried out for the individual rat.

8.4.3 Acclimation and device jamming

During the acclimation phase, as observed in the previous study (Chapter 7) rats responded cautiously to the RatBot in cage and similar behaviour of pushing cage bedding through the slit was observed. Jams and bedding obstructions that occurred were resolved on the following day. This delay indicates a pressing need to introduce a solution to prevent or further minimise the possibility of jamming due to bedding.

A fine grade bedding (LBS Biotech - micro chips) (Figure 8.17) was introduced to attempt to reduce sensor obstruction and jamming and this seemed to improve the situation, however this has not been quantified. Moving forward, investigation into bedding types and/or RatBot design improvements to mitigate the risk of jamming is required.

Figure 8.17 - A fine grain bedding (LBS Biotech - Micro Chips) was substituted for standard bedding during this study.

Due to jamming occurring in the early stages of the study, a finer grain bedding was used in place of standard cage bedding used by the Biological Services Unit (BSU) that housed the rats in this experiment.

8.4.4 Quality of fabrication

Prototypes used in this study were produced by Shapeways, a 3D printing service, using nylon components. While this is an improvement over previously used 3D printed PLA components, the overall quality and smoothness of various components is lacking. Components such as the auger, spoon and reservoir may benefit from fabrication methods that result in a smooth, mirror like surface (3.2 µm Ra or smoother) to reduce friction at the interface of these components. This may be more likely achieved through high quality subtractive machining methods (Routara et al., 2008).

8.4.5 Animal well-being

Throughout the study, rats had ad libitum access to food and water. No observable weight losses were observed post stroke and visual inspection of the rats revealed no observable negative disposition. Surgical wounds healed and required no additional attention. These positive welfare outcomes supports the case for longer term studies with the RatBot.

8.4.6 Maintenance

RatBots were cleaned and pellets were replenished daily in the following manner:

Step	Description
1	Disconnect the single Ethernet cable connected to the external electronics of the cage (Figure 8.3).
2	Remove the cage from the rack.
3	Relocate the rats to a temporary holding cage.
4	Remove and empty the magnetically coupled drop box (Figure 3.27).
5	Replenish the pellet reservoir.
6	Inspect the device for dirt, damage or other obstructions and clean were necessary using an air duster (Dust Off; Falcon safety products).
7	Place the RatBot back in position.
8	Place the rats back into the cage.
9	Return the cage to the cage rack.
10	Reconnect the single Ethernet cable.

Table 8.2 - Daily maintenance procedure.

If no corrective action was required, this 10-step process took approximately 3-5 minutes per device. Once weekly, bedding and cages were replaced as part of the normal cleaning and maintenance procedure in the BSU. Steps 1 to 6 remain the same. Steps 7 to 10 take place using the new cage. All cages used had female Velcro strips attached to the outside so that the electronics enclosure may be easily attached. Maintenance efficiencies are required to reduce overall daily time commitments as this can become excessive with larger arrays of devices. Improvements in reliability, pellet refilling and bedding jam resolving require investigation.

Chapter 9

Discussion

The key objective of this PhD is in-cage automation of the labour intensive (Schaar et al., 2010; Hurd et al., 2013) single pellet reaching task. This thesis presents evidence that this objective has been achieved.

I have successfully designed, fabricated (Chapter 3, Chapter 4, Chapter 5), validated (Chapter 6) and tested (Chapter 7, Chapter 8) an in-cage apparatus (RatBot™) capable of automatically acclimating, training and assessing cohorts of rats in the single pellet reaching task. The data presented indicates that the device can be used to determine handedness and detect a reaching deficit affecting the preferred forepaw of a cohort of Lister Hooded female rates after CNS injury. We have also shown that the grasping success of the forepaw ipsilateral to the lesioned hemisphere had experienced a deficit in the days immediately after stroke and then recovered to pre-stroke levels in week 2. This may be attributed to a transient dysfunction of the contralesional hemisphere. This dysfunction might be due to diaschisis (Infeld et al., 1995; Seitz et al., 1999; Garbuzova-Davis et al., 2013) as a result of compression from the swollen hemisphere (McBride et al., 2016) or perhaps due to the contralesional hemisphere undergoing plasticity after losing inputs from the affected hemisphere. It may also be an ipsilateral deficit due to the stroke as seen in human patients (Sunderland et al., 1999; Battelli et al., 2001; Kim et al., 2003).

In many studies using animals, behavioural assessments are key to measuring outcomes. The labour intensive nature of these tasks (Hurd et al., 2013) introduce experimental overhead, distracting researchers from core research. We have shown that an array of RatBots can operate unattended overnight and can automatically acclimate, train and assess rats using this task. This allows researchers to design and execute studies involving larger numbers of rats to provide more powerful, repeatable results (Ioannidis, 2005; Button et al., 2013; Card and Srivastava, 2014).

The RatBot (Chapter 3) was designed to make the task more difficult so that it may be less prone to ‘cheating’ or compensatory grasping behaviour (Cirstea and Levin, 2000; Gharbawie and Whishaw, 2006; Alaverdashvili and Whishaw, 2010; 2013). The design of the spoon described in section 3.3.5 is such that it may reduce the likelihood of pellet scooping or dragging. Any attempt to drag the pellet without grasping would result in the pellet falling off the spoon, as there is no platform on which the pellet may be dragged between the spoon and the slit when at the final testing positions.

The device runs unattended so the effect of the researcher (Rosenthal and Fode, 2007) on the task may be diminished. The effect of the researcher has not been quantified but may be the subject of further investigation into result consistency between technicians using the manual version of this task.

The task objectivity and consistency that comes with automated task execution enables collaboration between research groups. This reinforces the need for a reporting standard (Rice et al., 2008) and an immutable, centralised data store where this type of data may be persisted and shared. Automation also enables larger studies with large cohorts of rats executing the task in parallel and generating large volumes of data. In the latest study (Chapter 8) 63326 reaching trials were executed in the 44 days pre-stroke by 24 rats housed 3 per cage. This requires a big-data approach to the centralised persistence, access and management of the trial results.

It has been shown that the RatBot brings with it benefits such as reduced researcher interaction, reduced time commitments, and higher trial numbers in a study, but it must be highlighted that daily maintenance with larger numbers of cages may become tedious. Feature changes and new facilities are required to ensure that maintenance activities such as cleaning and replenishing pellet reservoirs can be done quickly and easily, possibly without the need to remove the cage from the rack. It must also be noted that the weight of the cage increases by approximately 1.8kg with the device installed. This makes cage removal and replacement potentially difficult for cages positioned higher within the same rack. Part of the focus of upcoming changes must focus on reducing the overall weight. This may be achieved by altering the density of the fabricated components as well as the thickness and size of the internal acrylic enclosure.

During the acclimation stages of the study the rats actively pushed bedding through the slit (Figure 7.13, Figure 7.14). This resulted in obstruction of the reach and drop sensors. In extreme cases, enough bedding was pushed in far enough to restrict movement of the device, causing further jamming. A solution to this issue is required to reduce the overall overhead during the acclimation phase. Possible options are:

1. Introduce a door across the slit to prevent the rat from pushing bedding through and only open when a pellet is presented.
2. Change the dimensions of the drop chutes and drop sensors to allow the bedding to fall straight through.
3. Introduce a grid at the RFID tunnel to allow the bedding to fall straight through, preventing the rat from pushing it through the slit.

4. Provide a facility to ensure that the pellet is more readily available beyond the slit to provide an awareness of a reward more efficiently than it currently is.

These options will be explored in future iterations of the device as we move closer towards commercialisation.

9.1 Future Directions

9.1.1 Patent

All intellectual property rights were acquired from King's College London and a United Kingdom patent application 1607278.7 was submitted to protect the innovation and ensure that the device can be commercialised. A Patent Cooperation Treaty (PCT) filing has subsequently been made to protect our right to commercialise the device internationally.

9.1.2 Commercialisation

A Proof of Concept (PoC) grant (EUR 150,000) was awarded by the European Research Council (ERC) to develop the RatBot concept further with the intention of taking the product to market. A company, Research Devices Ltd (Company number: 09993367) was incorporated to refine, market and sell the device and all intellectual property rights has been acquired from King's College London. The device will be refined with various improvements in both hardware and software and distributed to specific beta testing partners for evaluation and feedback.

9.1.3 Size adaptation

Funding has also been secured to develop the device further to work with mice and smaller pellet sizes, in a smaller environment.

9.1.4 Further device development and research

The device was designed to automate the single pellet reaching task (SPRT), but the device is not limited to this specific use. With enhancements, the device may also be tailored to assess forelimb trajectories of rats in a similar fashion to current mechanisms used in human studies (Wycherley et al., 2005; Balslev et al., 2007; Goble and Anguera, 2010; Henriques et al., 2014; Contu et al., 2016; Kuczynski et al., 2017; Shaffer and Taylor, 2017)

Rats come in varying sizes but the manual or this automated version does not cater to the physiology of the animals being assessed. We plan to programmatically tailor the task to the physical reaching capability of individual rats. It has been observed previously that gender and physiology may have an impact on several behavioural tasks (Field and Whishaw, 2005; Sutcliffe et al., 2007).

By obscuring the view of the pellet and utilising the current variable lighting capability, the device may be used to investigate and understand the effect of vision and possibly olfactory base pellet reach trajectories (Whishaw and Tomie, 1988). Other applications for the device may be in stress (Hu et al., 2014; Moore et al., 2016) and dominance (Ramirez, 2013; Jupp et al., 2016; Melhorn et al., 2017) related studies comparing the effect of the execution environment using this task.

The current device manufacturing process comprises of the assembly of a variety of components which introduces multiple points of failure. Moving forward the design of the device will be changed to reduce this complexity. Alternate materials will be investigated to reduce wear and tear, reducing the maintenance required over the lifespan of the device. Several enhancements have been identified during the validation (Chapter 6) process and these will be incorporated into future versions of the device.

At present, the device is controlled by a Raspberry Pi, which increases the power requirements for device operation. Moving forward, custom embedded electronics will be designed to replace the current controller. This may incorporate inductive charging and wireless data transfer so that there is no physical connectivity requirement between the inside of the rat cage and the outside. This also allows for repositioning of the device to suit different cage styles.

New sensors and design adjustments will be made to help mitigate or prevent the jamming that was observed in the previous reaching studies described in Chapter 7 and Chapter 8.

The RatBot currently operates in a single Z plane, which means that it can currently only position a pellet in the XY Cartesian space. There is evidence that high reaching heights negatively affected reaching success (Miklyaeva and Whishaw, 1996). Height of the spoon may be a useful feature to programmatically control as it may be used to change the task difficulty or facilitate investigations where XYZ reach trajectories are studied.

Reach success is determined by the firmware using a variety of sensors described in section 3.3.8. While this is shown to be successful when manually observing random trials, it would be useful to include a confirmation feature that would allow for an audit of the reaching result. This may be in the form of a camera or set of cameras installed into the device and positioned appropriately such that a video recording of each trial is captured. This may also prove to be useful in analysing the reaching trajectories, dispense position and possibly any compensation behaviours (Whishaw et al., 1991; Cirstea and Levin, 2000; Alaverdashvili and Whishaw, 2010) that may have developed.

Although a sound level of 52dB was measured during operation of the device, this effect on the rats was not studied. Further development is required to reduce the overall noise footprint of the device. Further studies are required to determine if any high frequency sounds are emitted by the device that may have a negative impact on the behaviour of the rats (Chrousos and Gold, 1992; Hu et al., 2014; Yang et al., 2014). Non-quantifiable visual observations of the rats during the operation of the RatBot did not provide any indication of rat discomfort or stress. In some cases, it was observed that rats slept on top of the RatBot whilst others were executing trials in the same cage.

The introduction of a Pavlovian style cue (Cambiaghi and Sacchetti, 2015; Mosberger et al., 2016) capability to the device may support grouping of trials into sessions where a pre-defined number of reaching trials may be carried out. Rats would be cued using a tone or using the LEDs to indicate when a session is about to start. This may be taken even further whereby cues may be directed at individual rats, whereby a specific rat may be requested to approach the device and execute a reaching trial. This may also provide support for other cue or learning based investigations.

9.2 Conclusion

An in-cage automated apparatus (RatBot™) has been designed and fabricated using rapid prototyping techniques to automate the Single Pellet Reaching Task (SPRT). The device can automatically acclimate, train and assess rats in-cage using 45mg sucrose pellets, by making the pellet accessible by the rats' tongue initially and progressively retracting the pellet on subsequent tasks ensuring that reaching occurs. We have shown that the device can identify a motor deficit after a unilateral cortical injury in both adult and middle age rats and is sensitive to learning and recovery trends. The device can run unattended overnight with programmable schedules and positioning regimes and automatically assesses and stores summarised reaching results of individually identified rats.

Appendix A. Included in the attached DVD

The included DVD contains the following material

1. Solidworks CAD drawings for all RatBot versions.
2. Eagle PCB schematics and routings for all PCB versions including datasheets and Bill of Materials.
3. Videos of rat interaction with the RatBot.
4. All source code for the firmware and management applications.
5. The Ratbot Patent Application.

Videos on the DVDs:

Video	Description
Video 1	Presents a trial at position $0,0_{device}$ with a grid overlay to demonstrate correct positioning.
Video 2	Presents a trial at position $4,4_{device}$ with a grid overlay to demonstrate correct positioning.
Video 3	Presents a trial at position $8,5_{device}$ with a grid overlay to demonstrate correct positioning.
Video 4	Presents the pellet dispensing portion of a trial with a log overlay to demonstrate correct function of the pellet dispenser
Video 5	The proximity sensor is tested by manually placing a pellet on the sensor and removing it. A real-time log overlay provides a stream of proximity data feedback to indicate pellet detection.
Video 6	The chute sensor is tested by manually dropping a pellet down the dispensing chute and monitoring the state of the chute sensor, which has been overlaid onto the video.
Video 7	The development test of the drop sensor prototype is presented here with visual verification of the sensor being triggered.
Video 8	The drop sensor of the device is manually tested by dropping pellets down each drop chute and monitoring the status of the drop sensors.
Video 9	The slit sensor of the device is manually tested by obscuring the slit using a spatula, whilst monitoring the status of the slit sensor.
Video 10	The initialisation sequence of the RatBot is presented here with real-time device logs overlaid and on screen narration of the various steps of the initialisation sequence.

Video 11	A manual dispense trial is performed at position $(4,4)_{device}$ to demonstrate the correct functioning of a pellet grasp and dropped pellet trial. Log overlays confirm states and results.
Video 12	A cleaning operation is demonstrated here for when a pellet is left on the spoon between trials.
Video 13	A 55-minute set of trials at position $\pm4,4_{device}$ and $\pm8,5_{device}$ is presented here to validate the device result against a manual action.
Video 14	An RFID tag read of a rat executing a trial in-cage is presented here. Sensor and log feedback overlays are provided to confirm operation.
Video 15	The RatBot correctly determines the result of the trial to be a 'Pellet Retrieval'. Sensor and log feedback overlays are provided to confirm operation.
Video 16	The RatBot correctly determines the result of the trial to be a 'Dropped. Sensor and log feedback overlays are provided to confirm operation.

Table 9.1 – Descriptions of the validation videos included within Appendix A

Appendix B. The design evolution of the RatBot™

In this section, 11 design milestones in the design history of the RatBot™ is presented to outline the iterative nature of the development process. All detailed designs were developed using Solidworks 2013-2017, printed out of PLA using a MakerBot Replicator 2 for evaluation. For accurate dimensioned 3D CAD models of the figures please refer to Appendix A.

3D Overview	Cross Section View
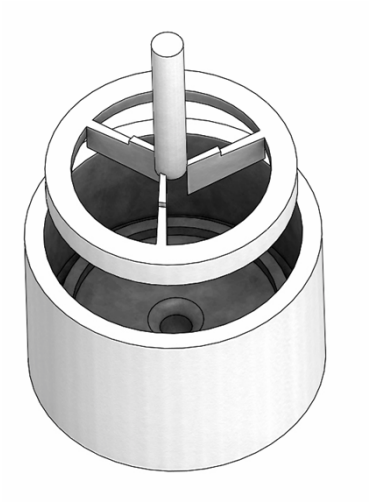	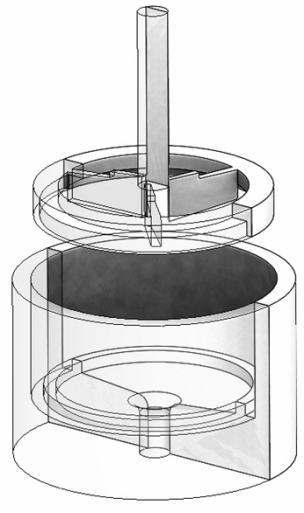

Figure B.1 - Dispenser version 1

A reservoir with a top driven stirrer was attempted. Pellets fell through the central hole in the base. The stirring shaft reduced the overall volume of pellets that could be stored in the reservoir and the decision was made for it to be replaced with an alternate mechanism described in Figure B.2 - Dispenser version

3D Overview	Cross Section View
	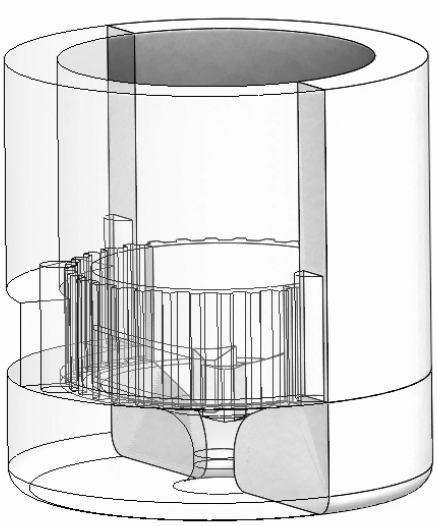

Figure B.2 - Dispenser version 2

The previous top driven stirring mechanism was replaced by a side driven mechanism to allow for a greater number of pellets to be stored within the same space.

3D Overview	Cross Section
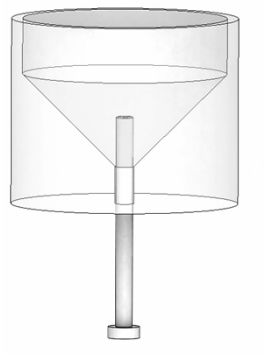	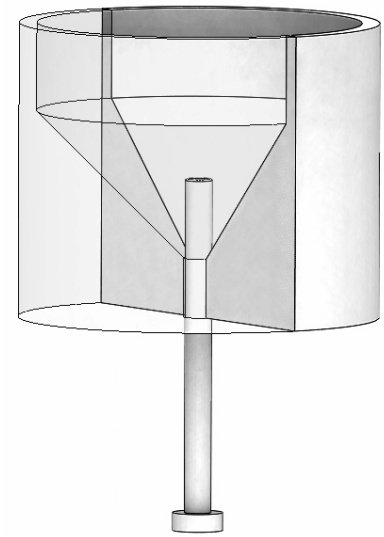

Figure B.3 - Dispenser version 3

Parallel design attempt: An alternate method inspired by the pedestal variation (Buitrago et al., 2004a) of the SPRT was attempted. This was abandoned due to the rapid accumulation of pellet dust around the pedestal shaft resulting in the shaft jamming.

3D Overview	Cross Section View
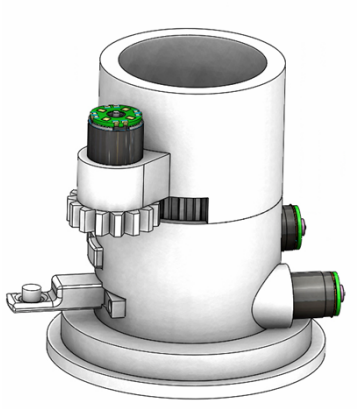	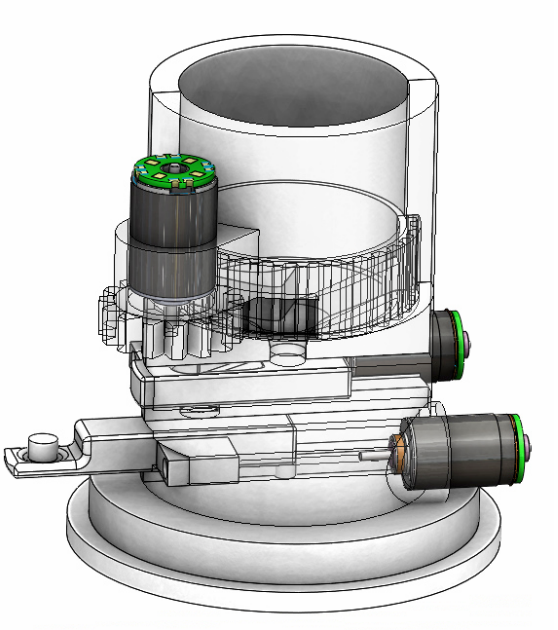

Pellet isolation and location sequence

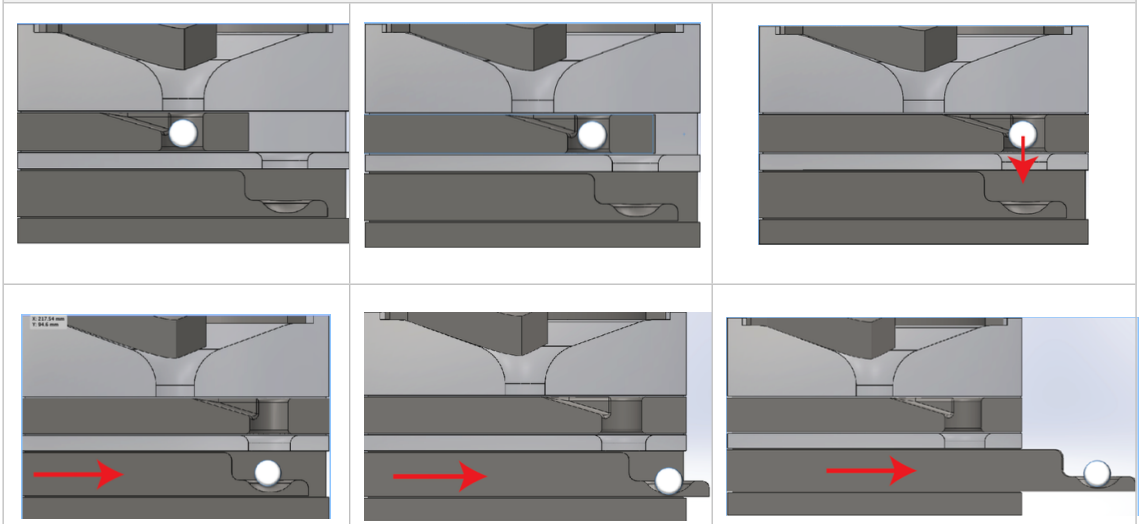

Figure B.4 - Dispenser version 14

The side driven stirrer design was further developed and a two-stage dispenser inspired by standard sweetener dispensers was designed. A stirrer which would agitate pellets coaxing them towards the hole in the centre. A ‘Single-Shot’ mechanism will isolate a single pellet and move it forward to be dropped onto a spoon. The spoon will then move the pellet into the desired trial position. The reservoir and agitation mechanism was abandoned because of jamming due to pellet dust accumulation at the base of the dispenser.

3D Overview	Cross Section View
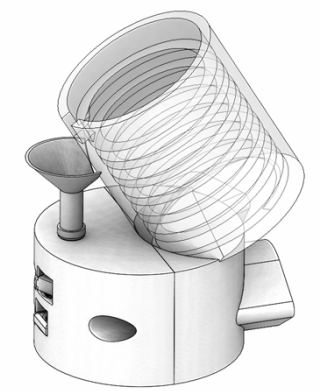	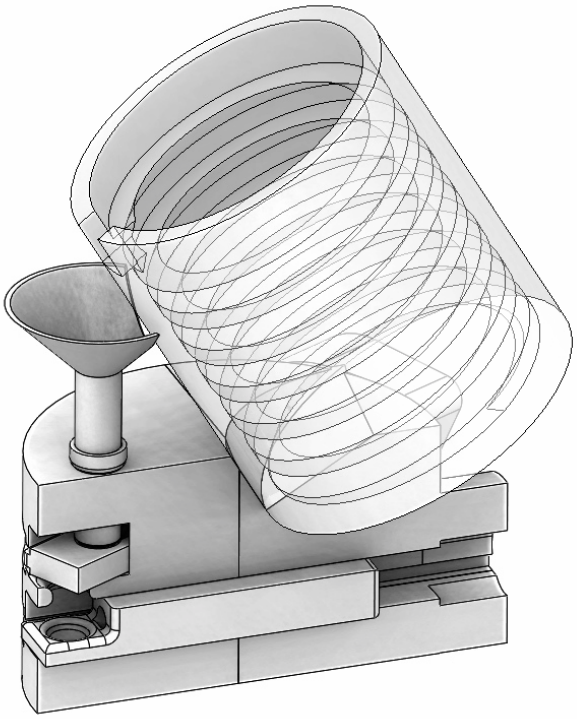

Figure B.5 - Dispenser version 19

The reservoir was redesigned inspired by vibrational feeding bowls to be a ‘top dispenser’ whereby pellets are driven up the reservoir channels either by rotating the reservoir or by vibrating the reservoir. This method was abandoned because

a. The manufacturing of the reservoir to a smooth finish proved difficult.
b. The rotation attempt resulted in excessive pellet grinding
c. The vibration feeding was not attempted because of the possibility of excessive noise and high frequency noises affecting the rats.

3D Overview	Cross Section View
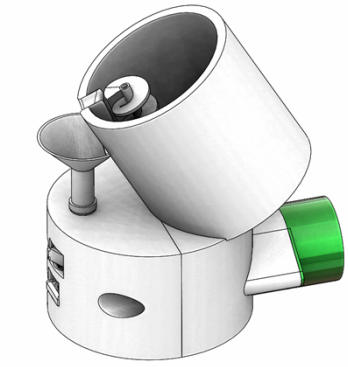	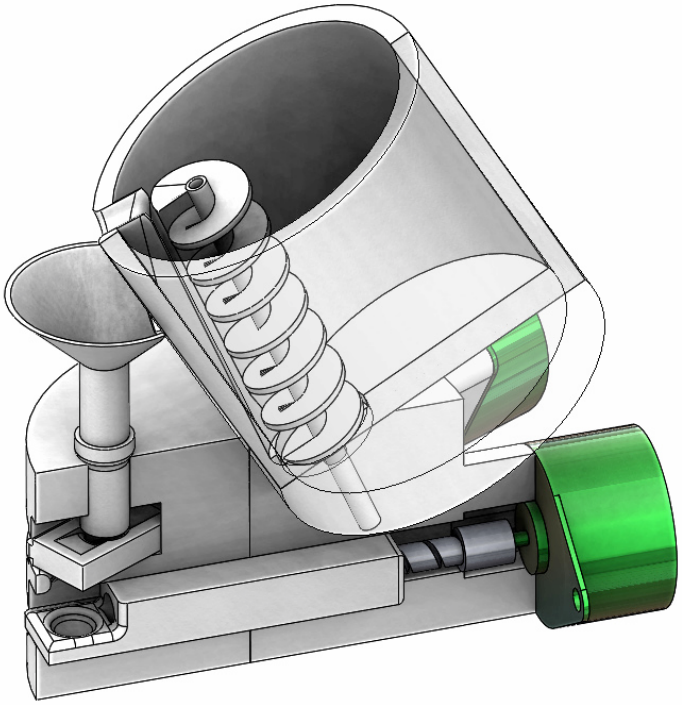

Figure B.6 - Dispenser version 21

An auger driven dispenser was designed as a ‘top dispenser’ whereby pellets are driven upwards along a pellet guide. This mechanism proved to be successful and the design persisted up to the latest revision.

3D Overview	Cross Section View
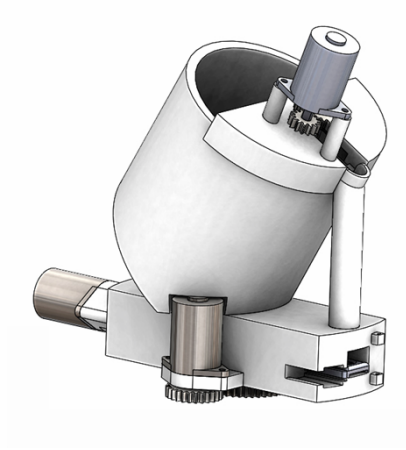	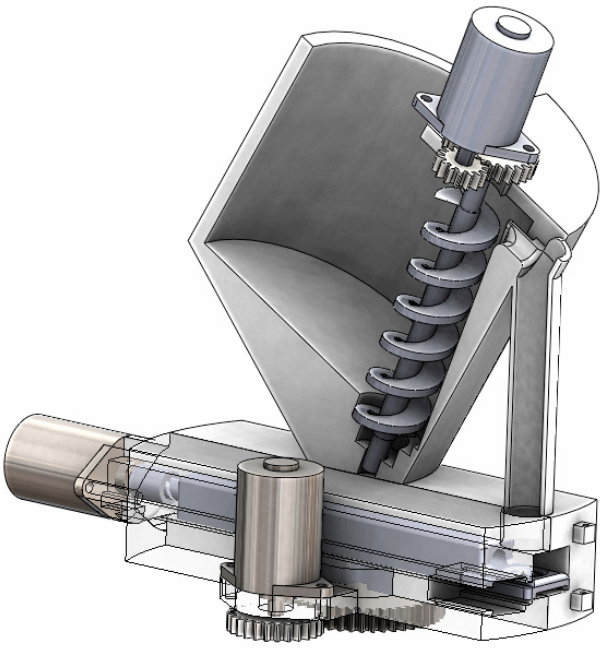

Figure B.7 - Dispenser version 36

It was found that the auger driven approach was sufficiently accurate in dispensing pellets in a single file and thus the ‘single shot’ mechanism which was responsible for isolating individual pellets became a redundant feature and was removed from the design. This also reduced the overall volume and weight of the device as the base could now be made smaller.

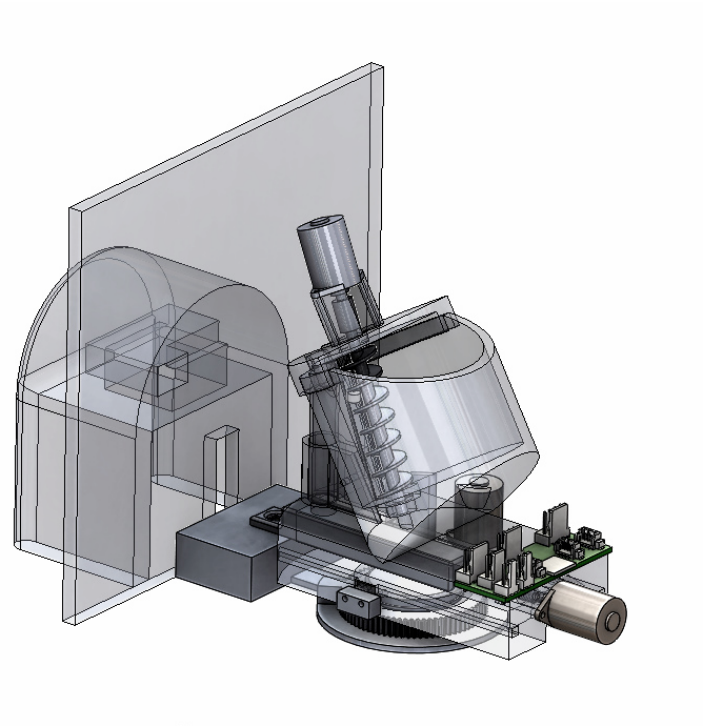

Figure B.8 - Dispenser version 51

At iteration 51, the RFID tunnel and on-board electronics and acrylic enclosure with slit was introduced into the design.

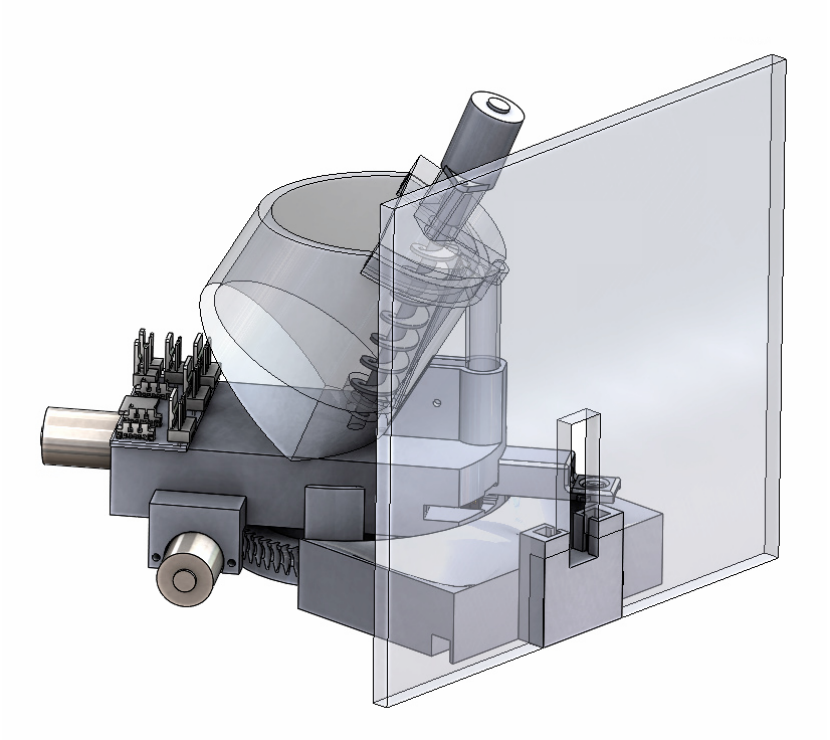

Figure B.9 - Dispenser version 60

The drop box, reach sensor, drop sensors and worm gear driven rotational components were introduced into the design.

Top Left View

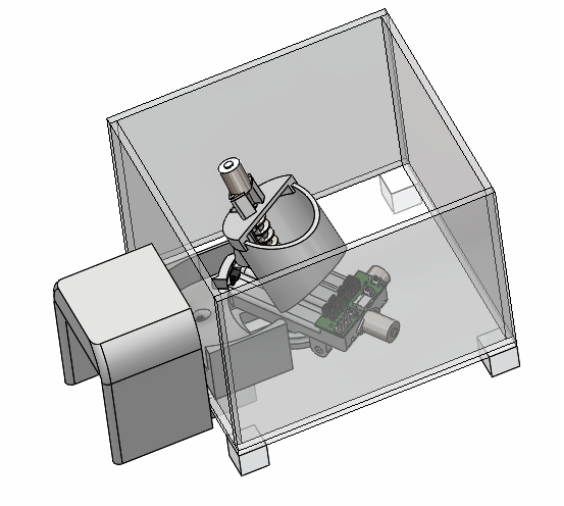

Bottom Left View

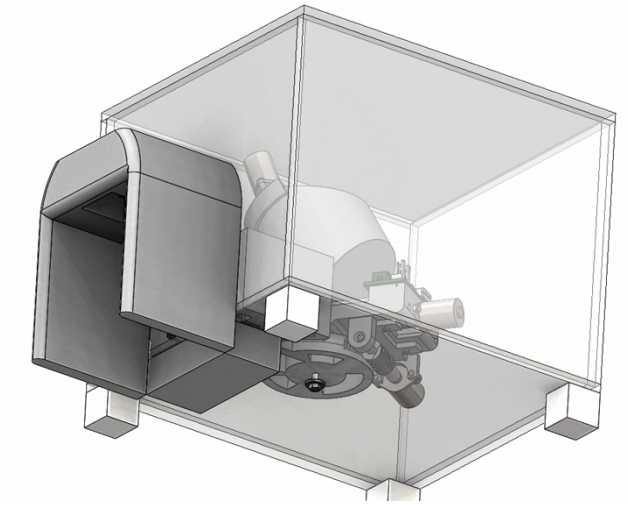

Figure B.10 - Dispenser version 90

Version 90 is a near final design of the RatBot described in this thesis. Minor adjustments to the auger, cleaning station and spoon designs were made between this variant and the final variant presented in this thesis. These adjustments were made due to a change in the fabrication process which was up this point, carried out using a MakerBot Replicator 2 3D printer. Subsequent designs were fabricated using Shapeways printed Nylon components which are of a higher accuracy and differing surface finish.

Bibliography

Adkins, D.L., Ferguson, L., Lance, S., Pevtsov, A., McDonough, K., Stamschror, J., et al. (2015). Combining Multiple Types of Motor Rehabilitation Enhances Skilled Forelimb Use Following Experimental Traumatic Brain Injury in Rats. Neurorehabilitation and Neural Repair *29*: 989–1000.

Alaverdashvili, M., and Whishaw, I.Q. (2008). Motor cortex stroke impairs individual digit movement in skilled reaching by the rat. Eur J Neurosci *28*: 311–322.

Alaverdashvili, M., and Whishaw, I.Q. (2010). Compensation aids skilled reaching in aging and in recovery from forelimb motor cortex stroke in the rat. Neuroscience *167*: 21–30.

Alaverdashvili, M., and Whishaw, I.Q. (2013). A behavioral method for identifying recovery and compensation: Hand use in a preclinical stroke model using the single pellet reaching task. Neuroscience and Biobehavioral Reviews *37*: 950–967.

Amki, El, M., Baumgartner, P., Bracko, O., Luft, A.R., and Wegener, S. (2017). Task-Specific Motor Rehabilitation Therapy After Stroke Improves Performance in a Different Motor Task: Translational Evidence. Transl. Stroke Res. *5*: 77–4.

Ballermann, McKenna, J., and Whishaw, I.Q. (2001). A grasp-related deficit in tactile discrimination following dorsal column lesion in the rat. 1–6.

Ballermann, Tompkins, G., and Whishaw, I.Q. (1999). Skilled forelimb reaching for pasta guided by tactile input in the rat as measured by accuracy, spatial adjustments, and force. 1–9.

Balslev, D., Cole, J., and Miall, R.C. (2007). Proprioception contributes to the sense of agency during visual observation of hand movements: evidence from temporal judgments of action. Journal of Cognitive Neuroscience *19*: 1535–1541.

Bar-Yona, I., Teicher, M., and Products, L.-P. (1994). Tablet dispenser.

Battelli, L., Cavanagh, P., Intriligator, J., Tramo, M.J., Hénaff, M.A., Michèl, F., et al. (2001). Unilateral right parietal damage leads to bilateral deficit for high-level motion. Neuron *32*: 985–995.

Becker, A.M., Meyers, E., Sloan, A., Rennaker, R., Kilgard, M., and Goldberg, M.P. (2016). An automated task for the training and assessment of distal forelimb function in a mouse model of ischemic stroke. Journal of Neuroscience Methods *258*: 16–23.

Borton, D., Yin, M., Aceros, J., Agha, N., Minxha, J., Komar, J., et al. (2011). Developing implantable neuroprosthetics: a new model in pig. Conf Proc IEEE Eng Med Biol Soc *2011*: 3024–3030.

Brösamle, C., and Schwab, M.E. (2000). Ipsilateral, ventral corticospinal tract of the adult rat: ultrastructure, myelination and synaptic connections. J. Neurocytol. *29*: 499–507.

Buitrago, M.M., Ringer, T., Schulz, J.B., Dichgans, J., and Luft, A.R. (2004a). Characterization of motor skill and instrumental learning time scales in a skilled reaching task in rat. Behavioural Brain Research *155*: 249–256.

Buitrago, M.M., Ringer, T., Schulz, J.B., Dichgans, J., and Luft, A.R. (2004b).

Characterization of motor skill and instrumental learning time scales in a skilled reaching task in rat. Behavioural Brain Research *155*: 249–256.

Button, K.S., Ioannidis, J.P.A., Mokrysz, C., Nosek, B.A., Flint, J., Robinson, E.S.J., et al. (2013). Power failure: why small sample size undermines the reliability of neuroscience. 1–12.

Cambiaghi, M., and Sacchetti, B. (2015). Ivan Petrovich Pavlov (1849-1936). (Springer Berlin Heidelberg).

Campos, A.C., Fogaça, M.V., Aguiar, D.C., and Guimarães, F.S. (2013). Animal models of anxiety disorders and stress. Rev Bras Psiquiatr *35 Suppl 2*: S101–11.

Card, D., and Srivastava, S. (2014). Summary and discussion of: 'Why Most Published Research Findings Are False'. 1–15.

Cenci, M.A., Whishaw, I.Q., and Schallert, T. (2002). Animal models of neurological deficits: how relevant is the rat? Nat. Rev. Neurosci. *3*: 574–579.

Chang, J.-J., Tung, W.-L., Wu, W.-L., Huang, M.-H., and Su, F.-C. (2007). Effects of Robot-Aided Bilateral Force-Induced Isokinetic Arm Training Combined With Conventional Rehabilitation on Arm Motor Function in Patients With Chronic Stroke. Archives of Physical Medicine and Rehabilitation *88*: 1332–1338.

Cheng, N.G. (2012). Design and Analysis of a Robust, Low-cost, Highly Articulated Manipulator Enabled by Jamming of Granular Media. 1–6.

Chrousos, G.P., and Gold, P.W. (1992). The concepts of stress and stress system disorders. Overview of physical and behavioral homeostasis. Jama *267*: 1244–1252.

Cirstea, and Levin, M.F. (2000). Compensatory strategies for reaching in stroke. 1–14.

Contu, S., Hussain, A., Masia, L., and Campolo, D. (2016). A preliminary study for quantitative assessment of upper limb proprioception. Conf Proc IEEE Eng Med Biol Soc *2016*: 4614–4617.

Courtine, G., and Bloch, J. (2015). Defining Ecological Strategies in Neuroprosthetics. Neuron *86*: 29–33.

del Zoppo, G.J., Saver, J.L., Jauch, E.C., Adams, H.P., on behalf of the American Heart Association Stroke Council (2009). Expansion of the Time Window for Treatment of Acute Ischemic Stroke With Intravenous Tissue Plasminogen Activator: A Science Advisory From the American Heart Association/American Stroke Association. Stroke *40*: 2945–2948.

Dominici, N., Keller, U., Vallery, H., Friedli, L., van den Brand, R., Starkey, M.L., et al. (2012). Versatile robotic interface to evaluate, enable and train locomotion and balance after neuromotor disorders. Nature Publishing Group *18*: 1142–1147.

Donnan, G.A., Fisher, M., Macleod, M., and Davis, S.M. (2008). Stroke. The Lancet *371*: 1612–1623.

Dukelow, S.P. (2017). The potential power of robotics for upper extremity stroke rehabilitation. Int J Stroke *12*: 7–8.

Duricki, D.A., Soleman, S., and Moon, L.D.F. (2016). Analysis of longitudinal data from animals with missing values using SPSS. Nat Protoc *11*: 1112–1129.

Eapen, B.C., Murphy, D.P., and Cifu, D.X. (2017). Neuroprosthetics in amputee and brain injury rehabilitation. Experimental Neurology *287*: 479–485.

Einon, D. (2007). Spatial Memory and Response Strategies in Rats: Age, Sex and Rearing Differences in Performance. Quarterly Journal of Experimental Psychology *32*: 473–489.

Ellens, D.J., Gaidica, M., Toader, A., Peng, S., Shue, S., John, T., et al. (2016). An automated rat single pellet reaching system with high-speed video capture. Journal of Neuroscience Methods *271*: 119–127.

European heart network (2017). European Cardiovascular Disease Statistics 2017 edition. 1–192.

Evenden, J.L., and Robbins, T.W. (1984). Effects of unilateral6-Hydroxydopamine lesions of the caudate-putamen on skilled forepaw use in the rat. 1–8.

Farr, T.D., and Whishaw, I.Q. (2002). Quantitative and qualitative impairments in skilled reaching in the mouse (Mus musculus) after a focal motor cortex stroke. Stroke *33*: 1869–1875.

Fasoli, S.E., Krebs, H.I., Stein, J., Frontera, W.R., and Hogan, N. (2003). Effects of robotic therapy on motor impairment and recovery in chronic stroke. Archives of Physical Medicine and Rehabilitation *84*: 477–482.

Fenrich, K.K., May, Z., Hurd, C., Boychuk, C.E., Kowalczewski, J., Bennett, D.J., et al. (2015a). Improved single pellet grasping using automated ad libitum full-time training robot. Behavioural Brain Research *281*: 137–148.

Fenrich, K.K., May, Z., Hurd, C., Boychuk, C.E., Kowalczewski, J., Bennett, D.J., et al. (2015b). Improved single pellet grasping using automated ad libitum full-time training robot. Behavioural Brain Research *281*: 137–148.

Fenrich, K.K., May, Z., Torres-Espín, A., Forero, J., Bennett, D.J., and Fouad, K. (2016). Single pellet grasping following cervical spinal cord injury in adult rat using an automated full-time training robot. Behavioural Brain Research *299*: 59–71.

Field, E.F., and Whishaw, I.Q. (2005). Sexually dimorphic postural adjustments are used in a skilled reaching task in the rat. Behavioural Brain Research *163*: 237–245.

FINK, A., BENEDEK, M., GRABNER, R., STAUDT, B., and NEUBAUER, A. (2007). Creativity meets neuroscience: Experimental tasks for the neuroscientific study of creative thinking. Methods *42*: 68–76.

Fouad, K. (2013). Functional testing in animal models of spinal cord injury: not as straight forward as one would think. 1–8.

Garbuzova-Davis, S., Rodrigues, M.C.O., Hernandez-Ontiveros, D.G., Tajiri, N., Frisina-Deyo, A., Boffeli, S.M., et al. (2013). Blood-brain barrier alterations provide evidence of subacute diaschisis in an ischemic stroke rat model. PLoS ONE *8*: e63553.

García-Alías, G., Barkhuysen, S., Buckle, M., and Fawcett, J.W. (2009). Chondroitinase ABC treatment opens a window of opportunity for task-specific rehabilitation. Nat Neurosci *12*: 1145–1151.

Gharbawie, O.A., and Whishaw, I.Q. (2006). Parallel stages of learning and recovery of skilled reaching after motor cortex stroke: ‘Oppositions’ organize normal and

compensatory movements. Behavioural Brain Research *175*: 249–262.

Girgis, J., Merrett, D., Kirkland, S., Metz, G.A.S., Verge, V., and Fouad, K. (2007). Reaching training in rats with spinal cord injury promotes plasticity and task specific recovery. Brain *130*: 2993–3003.

Goble, D.J., and Anguera, J.A. (2010). Plastic changes in hand proprioception following force-field motor learning. Journal of Neurophysiology *104*: 1213–1215.

Gonzalez, C.L.R., and Kolb, B. (2003). A comparison of different models of stroke on behaviour and brain morphology. Eur J Neurosci *18*: 1950–1962.

Gonzalez, C.L.R., Gharbawie, O.A., Williams, P.T., Kleim, J.A., Kolb, B., and Whishaw, I.Q. (2004). Evidence for bilateral control of skilled movements: ipsilateral skilled forelimb reaching deficits and functional recovery in rats follow motor cortex and lateral frontal cortex lesions. Eur J Neurosci *20*: 3442–3452.

Hakim, R.M., Tunis, B.G., and Ross, M.D. (2016). Rehabilitation robotics for the upper extremity: review with new directions for orthopaedic disorders. Disabil Rehabil Assist Technol *48*: 1–7.

Hankey, G.J. (2003). Angiotensin-Converting Enzyme Inhibitors for Stroke Prevention: Is There HOPE for PROGRESS After LIFE? Stroke *34*: 354–356.

Hays, S.A., Khodaparast, N., Sloan, A.M., Hulsey, D.R., Pantoja, M., Ruiz, A.D., et al. (2013). The isometric pull task: a novel automated method for quantifying forelimb force generation in rats. Journal of Neuroscience Methods *212*: 329–337.

Henriques, D.Y.P., Filippopulos, F., Straube, A., and Eggert, T. (2014). The cerebellum is not necessary for visually driven recalibration of hand proprioception. Neuropsychologia *64*: 195–204.

Hesse, S., Schmidt, H., and Werner, C. (2006). Machines to support motor rehabilitation after stroke: 10 years of experience in Berlin. J Rehabil Res Dev *43*: 671–678.

Hesse, S., Schmidt, H., Werner, C., and Bardeleben, A. (2003a). Upper and lower extremity robotic devices for rehabilitation and for studying motor control. Curr. Opin. Neurol. *16*: 705–710.

Hesse, S., Schulte-Tigges, G., Konrad, M., Bardeleben, A., and Werner, C. (2003b). Robot-assisted arm trainer for the passive and active practice of bilateral forearm and wrist movements in hemiparetic subjects. Archives of Physical Medicine and Rehabilitation *84*: 915–920.

Hogg, S. (1996). A review of the validity and variability of the elevated plus-maze as an animal model of anxiety. Pharmacol. Biochem. Behav. *54*: 21–30.

Holley, K. (2008). The challenge of an interdisciplinary curriculum: a cultural analysis of a doctoral-degree program in neuroscience. High Educ *58*: 241–255.

Home Office (2014). Code of Practice for the Housing and Care of Animals Bred, Supplied or Used for Scienti c Purposes. 1–226.

Hu, L., Yang, J., Song, T., Hou, N., Liu, Y., Zhao, X., et al. (2014). A new stress model, a scream sound, alters learning and monoamine levels in rat brain. Physiol. Behav. *123*: 105–113.

Humm, J.L., Kozlowski, D.A., James, D.C., Gotts, J.E., and Schallert, T. (1998). Use-dependent exacerbation of brain damage occurs during an early post-lesion vulnerable period. Brain Research *783*: 286–292.

Hurd, C., Weishaupt, N., and Fouad, K. (2013). Anatomical correlates of recovery in single pellet reaching in spinal cord injured rats. Experimental Neurology *247*: 605–614.

Hurst, J.L., and West, R.S. (2010). Taming anxiety in laboratory mice. Nat. Methods *7*: 825–826.

Infeld, B., Davis, S.M., Lichtenstein, M., Mitchell, P.J., and Hopper, J.L. (1995). Crossed cerebellar diaschisis and brain recovery after stroke. Stroke *26*: 90–95.

Ioannidis, J.P.A. (2005). Why Most Published Research Findings Are False. PLoS Med *2*: e124–6.

Ishikawa, Y., Imagama, S., Ohgomori, T., Ishiguro, N., and Kadomatsu, K. (2015). A combination of keratan sulfate digestion and rehabilitation promotes anatomical plasticity after rat spinal cord injury. Neurosci. Lett. *593*: 13–18.

Iwaniuk, A.N., and Whishaw, I.Q. (2000). On the origin of skilled forelimb movements. 1–5.

Janda, A., Maza, D., Garcimartín, A., Kolb, E., Lanuza, J., and Clément, E. (2009). Unjamming a granular hopper by vibration. Europhys. Lett. *87*: 24002–7.

Jupp, B., Murray, J.E., Jordan, E.R., Xia, J., Fluharty, M., Shrestha, S., et al. (2016). Social dominance in rats: effects on cocaine self-administration, novelty reactivity and dopamine receptor binding and content in the striatum. Psychopharmacology (Berl.) *233*: 579–589.

Karl, J.M., and Whishaw, I.Q. (2011). Rodent Skilled Reaching for Modeling Pathological Conditions of the Human Motor System. In Animal Models of Movement Disorders, (Totowa, NJ: Humana Press), pp 87–107.

Kim, S.H., Pohl, P.S., Luchies, C.W., Stylianou, A.P., and Won, Y. (2003). Ipsilateral deficits of targeted movements after stroke. Archives of Physical Medicine and Rehabilitation *84*: 719–724.

Kleim, J.A., Boychuk, J.A., and Adkins, D.L. (2007). Rat models of upper extremity impairment in stroke. Ilar J *48*: 374–384.

Kleinholdermann, U., Franz, V.H., and Gegenfurtner, K.R. (2013). Human grasp point selection. Journal of Vision *13*: 23–23.

Kodandaramaiah, S.B., Boyden, E.S., and Forest, C.R. (2013). In vivorobotics: the automation of neuroscience and other intact-system biological fields. Ann. N.Y. Acad. Sci. *1305*: 63–71.

Kuczynski, A.M., Carlson, H.L., Lebel, C., Hodge, J.A., Dukelow, S.P., Semrau, J.A., et al. (2017). Sensory tractography and robot-quantified proprioception in hemiparetic children with perinatal stroke. Hum. Brain Mapp. *38*: 2424–2440.

Lees, K.R., Bluhmki, E., Kummer, von, R., Brott, T.G., Toni, D., Grotta, J.C., et al. (2010). Time to treatment with intravenous alteplase and outcome in stroke: an updated pooled analysis of ECASS, ATLANTIS, NINDS, and EPITHET trials. Lancet

375: 1695–1703.

Liggesmeyer, P., and Trapp, M. (2009). Trends in Embedded Software Engineering. IEEE Softw. *26*: 19–25.

Lindau, N.T., Banninger, B.J., Gullo, M., Good, N.A., Bachmann, L.C., Starkey, M.L., et al. (2014). Rewiring of the corticospinal tract in the adult rat after unilateral stroke and anti-Nogo-A therapy. Brain *137*: 739–756.

Livingston-Thomas, J.M., and Tasker, R.A. (2013). Animal models of post-ischemic forced use rehabilitation: methods, considerations, and limitations. Experimental & Translational Stroke Medicine *5*: 1–1.

Loureiro, R.C.V., Harwin, W.S., Lamperd, R., and Collin, C. (2014). Evaluation of reach and grasp robot-assisted therapy suggests similar functional recovery patterns on proximal and distal arm segments in sub-acute hemiplegia. IEEE Trans. Neural Syst. Rehabil. Eng. *22*: 593–602.

Loureiro, R.C.V., Harwin, W.S., Nagai, K., and Johnson, M. (2011). Advances in upper limb stroke rehabilitation: a technology push. Med Biol Eng Comput *49*: 1103–1118.

Luengo-Fernandez, R., Leal, J., and Gray, A.M. (2012). UK research expenditure on dementia, heart disease, stroke and cancer: are levels of spending related to disease burden? Eur. J. Neurol. *19*: 149–154.

Lum, P.S., Burgar, C.G., Shor, P.C., Majmundar, M., and Van der Loos, M. (2002). Robot-assisted movement training compared with conventional therapy techniques for the rehabilitation of upper-limb motor function after stroke. Archives of Physical Medicine and Rehabilitation *83*: 952–959.

MacLellan, C.L., Gyawali, S., and Colbourne, F. (2006). Skilled reaching impairments follow intrastriatal hemorrhagic stroke in rats. Behavioural Brain Research *175*: 82–89.

McBride, D.W., Legrand, J., Krafft, P.R., Flores, J., Klebe, D., Tang, J., et al. (2016). Acute Hyperglycemia Is Associated with Immediate Brain Swelling and Hemorrhagic Transformation After Middle Cerebral Artery Occlusion in Rats. Acta Neurochir. Suppl. *121*: 237–241.

Melhorn, S.J., Elfers, C.T., Scott, K.A., and Sakai, R.R. (2017). A closer look at the subordinate population within the visible burrow system. Physiol. Behav.

Metz, G.A., and Whishaw, I.Q. (2013). Skilled reaching an action pattern: stability in rat (Rattus norTegicus) grasping movements as a function of changing food pellet size. 1–12.

Metz, G.A., Antonow-Schlorke, I., and Witte, O.W. (2005). Motor improvements after focal cortical ischemia in adult rats are mediated by compensatory mechanisms. Behavioural Brain Research *162*: 71–82.

Metz, G.A., Merkler, D., Dietz, V., Schwab, M.E., and Fouad, K. (2000). Efficient testing of motor function in spinal cord injured rats. Brain Research *883*: 165–177.

Metz, G.A.S., and Whishaw, I.Q. (2000). Skilled reaching an action pattern: stability in rat (Rattus norvegicus) grasping movements as a function of changing food pellet size. Behavioural Brain Research *116*: 111–122.

Meyers, E., Sindhurakar, A., Choi, R., Solorzano, R., Martinez, T., Sloan, A., et al.

(2016). The supination assessment task: an automated method for quantifying forelimb rotational function in rats. Journal of Neuroscience Methods 1–28.

Miklyaeva, E.I., and Whishaw, I.Q. (1996). HemiParkinson analogue rats display active support in good limbs versus passive support in bad limbs on a skilled reaching task of variable height. Behav. Neurosci. *110*: 117–125.

Miklyaeva, E.I., Castañeda, E., and Whishaw, I.Q. (1994). Skilled reaching deficits in unilateral dopamine-depleted rats: impairments in movement and posture and compensatory adjustments. Journal of Neuroscience *14*: 7148–7158.

Moneo, M., Martín Zúñiga, J., and Morón, I. (2017). Caloric restriction in grouped rats: aggregate influence on behavioural and hormonal data. Lab. Anim. *12*: 23677216686805.

Montoya, C.P., Campbell-Hope, L.J., Pemberton, K.D., and Dunnett, S.B. (1991). The 'staircase test': a measure of independent forelimb reaching and grasping abilities in rats. Journal of Neuroscience Methods *36*: 219–228.

Moore, N.L.T., Altman, D.E., Gauchan, S., and Genovese, R.F. (2016). Adulthood stress responses in rats are variably altered as a factor of adolescent stress exposure. Stress *19*: 295–302.

Mosberger, A.C., de Clauser, L., Kasper, H., and Schwab, M.E. (2016). Motivational state, reward value, and Pavlovian cues differentially affect skilled forelimb grasping in rats. Learn. Mem. *23*: 289–302.

Mosberger, A.C., Miehlbradt, J.C., Bjelopoljak, N., Schneider, M.P., Wahl, A.-S., Ineichen, B.V., et al. (2017). Axotomized Corticospinal Neurons Increase Supra-Lesional Innervation and Remain Crucial for Skilled Reaching after Bilateral Pyramidotomy. Cereb. Cortex.

Moxon, K.A., and Foffani, G. (2015). Brain-machine interfaces beyond neuroprosthetics. Neuron *86*: 55–67.

NICE (2017). Alteplase for treating acute ischaemic stroke. 1–37.

Nielsen, R.K., Samson, K.L., Simonsen, D., and Jensen, W. (2013). Effect of Early and Late Rehabilitation Onset in a Chronic Rat Model of Ischemic Stroke— Assessment of Motor Cortex Signaling and Gait Functionality Over Time. IEEE Trans. Neural Syst. Rehabil. Eng. *21*: 1006–1015.

O'Collins, V.E., Macleod, M.R., Donnan, G.A., Horky, L.L., van der Worp, B.H., and Howells, D.W. (2006). 1,026 Experimental treatments in acute stroke. Ann Neurol. *59*: 467–477.

Otwell, J.L., Phillippe, H.M., and Dixon, K.S. (2010). Efficacy and safety of i.v. alteplase therapy up to 4.5 hours after acute ischemic stroke onset. Am J Health Syst Pharm *67*: 1070–1074.

Palmér, T., Tamtè, M., Halje, P., Enqvist, O., and Petersson, P. (2012). A system for automated tracking of motor components in neurophysiological research. Journal of Neuroscience Methods *205*: 334–344.

Pappas, K.M., and DeVoll, J.R. (2012). Neuroprosthetics. Aviat Space Environ Med *83*: 537–538.

Peikon, I.D., Fitzsimmons, N.A., Lebedev, M.A., and Nicolelis, M.A.L. (2009). Three-dimensional, automated, real-time video system for tracking limb motion in brain–machine interface studies. Journal of Neuroscience Methods *180*: 224–233.

PhD, M.W., MSPT, J.M.L., MPT, J.K., PhD, B.D.S., PhD, S.-C.Y.P., and DPT, J.M. (2014). Robotic Resistance/Assistance Training Improves Locomotor Function in Individuals Poststroke: A Randomized Controlled Study. Archives of Physical Medicine and Rehabilitation *95*: 799–806.

Poddar, R., Kawai, R., and Ölveczky, B.P. (2013). A Fully Automated High-Throughput Training System for Rodents. PLoS ONE *8*: e83171–10.

Pourghodrat, A., and Nelson, C.A. (2017). Disposable Fluidic Actuators for Miniature In-Vivo Surgical Robotics. J Med Device *11*: 0110031–0110038.

Ramirez, J.M. (2013). Behavioral parameters of social dominance in rats. Bulletin of the Psychonomic Society *15*: 96–98.

Rice, A.S.C., Cimino-Brown, D., Eisenach, J.C., Kontinen, V.K., Lacroix-Fralish, M.L., Machin, I., et al. (2008). Animal models and the prediction of efficacy in clinical trials of analgesic drugs: a critical appraisal and call for uniform reporting standards. Pain *139*: 243–247.

Rosenthal, R., and Fode, K.L. (2007). The effect of experimenter bias on the performance of the albino rat. Behavioral Science *8*: 183–189.

Routara, B.C., Bandyopadhyay, A., and Sahoo, P. (2008). Roughness modeling and optimization in CNC end milling using response surface method: effect of workpiece material variation. Int J Adv Manuf Technol *40*: 1166–1180.

Rowe, W.A. (2014). Motor Rehabilitation Based on Brain Machine Interface and Microsoft Kinect. 1–4.

Schaar, K.L., Brenneman, M.M., and Savitz, S.I. (2010). Functional assessments in the rodent stroke model. Experimental & Translational Stroke Medicine *2*: 13.

Schaller, R.R. (1997). Moore's law: past, present and future. IEEE Spectrum *34*: 52–59.

Schallert, T., Fleming, S.M., Leasure, J.L., Tillerson, J.L., and Bland, S.T. (2000). CNS plasticity and assessment of forelimb sensorimotor outcome in unilateral rat models of stroke, cortical ablation, parkinsonism and spinal cord injury. Neuropharmacology *39*: 777–787.

Schlinger, H.D. (2015). Behavior analysis and behavioral neuroscience. Front. Hum. Neurosci. *9*: 210.

Schmidt, H., Hesse, S., Werner, C., and Bardeleben, A. (2004). Upper and lower extremity robotic devices to promote motor recovery after stroke -recent developments. Conf Proc IEEE Eng Med Biol Soc *7*: 4825–4828.

Schneider, J.S., and Olazabal, U.E. (1984). Behaviorally specific limb use deficits following globus pallidus lesions in rats. Brain Research *308*: 341–346.

Schwartz, I., and Meiner, Z. (2015). Robotic-Assisted Gait Training in Neurological Patients: Who May Benefit? Ann Biomed Eng *43*: 1260–1269.

Seitz, R.J., Azari, N.P., Knorr, U., Binkofski, F., Herzog, H., and Freund, H.J. (1999). The role of diaschisis in stroke recovery. Stroke *30*: 1844–1850.

Shaffer, D.M., and Taylor, A. (2017). Free hand proprioception is well calibrated to verbal estimates of slanted surfaces. Atten Percept Psychophys *79*: 691–697.

Silasi, G., Hamilton, D.A., and Kolb, B. (2008). Social instability blocks functional restitution following motor cortex stroke in rats. Behavioural Brain Research *188*: 219–226.

Smith, L.K., and Metz, G.A. (2005). Dietary restriction alters fine motor function in rats. Physiol. Behav. *85*: 581–592.

Soblosky, J.S., Colgin, L.L., Chorney-Lane, D., Davidson, J.F., and Carey, M.E. (1997). Ladder beam and camera video recording system for evaluating forelimb and hindlimb deficits after sensorimotor cortex injury in rats. Journal of Neuroscience Methods *78*: 75–83.

Soleman, S., Yip, P., Leasure, J.L., and Moon, L. (2010). Sustained sensorimotor impairments after endothelin-1 induced focal cerebral ischemia (stroke) in aged rats. Experimental Neurology *222*: 13–24.

Soleman, S., Yip, P.K., Duricki, D.A., and Moon, L.D.F. (2012). Delayed treatment with chondroitinase ABC promotes sensorimotor recovery and plasticity after stroke in aged rats. Brain *135*: 1210–1223.

Stinear, C., Ackerley, S., and Byblow, W. (2013). Rehabilitation is Initiated Early After Stroke, but Most Motor Rehabilitation Trials Are Not: A Systematic Review. Stroke *44*: 2039–2045.

Stroke Association (2017). Stroke Association Statistics 2017. 1–38.

Stutzmann, J.-M., Mary, V., Wahl, F., Grosjean-Piot, O., Uzan, A., and Pratt, J. (2002). Neuroprotective profile of enoxaparin, a low molecular weight heparin, in in vivo models of cerebral ischemia or traumatic brain injury in rats: a review. CNS Drug Rev *8*: 1–30.

Sunderland, A., Bowers, M.P., Sluman, S.M., Wilcock, D.J., and Ardron, M.E. (1999). Impaired dexterity of the ipsilateral hand after stroke and the relationship to cognitive deficit. Stroke *30*: 949–955.

Sutcliffe, J.S., Marshall, K.M., and Neill, J.C. (2007). Influence of gender on working and spatial memory in the novel object recognition task in the rat. Behavioural Brain Research *177*: 117–125.

Tian, S., Zhang, Y., Tian, S., Yang, X., Yu, K., Zhang, Y., et al. (2013). Early exercise training improves ischemic outcome in rats by cerebral hemodynamics. Brain Research *1533*: 114–121.

To, K., Lai, P.-Y., and Pak, H.K. (2001). Jamming of Granular Flow in a Two-Dimensional Hopper. Phys. Rev. Lett. *86*: 71–74.

Tsai, S.Y., Papadopoulos, C.M., Schwab, M.E., and Kartje, G.L. (2010). Delayed Anti-Nogo-A Therapy Improves Function After Chronic Stroke in Adult Rats. Stroke *42*: 186–190.

Vigaru, B. (2013). A Robotic Platform to Assess, Guide and Perturb Rat Forelimb Movements. 1–11.

Wahl, A.S., Omlor, W., Rubio, J.C., Chen, J.L., Zheng, H., Schroter, A., et al. (2014). Asynchronous therapy restores motor control by rewiring of the rat corticospinal tract after stroke. Science *344*: 1250–1255.

Weishaupt, N., Li, S., Di Pardo, A., Sipione, S., and Fouad, K. (2013). Synergistic effects of BDNF and rehabilitative training on recovery after cervical spinal cord injury. Behavioural Brain Research *239*: 31–42.

Wentworth, C.K. (1933). FUNDAMENTAL LIMITS TO THE SIZES OF CLASTIC GRAINS. Science *77*: 633–634.

Whishaw, I.Q. (1989). Dissociating performance and learning deficits on spatial navigation tasks in rats subjected to cholinergic muscarinic blockade. Brain Research Bulletin *23*: 347–358.

Whishaw, I.Q., Alaverdashvili, M., and Kolb, B. (2008a). The problem of relating plasticity and skilled reaching after motor cortex stroke in the rat. Behavioural Brain Research *192*: 124–136.

Whishaw, I.Q., Alaverdashvili, M., and Kolb, B. (2008b). The problem of relating plasticity and skilled reaching after motor cortex stroke in the rat. Behavioural Brain Research *192*: 124–136.

Whishaw, I.Q., and Coles, B.L. (1996). Varieties of paw and digit movement during spontaneous food handling in rats: Postures, bimanual coordination, preferences, and the effect of forelimb cortex lesions. 1–14.

Whishaw, I.Q., and Pellis, S.M. (1990a). The structure of skilled forelimb reaching in the rat" a proximally driven movement with a single distal rotatory component. 1–11.

Whishaw, I.Q., and Pellis, S.M. (1990b). The structure of skilled forelimb reaching in the rat: a proximally driven movement with a single distal rotatory component. Behavioural Brain Research *41*: 49–59.

Whishaw, I.Q., and Tomie, J.-A. (1988). Olfaction directs skilled forelimb reaching in the rat. 1–11.

Whishaw, I.Q., Haun, F., and Kolb, B. (2013). Analysis of Behavior in Laboratory Rodents. 1–33.

Whishaw, I.Q., O'Connor, W.T., and Dunnett, S.B. (1986a). The contributions of motor cortex, nigrostriatal dopamine and caudate-putamen to skilled forelimb use in the rat. Brain *109 (Pt 5)*: 805–843.

Whishaw, I.Q., Pellis, S.M., and Gorny, B.P. (1992). Skilled reaching in rats and humans: evidence for parallel development or homology. Behavioural Brain Research *47*: 59–70.

Whishaw, I.Q., Pellis, S.M., Gorny, B.P., and Pellis, V.C. (1991). The impairments in reaching and the movements of compensation in rats with motor cortex lesions: an endpoint, videorecording, and movement notation analysis. Behavioural Brain Research *42*: 77–91.

Whishaw, I.Q., Sutherland, R.J., Kolb, B., and Becker, J.B. (1986b). Effects of neonatal forebrain noradrenaline depletion on recovery from brain damage: performance on a spatial navigation task as a function of age of surgery and postsurgical housing. Behav. Neural Biol. *46*: 285–307.

Whishaw, I.Q., Whishaw, P., and Gorny, B. (2008c). The Structure of Skilled Forelimb Reaching in the Rat: A Movement Rating Scale. JoVE.

Wong, C.C., Ramanathan, D.S., Gulati, T., Won, S.J., and Ganguly, K. (2015). An automated behavioral box to assess forelimb function in rats. Journal of Neuroscience Methods *246*: 30–37.

Wycherley, A.S., Helliwell, P.S., and Bird, H.A. (2005). A novel device for the measurement of proprioception in the hand. Rheumatology (Oxford) *44*: 638–641.

Yang, J., Hu, L., Wu, Q., Liu, L., Zhao, L., Zhao, X., et al. (2014). A terrified-sound stress induced proteomic changes in adult male rat hippocampus. Physiol. Behav. *128*: 32–38.

Zunzunegui, C., Gao, B., Cam, E., Hodor, A., and Bassetti, C.L. (2011). Sleep disturbance impairs stroke recovery in the rat. Sleep *34*: 1261–1269.